Macroeconomic Forecasting and Business Cycle Analysis with Nonlinear Models

Inaugural-Dissertation
zur Erlangung des akademischen Grades eines Doktors
der Wirtschafts- und Sozialwissenschaften
der Wirtschafts- und Sozialwissenschaftlichen Fakultät
der Christian-Albrechts-Universität zu Kiel

vorgelegt von
M.Sc.
Markus Heinrich
aus Flensburg

Kiel, 2020

Erstbegutachtung:
Prof. Dr. Kai Carstensen

Zweitbegutachtung:
Prof. Dr. Matei Demetrescu

Tag der Abgabe der Arbeit:
14. Juli 2020

Tag der mündlichen Prüfung:
17. November 2020

Acknowledgements

The process of writing this thesis has been quite a journey and I would like to thank everyone who has been a major part of it. First and foremost, I would like to express my gratitude to Prof. Dr. Kai Carstensen, my main PhD supervisor, who, by supervising me and always having an open door for discussions, made an fundamental contribution to my succeeding with the dissertation. Through him I learned not only a lot about economics and econometrics, but also the ways and nuances of sound research. In addition, I am indebted to Prof. Dr. Maik Wolters and Dr. Magnus Reif for the close and successful cooperation together with Prof. Dr. Kai Carstensen on the first project. In addition, I worked on a second project with Dr. Magnus Reif, who thus contributed significantly to the completion of my dissertation.

This thesis was written during my work as a research assistant at the Institute for Statistics and Econometrics at the Christian-Albrechts-University of Kiel. I would like to thank all colleagues at the Institute for a pleasant time on and off the job; especially Prof. Dr. Matei Demetrescu for being my second supervisor, Prof. Dr. Uwe Jensen as my office neighbor for every quick help and advice, and Albrecht Mengel and Julian Schröder for the excellent and extensive IT support during all this time.

I am truly thankful to all my friends for distracting me from research when I needed it the most at stressful times. Furthermore, I am very grateful to Daniel Gräber for encouraging me to apply for this position as a research assistant and thus sending me on this exciting and rewarding journey. Last but not least, I thank my parents, Peter and Sabine Heinrich, and my sister, Dr. Julia Hollenbach, for the moral support and words of cheer in strenuous times.

Contents

List of Figures

List of Tables

General Introduction

The Great Recession of 2008/09 led to a sharp and persistent decline in real output growth in many countries, resulting in a global economic crisis. This economic crisis had its worst slump in economic activity in late 2008 and early 2009. At this time economists failed to predict the economic slump, though some economic indicators have shown first stirrings for the sharp downturn and thus, a severe recession.

This failure raises two important questions: First, did economists use improper forecasting models? For instance, did these forecasting models not include information about the current state of the business cycle? Or did these forecasting models not account for the nonlinear dynamics inherent in the business cycle due to expansions and recessions? Generally, it is much more difficult to predict output growth during volatile recessions compared to calm expansions (see, i.e., Chauvet and Potter, 2013; Dovern and Jannsen, 2017). Second, did economists select the most informative economic indicators for their forecasting models at that time? Not all economic indicators are available at the same frequency and many models can not handle the frequency mismatch in the data. Furthermore, not all recessions are of the same origins, e.g. they might stem from financial, demand or supply shocks (see discussion in Ng and Wright, 2013). Hence, the importance of economic indicators for predicting recessions might change over time and economist need an appropriate variable selection method.

I examine in three independent articles different approaches to address these aspects and the problems associated with them in a real-time data analysis. Hence, my thesis consists of the chapters 1, 2 and 3, each comprising an independent article contributing to the literature.

In chapter 1, titled ***"Predicting Ordinary and Severe Recessions with a Three-State Markov-Switching Dynamic Factor Model. An Application to the German Business Cycle."***, we date the German business cycle and subsequently use this information to forecast GDP growth in real time. We date the business cycle with help of a Markov-Switching Dynamic Factor Model (MS-DFM) with three different regimes–namely expansion, ordinary recession and severe recession. Additionally, we implement the elastic-net regularized regression method to select the most informative indicators from a larger real-time data set. In this way, we contribute to the literature by circumventing the trade-off between the usage of a large information set and the computational infeasibility of the nonlinear MS-DFM that is associated with a large number of parameters to estimate. Furthermore, we obtain a time-varying selection of indicators by recursively implementing the elastic-net to account for the shifting importance of economic indicators in the prediction of recessions in real time.

In an ex-post validation, we demonstrate that the three regime specification is a better fit to the German business cycle compared to the standard two regime setting–namely expansion and recession. We argue that this result is driven by the Great Recession in Germany as it had a significantly stronger negative impact on the economy compared to previous recessions. In a real-time forecasting experiment, we show that the model can timely detect not only ordinary

recessions but also the severe recession with the economic slump during the Great Recession in 2008/09. In terms of real-time indicator selection, it becomes apparent that it is stable with only few changes and reflects the traditional dependence of the German business cycle on global developments.

This paper is joint work with Kai Carstensen, Maik Wolters and Magnus Reif. Magnus Reif and I constructed the first draft of the paper based on the initial concept of Maik Wolters. This first draft has been considerably advanced by Maik Wolters and Kai Carstensen during the later stage of this project. I contributed significantly to the implementation and estimation of the model as well to the co-writing of the paper. The paper is published online in the International Journal of Forecasting (see Carstensen et al., 2020).

In chapter 2, titled ***"Real-Time Forecasting Using Mixed-Frequency VARs with Time-Varying Parameters"***, we contribute to the literature by proving that combining nonlinearities in form of time-varying parameters and mixed-frequency can be beneficial for forecasting in real time. In this paper we introduce a mixed-frequency vector autoregressive model with time-varying parameter and stochastic volatility (MF-TVP-SV-VAR) as a novel model to the forecasting literature. The model allows for indicators sampled at different frequencies. At the same time, it takes potential structural changes in the economy, as probably caused by the Great Recession, into account. Moreover, we implement a hyperparameter optimization algorithm that partly determines the amount of time-variation in the parameters in a mixed-frequency setup.

A forecasting experiment on US real-time data highlights the importance of both features for point and density forecasts. In general, nowcasting benefits considerably from mixed-frequency while both mixed-frequency and time-variation in the parameters pays off in particular for inflation forecasts. We also provide evidence with help of an optimal forecast pool that the MF-TVP-SV-VAR has acquired an increased importance since the Great Recession and thus support the consideration of nonlinear models in forecasting due to the Great Recession.

This paper is joint work with Magnus Reif. Both of us contributed equally to the entire article. A current version is published as a Working Paper (see Heinrich and Reif, 2020).

The basis for chapter 3, titled ***"Does the Current State of the Business Cycle matter for Real-Time Forecasting? A Mixed-Frequency Threshold VAR approach."***, is provided by the first two chapters. In chapter 1, we contribute to the literature by showing that short-term forecasting of output–notably during recessions–improves from considering information about the state of the business cycle. In chapter 2, we add to the literature by demonstrating that mixed-frequency VARs particularly improve nowcasting. Motivated by these two important insights, I develop and implement a mixed-frequency threshold vector autoregressive model with common stochastic volatility in mean (MF-T-CSVM-VAR). With the MF-T-CSVM-VAR, I exploit the information about crucial characteristics of the state of the business cycle on forecasting in a multivariate nonlinear mixed-frequency setting. This allows me to account for nonlinear dynamics inherent in the business cycle due to expansions and recessions as well as economic indicators sampled at different frequencies.

My novel model includes three crucial characteristics of the state of the business cycle. First, it captures the asymmetry of the business cycle in form of expansion and recession regimes.

Second, it characterizes co-movements among a large set of different macroeconomic variables in form of an business cycle index. Third, it describes the change in macroeconomic uncertainty over time and its influence on the forecasting performance in form of common stochastic volatility in mean. A real-time forecasting experiment reveals the importance of the state of the business cycle on forecasting–notably for the nowcast of GDP growth and unemployment rate during recessions. It is worth emphasising that my model outperforms the nowcast of the US Survey of Professional Forecasters when it comes to the sharp decline in GDP during the Great Recession in the fourth quarter of 2008. This paper is a single-authored paper (see Heinrich, 2020).

Overall, this dissertation contributes to the research questions of how nonlinear models help to improve macroeconomic forecasting and business cycle analysis and how these two topics are interrelated. I propose several successful approaches to overcome the problem on how to timely detect recessions in real time and better forecast macroeconomic variables during recessions with a special focus on the Great Recession. But already Blanchard and Watson (1986) ask the question "*Are business cycles all alike*?". In chapter 1, we provide evidence that the Great Recession differs from the ordinary recession in Germany such that an additional regime must be added to the model. Generally, models with regime shifts assume constant parameters within each regime and hence, assume that all business cycles are alike. Hence, a promising topic for my future research is on the flexibility of these models in terms of different dynamics within each regime. This is especially interesting in the wake of the current economic crisis in 2020 caused by the COVID-19 epidemic. This new economic crisis has a different cause and most likely a different economic impact that will be reflected in a different severity of the recession compared to the Great Recession (see Perez-Quiros et al., 2020, for a first assesment).

Chapter 1

Predicting Ordinary and Severe Recessions with a Three-State Markov-Switching Dynamic Factor Model. An Application to the German Business Cycle.

Abstract

We estimate a Markov-switching dynamic factor model with three states based on six leading business cycle indicators for Germany preselected from a broader set using the Elastic Net soft-thresholding rule. The three states represent expansions, normal recessions and severe recessions. We show that a two-state model is not sensitive enough to reliably detect relatively mild recessions when the Great Recession of 2008/2009 is included in the sample. Adding a third state helps to clearly distinguish normal and severe recessions, so that the model identifies reliably all business cycle turning points in our sample. In a real-time exercise the model detects recessions timely. Combining the estimated factor and the recession probabilities with a simple GDP forecasting model yields an accurate nowcast for the steepest decline in GDP in 2009Q1 and a correct prediction of the timing of the Great Recession and its recovery one quarter in advance.

Keywords: Markov-Switching Dynamic Factor Model, Great Recession, Turning Points, GDP Nowcasting, GDP Forecasting
JEL-Codes: C53, E32, E37

This study is joint work with Kai Carstensen, Magnus Reif and Maik H. Wolters.
It is published in International Journal of Forecasting 36(3), 829-850.
https://doi.org/10.1016/j.ijforecast.2019.09.005

Chapter 2

Real-Time Forecasting Using Mixed-Frequency VARs with Time-Varying Parameters

Abstract

This paper provides a detailed assessment of the real-time forecast accuracy of a wide range of vector autoregressive models (VAR) that allow for both structural change and indicators sampled at different frequencies. We extend the literature by evaluating a mixed-frequency time-varying parameter VAR with stochastic volatility (MF-TVP-SV-VAR). Overall, the MF-TVP-SV-VAR delivers accurate now- and forecasts and, on average, outperforms its competitors. We assess the models' accuracy relative to expert forecasts and show that the MF-TVP-SV-VAR delivers better inflation nowcasts in this regard. Using an optimal prediction pool, we moreover demonstrate that the MF-TVP-SV-VAR has gained importance since the Great Recession.

Keywords: Time-varying parameters, Forecasting, Nowcasting, Mixed-frequency models, Bayesian methods
JEL-Codes: C11, C53, C55, E32

This study is joint work with Magnus Reif.
It is published as a Working Paper in CESifo Working Paper Series 8054, CESifo Group Munich.
`https://www.cesifo.org/w/cf4383bd`

2.1 Introduction

Macroeconomists and, in particular, macroeconomic forecasters face two major challenges. First, there are structural changes within an economy. Second, in real time forecasters need to process unbalanced datasets due to indicators sampled at different frequencies and idiosyncratic publication lags. Concerning structural change, it is commonly found that particularly modeling time-varying volatilities enhances VAR-based inference and estimation, while fluctuations in the VAR coefficients are frequently considered to be less vital (for example, Sims and Zha, 2006; Chan and Eisenstat, 2017). This finding is confirmed with respect to forecasting by, for example, D'Agostino et al. (2013). Since the onset of the Great Recession, which probably caused important structural shifts, modeling time-varying links between variables has attracted anew interest.[1] Concerning unbalanced datasets, a growing literature stresses the merits of mixed-frequency approaches in computing precise now- and forecasts, and tracking the current state of the economy in real time (for instance, Kuzin et al., 2011; Foroni and Marcellino, 2014; Schorfheide and Song, 2015).

However, evidence regarding the forecast performance of models allowing for structural shifts in a mixed-frequency setting is rather sparse. This study aims at filling this gap by providing a detailed assessment of the real-time forecast accuracy of a bundle mixed-frequency models that allow for structural change. To this end, we estimate nonlinear and linear VARs with and without mixed-frequencies, including a fully-fledged model incorporating time-varying parameters, stochastic volatilities, and mixed-frequencies—a MF-TVP-SV-VAR. This analysis enables us to trace out the relative impact of the models' mixed-frequency part and the time-variation in the models' coefficients on the forecast accuracy. Our comparison relies on real-time out-of-sample now- and forecast accuracy of both point and density forecasts for three key US macroeconomic variables: GDP growth, CPI inflation, and the unemployment rate.

Overall, our forecast comparison provides two major findings. First, modelling structural change *and* intra-quarterly dynamics is beneficial for point and density forecasts, notably for now and short-term forecasts. In particular, the accuracy of inflation and unemployment rate forecasts can be substantially increased. Second, the MF-TVP-SV-VAR delivers very competitive point and density forecasts—on average over all variables it outperforms each competitor. Our results moreover suggest that the combination of mixed-frequencies, stochastic volatility, and time-varying parameters is particularly beneficial for inflation nowcasts computed with only little information about the respective quarters. In those cases, the MF-TVP-SV provides the largest gains in forecast accuracy. Taking a closer look at the mixed-frequency models' forecasts during the Great Recession reveals that allowing for time-variation in the VAR coefficients and stochastic volatility is superior relative to only one of these specifications for inflation and the unemployment rate.

We put our results to the test along two dimensions. First, since it is commonly found that a combination of forecasts from several models outperforms individual models, we augment our analysis with a forecast combination exercise, including equal weighting and an optimal

[1] See Ng and Wright (2013) for a survey of business cycle facts of the U.S. economy with a focus on the Great Recession.

prediction pool á la Geweke and Amisano (2011). We find that when estimating the models' weights, the mixed-frequency models consistently receive a large share of the entire probability mass. In particular, the MF-TVP-SV-VAR receives a high weight since the onset of the Great Recession, indicating the benefits of modelling structural change combined with modelling within-quarter dynamics in that period. Moreover, this optimal prediction pool provides strong gains in point and density forecast accuracy across all variables and horizons. It even outperforms the equal weighting combination scheme in almost each case. Second, since precise forecasts may stem from an accurate assessment of the current state of the economy (Sims, 2002), we assess whether the mixed-frequency models' satisfying forecast performance flows from more precise nowcasts. We assess this channel, by—in a first step—comparing the MF-VARs' predictions with those of the Survey of Professional Forecasters (SPF). SPF predictions are superior for GDP growth and the unemployment rate, while for inflation, the nonlinear MF-VARs provide slightly more accurate nowcasts. In a second step, we follow Schorfheide and Song (2015) and Wolters (2015) by augmenting the quarterly datasets with SPF nowcasts. We find that the gains in accuracy of the quarterly models are rather small with respect to GDP growth and inflation, while unemployment rate forecasts can be substantially improved.

Estimation of the models' TVP-SV part mainly follows Primiceri (2005). However, we treat those hyperparameters that relate to the amount of time-variation in the parameters as an additional layer and estimate them using Bayesian methods (Amir-Ahmadi et al., 2020).[2] Estimation of the models' MF part is based on the idea that lower-frequency variables can be expressed as higher-frequency variables with latent observations (Zadrozny, 1988).[3] Adopting this notion, Mariano and Murasawa (2010) derive a state-space representation for VARs with missing observations, called mixed-frequency VAR (MF-VAR). We follow Schorfheide and Song (2015) and apply the MF-VAR approach in a Bayesian framework.

On the one hand, this paper contributes to the ongoing discussion on how structural change affects VAR-based forecast performance. D'Agostino et al. (2013) forecast US inflation, unemployment, and short-term interest rates with TVP-SV-VARs and find that allowing for parameter instability significantly improves forecast accuracy. Barnett et al. (2014) and Clark and Ravazzolo (2015) underpin these findings and show that models with time-varying parameters improve forecast performance, especially regarding inflation forecasts. Focusing on the period since the Great Recession, Aastveit et al. (2017) provide strong evidence against constant parameter VARs and document that TVP-SV-VAR tend to perform best with small models. Banbura and van Vlodrop (2018) illustrate that accounting for time-varying means in a Bayesian VAR substantially increases long-term forecast accuracy.

On the other hand, this article extends the literature on forecasting with nonlinear mixed-frequency VARs. Foroni et al. (2015) introduce mixed-frequency Markov-switching VARs and provide evidence that modelling discrete regime shifts in a mixed-frequency setting is particularly beneficial with regard to nowcasting and short-term forecasting. Closely related to this analysis

[2] Amir-Ahmadi et al. (2020) show that the magnitude of the hyperparameters changes significantly when estimated on monthly data compared to quarterly data, which affects the time-variation in the model's coefficients.

[3] Alternative approaches are mixed data sampling (MIDAS) provided by Ghysels et al. (2004) and the mixed frequency VAR in a stacked system introduced by Ghysels (2016). For an assessment of the stacked approach with regard to forecasting, see McCracken et al. (2015).

is the study by Götz and Hauzenberger (2018) that also uses a mixed-frequency VAR that allows for continuous parameter change. The latter, however, analyzes the forecast ability in a pseudo real-time setting of a more parsimonious model, restricting the parameter change to the intercept terms and employ common stochastic volatility, while we abstract form these restrictions.

The remainder of the paper is as follows. Section 2.2 provides a description of the dataset and outlines the forecast setup. Section 2.3 depicts the competing models and explains the estimation methodology. Section 2.4 describes the measures used for the forecast comparison. Section 2.5 presents the results. Section 2.6 concludes.

2.2 Data and forecast setup

2.2.1 Dataset

We use an updated version of the dataset used by Clark and Ravazzolo (2015) consisting of four macroeconomic time series, three of which are sampled at monthly frequency and one is observed quarterly. The quarterly series is US real GDP; the monthly series are CPI, the unemployment rate, and the 3-month Treasury bill rate. GDP and CPI enter the models in log first differences times 100 to obtain real GDP growth and CPI inflation in percentage point changes, respectively. The unemployment and interest rate remain untransformed. For the VARs estimated on quarterly frequency, the monthly indicators enter the models as quarterly averages. We obtain real-time data on inflation, unemployment, and GDP from the Archival FRED (ALFRED) database of the St. Louis Fed. Since the Treasury bill rate is not revised, we resort to the last available publication from the FRED database. The sample runs from January 1960 until September 2017. The first 8 years are used as a training sample to specify priors such that the estimation starts in January 1968.

Generally, macroeconomic variables are released with a publication lag, which implies that a certain vintage does not include the figures referring to the date of the vintage. The first release of quarterly GDP has a publication lag of roughly one month, thus, for example, the first figure for 2011Q4 is released at the end of 2012M1 and is then consecutively revised in the subsequent months. The value for the unemployment rate (CPI) is published in the first (second) week of the following month. Hence, following our previous example, at the end of 2012M1 the unemployment rate and CPI are available until 2011M12. Finally, the 3-month Treasury bill rate is available without any delay. Thus, we have so-called "ragged-edges" in our real-time dataset.

2.2.2 Forecast setup

To assess the predictions with regard to the intra-quarterly inflow of information, we follow Schorfheide and Song (2015) and establish three different information sets. We assume that the forecasts are generated around the middle of each month, when the current releases for GDP, CPI, and the unemployment rate are available.[4] The first information set, called I1, relates to the first month of each quarter such that the forecaster has information up to the

[4]We follow Schorfheide and Song (2015) and replace the missing observations for the T-Bill rate in the last month of each recursion by the expected monthly average.

middle of January, April, July, or October. In these months, the researcher has observations on inflation and unemployment until the end of the respective previous quarter and a first and preliminary estimate of GDP referring to the previous quarter. The second information set, called I2 (February, May, August, November), has one additional observation on inflation and unemployment referring to the current quarter and the first revision of GDP. The last set, I3 (March, June, September, December), includes one more observation on inflation and unemployment and the second GDP revision. Each information set is augmented with the observations of the T-Bill rate. Since the quarterly VARs cannot cope with "ragged-edges" in the data, we estimate them in each recursion based on the balanced information set I1, which accounts for new information only in terms of data revisions.

We use an expanding window to evaluate our forecasts for data vintages from January 1990 until September 2017. The predictions are evaluated based on quarterly averages, implying that for the mixed-frequency approaches we aggregate the predicted monthly time paths to quarterly frequency. To abstract from benchmark revisions, we evaluate GDP growth forecasts based on the second available estimate, that is the forecast for period $t+h$ is evaluated with the realization taken from the vintage published in $t+h+2$ (see, for example, Faust and Wright, 2009). Since the remaining variables are revised only rarely and slightly, we evaluate the forecast based on the latest vintage. The maximum forecast horizon h_{max} is set to 4 quarters. Thus, the mixed-frequency models generate forecasts for $h_m = 1, \ldots, 12$ months. Forecasts for horizons larger than one are obtained iteratively. We report results for 1, 2, 3, and 4 quarters ahead forecasts.

2.3 Models

Our baseline model is a standard VAR with all variables sampled at quarterly frequency. Based on this model, we evaluate the forecast performance of three extensions, namely, mixed-frequencies, stochastic volatilities, and time-varying parameters, as well as the forecast performance of combinations of these features. For the stochastic volatility models, we use random walk stochastic volatility, which is a parsimonious and competitive specification (Clark and Ravazzolo, 2015). Throughout the paper, $n = n_q + n_m$, where n, n_q, and n_m denote the number of total, quarterly, and monthly variables, respectively. Finally, p denotes the lag order.

2.3.1 Quarterly VAR

Our baseline quarterly VAR (Q-VAR) reads:

$$y_t = B_0 + \sum_{i=1}^{p} B_i y_{t-i} + \varepsilon_t, \qquad \varepsilon_t \sim N(0, \Omega), \tag{2.1}$$

where y_t and B_0 denote $n \times 1$ vectors of variables and constants, respectively. B_i for $i, \ldots, p$ are $n \times n$ matrices of coefficients and Ω is the time-invariant $n \times n$ variance-covariance matrix.

2.3.2 Quarterly VAR with stochastic volatility

The quarterly VAR with stochastic volatility (Q-SV-VAR) does not assume constant residual variances and includes a law of motion for the (log) volatilities. Following Primiceri (2005), we decompose the time-varying covariance matrix of the reduced-form residuals into a lower-triangular matrix A_t and a diagonal matrix Σ_t according to:

$$A_t \Omega_t A_t' = \Sigma_t \Sigma_t', \tag{2.2}$$

where the diagonal elements of Σ_t are the stochastic volatilities. A_t has ones on the main diagonal and nonzero entries for the remaining lower triangular elements, describing the contemporaneous relationships between the volatilities. This allows to rewrite the VAR in (2.1) as:

$$y_t = B_0 + \sum_{i=1}^{p} B_i y_{t-i} + A_t^{-1} \Sigma_t u_t, \qquad u_t \sim N(0, I_n). \tag{2.3}$$

The laws of motion are modeled by defining σ_t as the vector of the diagonal elements of Σ_t and a_t as the vector of nonzero elements stacked by rows of A_t as follows:

$$\log \sigma_t = \log \sigma_{t-1} + e_t, \qquad e_t = (e_{1,t}, \ldots, e_{n,t})' \sim N(0, \Psi), \tag{2.4}$$

$$a_t = a_{t-1} + \upsilon_t, \qquad \upsilon_t = (\upsilon_{1,t}', \ldots, \upsilon_{n,t}')' \sim N(0, \Phi). \tag{2.5}$$

Ψ is diagonal and Φ is block diagonal where the blocks relate to the equations of the VAR in (2.3).

2.3.3 Quarterly VAR with time-varying parameter

The quarterly VAR with time-varying parameter is estimated in a homoscedastic specification (Q-TVP-VAR) and with stochastic volatility (Q-TVP-SV-VAR). The Q-TVP-VAR extends the baseline Q-VAR for a random walk process governing the evolution of the VAR coefficients:

$$y_t = Z_t' \beta_t + \varepsilon_t, \qquad \varepsilon_t \sim N(0, \Omega), \tag{2.6}$$

$$\beta_t = \beta_{t-1} + \chi_t, \qquad \chi_t \sim N(0, Q), \tag{2.7}$$

where $Z_t = I_n \otimes [1, y_{t-1}', \ldots, y_{t-p}']$ contains all the right-hand side variables of the VAR, β_t is a $k_\beta \times 1$ vector of VAR coefficients, and $Q = diag(q_{\beta_1}^2, \ldots, q_{\beta_{k_\beta}}^2)$. For the Q-TVP-SV-VAR, the stochastic volatility part from (2.4) and (2.5) is added to the model.

2.3.4 Mixed-frequency VAR

Estimation of the mixed-frequency VAR (MF-VAR) follows the Bayesian state-space approach of Schorfheide and Song (2015), which can be combined with the former VAR specifications. To this end, we partition our vector of variables $y_t = [y_{q,t}', y_{m,t}']'$, where $y_{m,t}$ collects the monthly variables and $y_{q,t}$ denotes the quarterly variables at monthly frequency. Since the quarterly variables are observed only in the last month of each quarter, $y_{q,t}$ contains missing observations

for the first and second month of each quarter. To construct the measurement equation, we follow Mariano and Murasawa (2003) and assume that quarterly GDP in log levels ($\log Y_{q,t}$) can be expressed as the geometric mean of an unobserved monthly GDP ($\log \tilde{Y}_{q,t}$):

$$\log Y_{q,t} = \frac{1}{3}(\log \tilde{Y}_{q,t} + \log \tilde{Y}_{q,t-1} + \log \tilde{Y}_{q,t-2}). \tag{2.8}$$

This expression implies that the quarterly series is a first-order approximation to an arithmetic mean of the unobserved monthly series. To arrive at an expression for quarterly GDP growth ($y_{q,t}$) based on latent monthly GDP growth ($\tilde{y}_{q,t}$), we subtract $\log Y_{q,t-3}$ from (2.8):

$$\Delta_3 \log Y_{q,t} = y_{q,t} = \frac{1}{3}\tilde{y}_{q,t} + \frac{2}{3}\tilde{y}_{q,t-1} + \tilde{y}_{q,t-2} + \frac{2}{3}\tilde{y}_{q,t-3} + \frac{1}{3}\tilde{y}_{q,t-4}. \tag{2.9}$$

Combining the unobserved with the observed monthly variables in $\tilde{y}_t = [\tilde{y}'_{q,t}, y'_{m,t}]'$, we define the state vector by $z_t = [\tilde{y}'_t, \ldots, \tilde{y}'_{t-p+1}]$ and write the measurement equation as:

$$y_t = H_t z_t. \tag{2.10}$$

Assuming that GDP growth is ordered first in the model, H_t is given by:

$$H_t = \begin{bmatrix} H_{1,t} & H_{2,t} \end{bmatrix}', \tag{2.11}$$

$$H_{1,t} = \begin{bmatrix} 1/3 & 0_{1\times n-1} & 2/3 & 0_{1\times n-1} & 1 & 0_{1\times n-1} & 2/3 & 0_{1\times n-1} & 1/3 & 0_{1\times n-1} & 0_{1\times (p-4)n} \end{bmatrix}, \tag{2.12}$$

$$H_{2,t} = \begin{bmatrix} 0_{n-1\times 1} & I_{n-1} & 0_{n-1\times pn} \end{bmatrix}, \tag{2.13}$$

where $H_{1,t}$ translates the disaggregation constraint in (2.9) into the state-space framework. The missing observations in z_t are replaced by estimated states using the Carter and Kohn (1994) simulation smoother (hereafter CK) with a time-varying dimension of the state-space system (Durbin and Koopman, 2001).[5] If an indicator exhibits a missing observation in t, the corresponding entry in y_t and the corresponding row of H_t are deleted. The transition equation of the MF-VAR in state-space form is given by:

$$z_t = \mu + F z_{t-1} + \upsilon_t, \qquad \upsilon_t \sim N(0, S), \tag{2.14}$$

where μ and F contain the intercepts and AR-coefficients, respectively. S is a $pn \times pn$ variance-covariance matrix where the first $n \times n$ elements equal Ω and all remaining entries are zero.

We obtain the MF-SV-VAR by setting the first $n \times n$ elements of S to Ω_t using the decomposition in (2.2) and following the laws of motion in (2.4) and (2.5). The MF-TVP-VAR is obtained by allowing F to change over time according to (2.7). Including both specifications leads to the MF-TVP-SV-VAR. To summarize, we have a total of eight competing models:

[5] To increase computational efficiency, we eliminate the monthly series, which are observed in each period of the balanced part of the sample, from the state vector for $t = 1, \ldots, T_B$, where T_B denotes the end of the balanced sample. For a detailed description of this "compact" system we refer to the appendix of Schorfheide and Song (2015).

1. MF-TVP-SV-VAR: Mixed-frequency VAR with time-varying parameters and stochastic volatility
2. MF-SV-VAR: Mixed-frequency VAR with stochastic volatility
3. MF-TVP-VAR: Mixed-frequency VAR with time-varying parameters
4. MF-VAR: Mixed-frequency VAR
5. Q-TVP-SV-VAR: Quarterly VAR with time-varying parameters and stochastic volatility
6. Q-SV-VAR: Quarterly VAR with stochastic volatility (benchmark)
7. Q-TVP-VAR: Quarterly VAR with time-varying parameters
8. Q-VAR: Quarterly linear VAR

2.3.5 Estimation procedure and prior specification

All models are estimated with Bayesian estimation techniques, since most models depend on a large number of parameters and thus make estimation based on frequentist approaches infeasible. The mixed-frequency models are estimated with 4 lags; the quarterly models are estimated with 2 lags.[6] In the following, we provide a brief description of the estimation procedure and the prior specifications. A detailed description is provided in Appendices 2.A.1 and 2.A.2.

For the Q-VAR, we impose a Jeffrey's prior to abstract from shrinkage, since we use a small-scale VAR with only four variables. For the models' stochastic volatility part, we apply normal priors for the diagonal elements of Σ_t and the lower-triangular elements of A_t and obtain draws using CK algorithm and the mixture sampler of Kim et al. (1998) (hereafter KSC). Inverse-Wishart priors are applied for Ψ and Φ, respectively. For the SV-VAR and the MF-SV-VAR, we use normal priors for the VAR coefficients and obtain draws using the GLS-based posterior provided by Clark (2011). For the TVP models, we apply the Gibbs sampler of Del Negro and Primiceri (2015). Specifically, we apply the CK algorithm to draw the VAR coefficients, using a normal prior for β^T and an inverse-Wishart prior for Q.

The amount of time-variation in β_t, a_{it}, and $\log \sigma_{it}$ depends on the magnitude of the random walk variances Q, Ψ, and Φ and their corresponding prior distributions, which are—in part—determined by the hyperparameters k_Q, k_Ψ, and k_Φ:

$$p(Q) \sim IW(k_Q^2 \times T_0 \times V(\hat{\beta}_{OLS}), T_0), \tag{2.15}$$

$$p(\Psi) \sim IW(k_\Psi^2 \times (1+n) \times I_n, 4), \tag{2.16}$$

$$p(\Phi_i) \sim IW(k_\Phi^2 \times (i+1) \times V(\hat{A}_{i,OLS}), i+1), \qquad i = 1, \ldots, k-1, \tag{2.17}$$

[6] We set $p = 2$ for the quarterly model to be consistent with the literature on US data (see, e.g., Primiceri, 2005; D'Agostino et al., 2013; Clark and Ravazzolo, 2015). The monthly models have 4 lags to keep them computationally feasible. Furthermore, we require at least four lags to disaggregate quarterly GDP into monthly GDP (see (2.9)).

where OLS denotes OLS estimates based on the training sample. The literature commonly adopts the hyperparameter values proposed by Primiceri (2005). However, these values are calibrated for a quarterly three-variable TVP-SV-VAR and it is not clear, whether they are useful in case of monthly data or other model specifications. Therefore, we follow Amir-Ahmadi et al. (2020) by implementing another layer of priors for those hyperparameters. Moreover, we split k_Q into k_{Q_C} and $k_{Q_{AR}}$, where k_{Q_C} relates to intercept coefficients and $k_{Q_{AR}}$ to AR-coefficients, respectively. By this means, we allow for different degrees of time-variation across these groups of coefficients. The latter is motivated by the observations that time-variation seems to be more pronounced in the intercepts than in AR-coefficients (see, for example, D'Agostino et al., 2013). To be agnostic about the coefficients' degree of time-variation, we use, for each hyperparameter, an inverse-Gamma prior with scale parameter and degrees of freedom equal to 0.1 and 2, respectively, as recommended by Amir-Ahmadi et al. (2020).

For the mixed-frequency models, we initialize the state vector with a normal prior. The prior mean is set to the observed values, implying that for GDP the within-quarter figures equal the quarterly observations. The prior variance is the identity matrix. After having drawn the latent states, the remaining coefficients are drawn conditional on the drawn states (instead of conditional on the observed data).

2.3.6 In-sample analysis

To illustrate the importance of modeling variability in volatility and the VAR-coefficients, as well as the hyperparameter estimation, this sections provides a brief in-sample analysis based on the final data vintage. Figure 2.1 depicts the posterior distributions of the estimated hyperparameters along with the values proposed by Primiceri (2005) (dashed lines) and the prior distributions (dotted lines). While a direct comparison between Primiceri's values and ours is not straightforward, Figure 2.1, nevertheless, provides interesting observations.[7] Although we impose the same prior for each hyperparameter, the posterior distributions differ considerably from each other and, in some cases, Primiceri's values. The distributions for k_{Q_C} assign only minor probability mass to Primiceri's values, but imply a stronger prior belief on time variation in the intercept terms. The posterior of $k_{Q_{AR}}$ is (almost) centered around Primiceri's value with a rather low variance for the MF-TVP-SV-VAR, while it induces a stronger prior belief on time variation in the AR coefficients according to the Q-TVP-SV-VAR. Finally, the posteriors of k_Ψ and k_Φ parameterize—for both models—a stronger prior belief about time-variation in the stochastic volatilities, but a weaker one for time-variation in the correlations among the residuals. These results suggest that both estimating the hyperparameters and allowing for heterogeneity among the hyperparameters might provide a better description of the data generating process and thus, might increase the forecast performance.

Figure 2.2 plots the posterior means of the standard deviations of the reduced-form residuals from the MF-TVP-SV-VAR and Q-TVP-SV-VAR.[8] We assume that the volatility estimates from

[7] On the one hand, we employ a different model specification. On the other hand, the remaining parts of the priors are based on a different training sample. Both can lead to different priors, in spite of identical hyperparameters, and hence, complicate comparison.

[8] We also examined the volatility for different data vintages to investigate the impact of data revisions and

Figure 2.1: Posterior distributions of hyperparameters

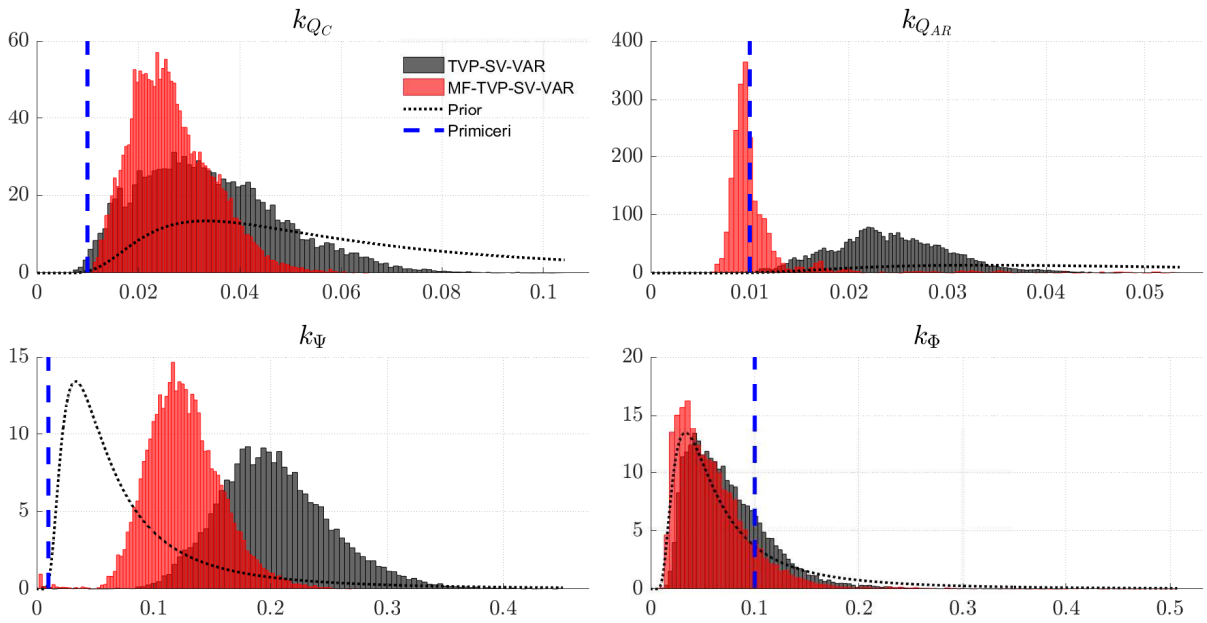

Notes: Figure shows the posterior distributions of the hyperparameters along with the respective prior distributions (dotted line) and the values proposed by Primiceri (2005) (dashed line).

the Q-TVP-SV-VAR are constant within a quarter to make them comparable across frequencies. The estimates of the Q-TVP-SV-VAR are smoother than those of Primiceri (2005), reflecting the weaker prior for time-variation in the residuals' correlations. Until the mid 1980s, the estimated volatilities are quite high and then fall sharply, indicating the beginning of the Great Moderation. Except for the increase during the burst of the dot-com bubble in 2000 and the rise during the Great Recession, they remain roughly at the levels of the mid 1980s. At the end of the sample, however, there is again a decline in volatility, indicating a time during which the US was remarkably less exposed to absolute shocks hitting the economy. Thus, as suggested by Clark (2009), the Great Recession seems to have simply interrupted, but not ended, the Great Moderation—the latest volatility estimates for GDP growth is the lowest of the entire sample.

The estimates from the MF-TVP-SV-VAR closely track the evolution of its quarterly counterpart. However, they are somewhat smaller, indicating that using monthly information absorbs part of the fluctuations in the volatility. This finding confirms the results of Carriero et al. (2015b), who employ a Bayesian mixed-frequency model without time-variation in the AR-coefficients.

With regard to the VAR coefficient, we obtain—for both models—the largest variability for the intercept coefficients; the remaining parameters exhibit only minor time-variation (see Figures 2.7 and 2.8 in Appendix 2.A.4). Overall, the results suggest that modeling variability in both volatility and the intercepts is more important for achieving precise forecasts than modeling time-varying autoregressive dynamics. Our results support the modeling strategy of

different values for the hyperparameters. Analogous to Clark (2011), we obtain very similar estimates for the different vintages, and thus we only report results for the latest vintage.

Figure 2.2: Standard deviations of reduced-form residuals

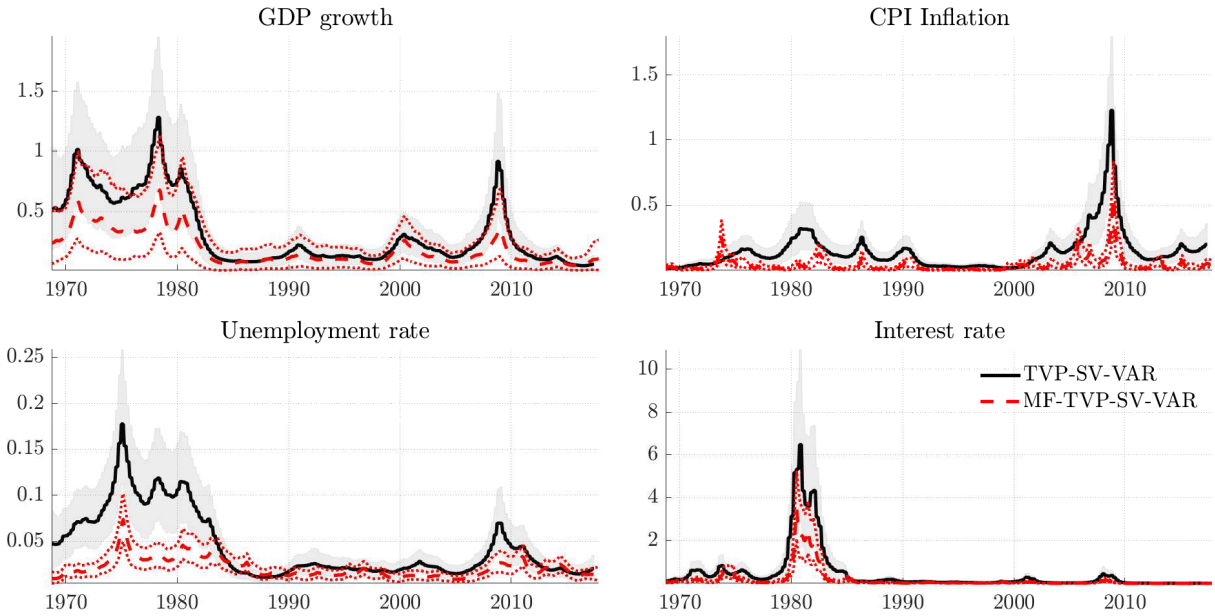

Notes: Figure depicts the posterior means of the residual standard deviations from the last data vintage at monthly frequency. Quarterly estimates are assumed to be constant within a quarter. Shaded areas and dotted lines refer to 68% posterior probability bands.

Götz and Hauzenberger (2018), who specify time-variation only in the intercepts, but treat the hyperparameters as exogenous values.

2.3.7 Now- and forecasting

The quarterly models are estimated on balanced datasets containing all available information from the previous quarter. To generate the predictive distributions, we compute sequences of h_{max} normally distributed innovations with covariance Φ, Ψ, and Q to produce time paths for the elements of A_t, Σ_t, and β_t, respectively. Based on these trajectories, we simulate y_t h_{max} periods into the future. The first forecast is a nowcast, since it is generated in and refers to the respective current quarter.

Additional notation is helpful in describing how we obtain the predictive distributions of the mixed-frequency models. Let T_M denote the last month of the indicator that has the shortest publication lag and let $Z^{T_M} = [z_1, \dots, z_{T_M}]$ denote the sequence of simulated state vectors. Note that the CK algorithm provides draws for the latent states until T_M. To obtain $Z^{T_m+1:T_m+h_{max}}$, we generate time paths for the elements of A_t, Σ_t, and β_t and simulate the state vector z_t forward using these time paths. Accordingly, if T_M belongs to I3, the CK algorithm provides draws for the entire last available quarter and by averaging over these draws we obtain the nowcasts. The forecasts are generated by averaging over the trajectories $Z^{T_m+1:T_m+h_{max}}$. However, if T_M belongs to I1 or I2, the CK algorithm does not provide draws of the latent states for the entire quarter since none of the indicators is available for the entire quarter. In this case, we average over the available CK draws and the simulated trajectories referring to this quarter to get the

nowcast. The forecasts are calculated from the averages of the remaining trajectories.[9]

2.4 Forecast metrics

We evaluate the models' forecasts with respect to point and density forecasts. Subsequently, m, i, and h denote the model, variable, and forecast horizon, respectively, for the forecast sample $t = 1, \ldots, N$. We measure point forecast accuracy using relative root mean squared errors:

$$\text{relative RMSE}_h^{i,m} = \frac{\sqrt{\frac{1}{N}\sum\left(\hat{y}_{t+h}^{i,m} - y_{t+h}^{i}\right)^2}}{\sqrt{\frac{1}{N}\sum\left(\hat{y}_{t+h}^{i,B} - y_{t+h}^{i}\right)^2}}, \tag{2.18}$$

where $\hat{y}_{t+h}^{i,B}$ refers to the forecast of the benchmark Q-SV-VAR.[10] We test for statistical differences in forecast accuracy by applying the Diebold and Mariano (1995) test.

Regarding density forecasts, we apply the continuous ranked probability score (CRPS). To compute the CRPS, we follow Gneiting and Ranjan (2011) and use the score function:

$$S(p_t^{i,m}, y_t^i, \nu(\alpha)) = \int_0^1 \text{QS}_\alpha(P_t(\alpha)^{-1}, y_t)\nu(\alpha)d\alpha, \tag{2.19}$$

where $\text{QS}_\alpha(P_t(\alpha)^{-1}, y_t^i) = 2(I\{y_t^i \leq P_t(\alpha)^{-1}\} - \alpha)(P_t(\alpha)^{-1} - y_t^i)$ is the quantile score for forecast quantile $P_t(\alpha)^{-1}$ at level $0 < \alpha < 1$. $I\{y_t^i \leq P_t(\alpha)^{-1}\}$ is an indicator function taking the value 1 when $y_t^i \leq P_t(\alpha)^{-1}$ and 0 otherwise. P_t^{-1} denotes the inverse of the cumulative predictive density function and $\nu(\alpha)$ is a weighting function. Using a uniform weighting scheme ($\nu(\alpha)=1$) and dividing by the number of generated densities yields the average CRPS:

$$\text{CRPS}_h^{i,m} = \frac{1}{N}\sum S(p_{t+h}^{i,m}, y_{t+h}^{i}, 1). \tag{2.20}$$

According to (2.20), a lower score indicates a better calibrated predictive density. We evaluate the CRPS as ratios relative to our benchmark:

$$\text{relative CRPS}_h^{i,m} = \frac{CRPS_h^{i,m}}{CRPS_h^{i,B}}. \tag{2.21}$$

We obtain approximate inference on whether the scores are significantly different from the benchmark by regressing the differences between the scores of each model and the benchmark on a constant. A t-test with Newey-West standard errors on the constant indicates whether these average differences are significantly different from zero (D'Agostino et al., 2013).

[9] For instance, in February, the T-Bill rate is available until February (T_M), while inflation and unemployment rate are available until January ($T_M - 1$). Hence, the CK algorithm provides draws for each indicator until T_M. The figures for March ($T_M + 1$) are generated using the time paths for A_t, Σ_t, and β_t. The forecast for the first quarter is the average over the figures referring to $T_M - 1$ to $T_M + 1$.

[10] Since several studies demonstrate that VARs with stochastic volatility outperform constant volatility VARs (see, for instance, Clark, 2011; Clark and Ravazzolo, 2015; Chiu et al., 2017), we do not use the Q-VAR as our benchmark.

2.5 Results

In this section, we discuss the results from the forecast experiment. We evaluate both point and density forecasts. Regarding the point forecasts, we first assess the models' nowcast accuracy. Second, we evaluate the accuracy of the point forecasts and predictive densities with respect to the subsequent quarters.[11] We provide results for the entire recursive sample (1995Q1–2017Q4) and for a shorter sample period of 2008Q1 until 2017Q4 to assess whether a possible structural break around the Great Recession affects the forecast performance.

2.5.1 Nowcast evaluation

Table 2.1 presents the results for the nowcast exercise taking into account the information sets I1 to I3. It provides three main takeaways. First, the mixed-frequency models outperform the quarterly models. On average, over all information sets and variables, the best nowcast performance is obtained by the MF-TVP-SV-VAR and the MF-SV-VAR, which improve on the benchmark (Q-SV-VAR) by roughly 35%. Second, most of the time, the nonlinear MF-models outperform the linear MF-VAR, indicating that—apart from using monthly information—parameter instability is beneficial also in a mixed-frequency setting. Third, the MF-models' relative performance improves with more information available, showing that the models are able to efficiently process the sequential data releases.

For GDP growth, only MF-models significantly outperform the benchmark. The best performance, for both samples, is obtained by the MF-SV-VAR. This result suggests that, from a nowcasting perspective, it is more important to account for the decline in output growth volatility than to account for changes in output growth dynamics. For inflation, the MF-TVP-SV-VAR delivers the best performance for the entire sample; it improves on the benchmark by, on average, 50%. Concerning the shorter sample, the MF-SV-VAR matches up with the MF-TVP-SV-VAR, suggesting that stochastic volatility has gained importance in the post-Great Recession period. Regarding both samples, the results indicate that notably with little information about the current quarter the MF-TVP-SV-VAR provides large gains in forecast accuracy relative to the competing models. The latter is particularly relevant because expert forecast, for example the SPF, are usually published in the second month of a quarter. With more information available, however, the differences towards the remaining MF-models vanish. For the unemployment rate, the MF-TVP-SV-VAR provides the most accurate nowcasts across all information sets with gains of about 40%. Though, it appears that nonlinearity is not as important as for the remaining variables—the differences to the linear MF are minor. The latter is maybe not surprising given that the fluctuations in volatility of the unemployment rate are less pronounced compared to the remaining variables (see Figure 2.2).

In total, the nowcast exercise provides strong evidence in favor of nonlinear forecasting models. In particular, stochastic volatility seems to be a major determinant of precise nowcasts,

[11] We abstract from evaluating the nowcasts with respect to predictive densities. Depending on the information sets, the nowcasts of the mixed-frequency models consist of quarterly averages over draws from the CK algorithm and realizations. Therefore, the nowcast densities of the mixed-frequency models are very narrow compared to the quarterly models and thus hardly comparable.

Table 2.1: Real-time nowcast RMSEs

Model	1990-2017 I1	1990-2017 I2	1990-2017 I3	2008-2017 I1	2008-2017 I2	2008-2017 I3
	GDP growth					
MF-TVP-SV-VAR	0.91	0.89	0.90	0.83	0.80	0.81
MF-SV-VAR	**0.85***	**0.80****	**0.78****	**0.80***	**0.74**	**0.72***
MF-TVP-VAR	0.88*	0.86*	0.82*	0.92	0.85	0.80
MF-VAR	0.99	0.96**	0.93	0.94	0.89	0.86
Q-TVP-SV-VAR	1.06	1.08	1.08	1.13	1.16	1.15
Q-TVP-VAR	0.98	0.99	0.99	0.99	1.00	1.01
Q-VAR	1.11***	1.12***	1.11***	1.12***	1.12***	1.12***
Q-SV-VAR	0.65	0.65	0.65	0.78	0.77	0.77
	Inflation					
MF-TVP-SV-VAR	**0.77***	**0.49****	**0.29****	**0.73***	0.46*	0.21*
MF-SV-VAR	0.86	0.52**	0.30***	0.77	**0.44**	0.21*
MF-TVP-VAR	0.85**	0.52*	**0.29*****	0.86*	0.50	0.22*
MF-VAR	0.89	0.53*	0.30***	0.80	0.45	**0.20***
Q-TVP-SV-VAR	0.87**	0.87**	0.88**	0.88	0.88	0.89
Q-TVP-VAR	0.93**	0.93**	0.93	0.94	0.94	0.95
Q-VAR	1.04***	1.04***	1.04***	1.03	1.03	1.03
Q-SV-VAR	0.56	0.56	0.56	0.76	0.76	0.76
	Unemployment rate					
MF-TVP-SV-VAR	**0.80***	**0.60****	**0.36*****	**0.74**	**0.54****	0.32**
MF-SV-VAR	0.83***	0.62***	0.38***	0.83**	0.59**	0.33**
MF-TVP-VAR	0.90	0.65**	**0.36*****	0.86	0.61**	**0.31****
MF-VAR	0.82***	0.61**	0.37***	0.80**	0.57**	0.32**
Q-TVP-SV-VAR	0.95	0.95	0.96	0.93	0.93	0.94
Q-TVP-VAR	1.01	1.01	1.01	1.01	1.01	1.02
Q-VAR	1.04*	1.04*	1.04	1.05	1.05	1.05
Q-SV-VAR	0.28	0.27	0.27	0.35	0.34	0.34

Notes: RMSEs are reported in absolute terms for the benchmark model (bottom row of each panel) and as ratios relative to the benchmark for the remaining models. A ratio below unity indicates that the model outperforms the benchmark. Bold figures indicate the best performance for the variable and information set. *, **, and *** denote significance at the 10%, 5%, and 1% level, respectively, according to the Diebold-Mariano test with Newey-West standard errors.

which is consistent with, for instance, Carriero et al. (2015b). Allowing for time-varying parameters without stochastic volatility improves accuracy relative to the benchmark but is—in most cases—inferior to models with stochastic volatility. Inflation nowcasts in turn benefit from combining both specifications.

2.5.2 Forecast evaluation

The results in Table 2.2 show that mixed-frequency VARs provide competitive forecasts even for higher horizons and for both samples.[12] In the case of the unemployment rate, modeling within-

[12]Since the marginal impact of an additional month of information becomes less important for forecasts at higher horizons, the RMSEs for higher horizons become similar across the information sets. For the forecast evaluation, we therefore compute total RMSEs by averaging over the entire forecast sample. Figure 9 in Appendix D plots the relative RMSE for each information set.

quarter dynamics is particularly beneficial—at each horizon even the worst performing mixed-frequency VAR outperforms the best performing quarterly VAR. Moreover, the results reveal that the models' forecast performance substantially differs across variables. The best relative performance, over all variables and horizons, is delivered by the MF-SV-VAR and the MF-TVP-SV-VAR; the corresponding RMSEs are roughly 10% lower than those of the benchmark.

Table 2.2: Real-time forecast RMSEs

	1990-2017			**2008-2017**		
Model	**h = 2**	**h = 3**	**h = 4**	**h = 2**	**h = 3**	**h = 4**
			GDP growth			
MF-TVP-SV-VAR	1.02	1.00	1.02	1.00	1.03	1.04
MF-SV-VAR	**1.00**	1.01	1.00	**0.97**	1.01	1.01
MF-TVP-VAR	1.09***	1.13***	1.05	1.08	1.19*	1.06
MF-VAR	1.13***	1.18***	1.16***	1.11***	1.18***	1.21***
Q-TVP-SV-VAR	1.06	**0.98**	1.01	1.10	1.03	1.02
Q-TVP-VAR	1.03	0.99	**0.97**	1.08	1.02	**0.97**
Q-VAR	1.14***	1.14***	1.13***	1.17***	1.17***	1.18***
Q-SV-VAR	0.66	0.66	0.68	0.84	**0.86**	0.86
			Inflation			
MF-TVP-SV-VAR	**0.81*****	0.84***	0.82***	**0.80*****	0.87***	0.91***
MF-SV-VAR	0.90**	0.89***	0.86***	0.86**	0.87***	**0.87*****
MF-TVP-VAR	0.93**	0.96**	0.93	0.97	1.05	1.11**
MF-VAR	0.98	1.09***	1.15***	0.92	1.02	1.06
Q-TVP-SV-VAR	0.84***	**0.83*****	**0.81*****	0.83***	**0.84*****	**0.87*****
Q-TVP-VAR	0.89***	0.89***	0.86***	0.92***	0.93***	0.94**
Q-VAR	1.08***	1.14***	1.22***	1.05**	1.10***	1.15***
Q-SV-VAR	0.63	0.64	0.64	0.89	0.87	0.78
			Unemployment rate			
MF-TVP-SV-VAR	**0.79*****	0.88**	0.95	**0.76****	0.85	0.95
MF-SV-VAR	0.86***	0.92**	0.95*	0.85**	0.91*	0.94
MF-TVP-VAR	0.83***	**0.87****	**0.89****	0.80**	**0.83****	**0.85****
MF-VAR	0.84***	0.91**	0.94*	0.83**	0.90*	0.93
Q-TVP-SV-VAR	1.00	1.04	1.08	0.98	1.04	1.09
Q-TVP-VAR	1.03	1.05	1.07	1.03	1.05	1.08
Q-VAR	1.03***	1.03***	1.03***	1.04***	1.04***	1.04***
Q-SV-VAR	0.48	0.71	0.93	0.65	1.00	1.33

Notes: RMSEs are reported in absolute terms for the benchmark model (bottom row of each panel) and as ratios to the benchmark model for the remaining models. A ratio below unity indicates that the model outperforms the benchmark. Bold figures indicate the best performance for the variable and horizon. *, **, and *** denote significance at the 10%, 5%, and 1% level, respectively, according to the Diebold-Mariano test with Newey-West standard errors.

For GDP growth, the benchmark is hard to beat. The MF-SV-VAR, the Q-TVP-VAR, and the Q-TVP-SV-VAR provide a better forecast performance for some horizons, albeit not statistically significant. For inflation, the Q-TVP-SV-VAR and the MF-TVP-SV-VAR deliver the best performance on average over all horizon, suggesting that time-variation in each coefficient is crucial for inflation forecasts. Thus, our results confirm the findings from previous studies based on quarterly models (see, among others, D'Agostino et al., 2013; Barnett et al., 2014; Faust and

Wright, 2013) by use of mixed-frequency models. Moreover, while the TVP-models' performance tends to deteriorate in the shorter sample, the SV-models' performance enhances, again providing evidence that stochastic volatility has gained importance in the shorter sample. For the unemployment rate, the MF-models consistently outperform the benchmark, while the quarterly models fail to do. Hence, the results provide evidence that both intra-quarterly dynamics and time-variation in the VAR-coefficients are particularly important.

In sum, the results are consistent with findings from previous studies, indicating that the gains in accuracy due to variations in the VAR-coefficients are smaller than the gains induced by stochastic volatility. However, using models with both features provides, on average over all variables, the most accurate forecasts. Finally, the results provide evidence that modeling within-quarter dynamics is beneficial also regarding short-term forecasts.

2.5.3 Comparison with survey-based forecasts

Since it is commonly found that survey-based forecasts are hard to beat (see, for example, Faust and Wright, 2013), we further assess the forecast performance of our MF-VARs relative to the forecasts provided by the SPF. To align the MF-VARs' information set with those of the SPF participants, we only resort to the forecasts from I2, providing 90 samples for the evaluation.[13]

Figure 2.3 depicts forecast errors of the MF-VARs relative to those of the SPF for the three variables. For GDP growth (left panel) and the unemployment rate (right panel), the SPF clearly outperforms each MF-VAR. The latter probably stems from the fact that survey participants consider a much broader information set than included in our small-scale VARs.[14] Regarding inflation, however, even small-scale MF-VARs provide very competitive nowcasts—each nonlinear specification slightly improves on the SPF, which itself is found to provide very accurate inflation nowcasts (Faust and Wright, 2013). For higher horizons, the SPF delivers more accurate inflation forecasts though. We moreover investigate whether the quarterly VARs' forecast performance can be improved by conditioning the latter on the SPF nowcasts.[15] Figure 2.10 in the Appendix 2.A.4 shows that this procedure indeed improves the Q-VARs' forecast accuracy. Overall, the gains are, however, small and die out quickly. In particular the MF-TVP-SV-VAR nevertheless provides very competitive predictions.

2.5.4 Predictive density evaluation

The results for the CRPS are displayed in Table 2.3. Overall, the results point to the usefulness of within-quarter information in delivering well calibrated predictive densities; the mixed-frequency models provide better results on average over all variables and horizons than their quarterly counterparts. The MF-TVP-SV-VAR provides the best performance with a reduction in CRPS

[13] The SPF participants' submission deadline for the first (second, third, fourth) quarter is the second to third week of February (May, August, November).

[14] For example, Brave et al. (2019) show that the forecast accuracy at medium-term horizons of a MF VAR with regard to GDP growth tends to improve with more information included in the model.

[15] Specifically, we estimate the Q-VARs until T_B, add the SPF nowcasts for T_{B+1}, and compute forecasts for T_{B+2} until $T_{B+h_{max}/3}$. Note that we do not update the coefficients given the SPF nowcasts. Alternatively, one could also use more sophisticated methods for utilizing external forecasts, for example, entropic tilting. For a comparison of methods to combine external and model-based predictions see Krüger et al. (2017).

Figure 2.3: Comparison of MF-VARs with Survey of Professional Forecasters

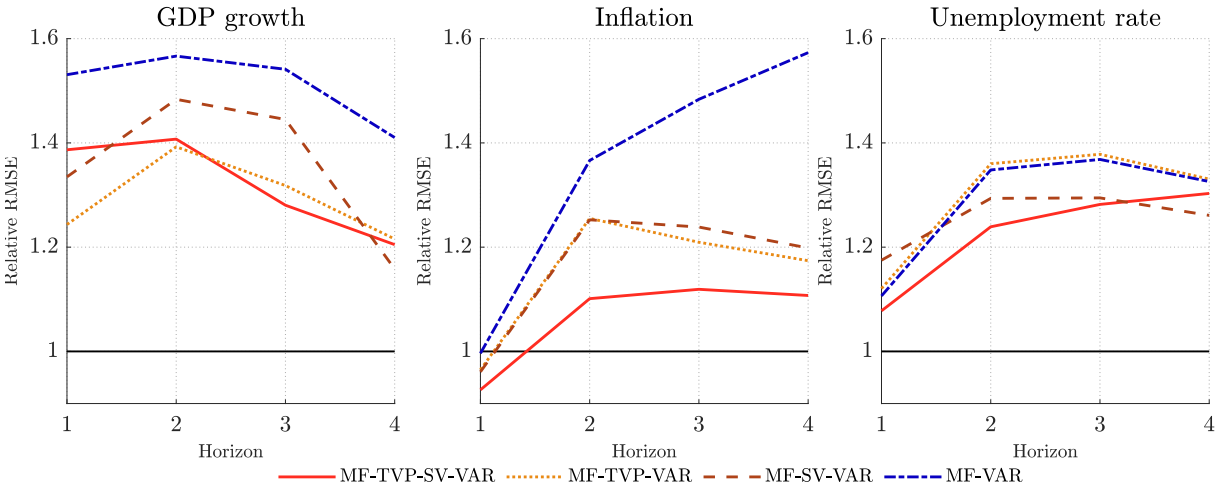

Notes: Comparison of MF-VAR forecasts with mean forecasts from the Survey of Professional Forecasters (SPF). GDP growth and inflation forecasts from MF-VARs are transformed into annualized rates. Figures below (above) unity indicate that the models provides smaller (larger) forecast errors than the SPF. Sample: 1990–2017.

of 19% followed by the MF-SV-VAR with 11% (on average over all variables and horizons). This emphasizes the importance of stochastic volatility for generating accurate predictive densities.

For GDP growth density forecasts, the benchmark is again difficult to beat—no model significantly improves on the benchmark. Only the MF-TVP-SV-VAR provides an (insignificant) improvement, although its points forecast are worse than those of the benchmark. Regarding inflation, the results indicate two outcomes. First, the Q-TVP-SV-VAR and the MF-TVP-SV-VAR deliver the largest (and significant) improvements on the benchmark. Hence, as for point forecasts, it is important to model time-variation in both the parameters and the residual variances to obtain precise predictive densities. Second, including time-variation in the parameters does play a vital role since both the MF-TVP-VAR and the Q-TVP-VAR offer strong improvements of roughly 10% over the benchmark.

For the unemployment rate, the results are different from the point forecasts evaluation. In this case, the MF-TVP-SV-VAR delivers the best performance, improving on the benchmark by up to 14% followed by the MF-SV-VAR with 11%. The MF-TVP-VAR, which provides very accurate point forecasts, in turn performs slightly worse with gains of up to 9%. Moreover and in contrast to inflation, each mixed-frequency model improves both on the benchmark and on its quarterly counterpart. Thus, it is crucial to include intra-quarterly information and stochastic volatility to generate precise predictive densities for the unemployment rate.

In summary, the results of the predictive density evaluation support the findings from the point forecast evaluation. Using mixed-frequency models is beneficial over all variables and horizons. It significantly improves results for inflation and the unemployment rate. In addition, we confirm the importance of stochastic volatility in density forecasting by use of mixed-frequency VARs. We provide evidence that combining stochastic volatility, time-varying parameters, and mixed-frequencies significantly improves the accuracy of predictive densities. However, for the

Table 2.3: Real-time forecast CRPS

Model	1990-2017 h = 2	h = 3	h = 4	2008-2017 h = 2	h = 3	h = 4
			GDP growth			
MF-TVP-SV-VAR	**1.00**	**0.95**	**0.97**	**0.94**	**0.90**	**0.90**
MF-SV-VAR	1.02	1.02**	1.01	0.97	1.01	1.02
MF-TVP-VAR	1.18***	1.39***	1.59***	1.21***	1.51***	1.85***
MF-VAR	1.15***	1.20***	1.19***	1.14***	1.24***	1.29***
Q-TVP-SV-VAR	1.02	0.96	1.00	1.02	0.95	0.96
Q-TVP-VAR	1.02	1.00	1.00	1.02	0.96	0.93
Q-VAR	1.17***	1.17***	1.15***	1.20***	1.22***	1.25***
Q-SV-VAR	0.35	0.36	0.37	0.37	0.38	0.39
			Inflation			
MF-TVP-SV-VAR	**0.80*****	0.81***	0.77***	**0.79*****	0.87**	0.87**
MF-SV-VAR	0.92*	0.95***	0.93***	0.81***	0.88**	0.89**
MF-TVP-VAR	0.88***	0.90**	0.85***	0.95	1.09	1.10
MF-VAR	0.98	1.12	1.16**	0.86**	1.01	1.02
Q-TVP-SV-VAR	0.83***	**0.80*****	**0.76*****	0.84***	**0.83*****	**0.83*****
Q-TVP-VAR	0.88***	0.86***	0.81***	0.91**	0.92**	0.88***
Q-VAR	1.11***	1.17***	1.23***	1.08**	1.13***	1.16***
Q-SV-VAR	0.31	0.33	0.35	0.40	0.39	0.39
			Unemployment rate			
MF-TVP-SV-VAR	**0.80*****	**0.86***	**0.91**	**0.80****	**0.86**	0.92
MF-SV-VAR	0.84***	0.91***	0.94***	0.82***	0.87**	**0.90****
MF-TVP-VAR	0.89**	0.92	0.94	0.87	0.89	**0.90**
MF-VAR	0.84***	0.89***	0.92***	0.83**	0.88**	0.91*
Q-TVP-SV-VAR	1.00	1.02	1.02	0.99	1.02	1.04
Q-TVP-VAR	1.06**	1.06	1.06	1.06	1.06	1.07
Q-VAR	1.03**	1.02	1.02	1.05	1.05	1.06*
Q-SV-VAR	0.24	0.36	0.47	0.27	0.41	0.55

Notes: The scores are reported in absolute terms for the benchmark model (the bottom row of each panel) and as ratios to the benchmark for the remaining models. A ratio below unity indicates that the model outperforms the benchmark. Bold figures indicate the best performance for the variable and horizon. *, **, and *** denote significance at the 10%, 5%, and 1% level, respectively, according to a t-test on the average difference in scores relative to the benchmark model with Newey-West standard errors.

inflation rate adding mixed frequency does not pay-off.

2.5.5 Forecasting during the Great Recession

So far we have demonstrated that modeling intra-quarterly dynamics, on average, significantly improves forecast accuracy. Now we take a closer look at the MF-models' absolute performance during the Great Recession, which is of great interest, because many structural and nonstructural models failed to provide accurate forecasts for the steep contraction and the following upswing in 2008/2009. Figures 2.4 and 2.5 depict real-time quarter-on-quarter CPI inflation and the unemployment rate (red lines) along with both the means (black lines) and 60% as well as 90% error bands (shaded areas) from the predictive distributions, respectively. The figures' columns refer to the data vintages of October 2008 until December 2008 and demonstrate how the arrival

Figure 2.4: Inflation forecasts during the Great Recession

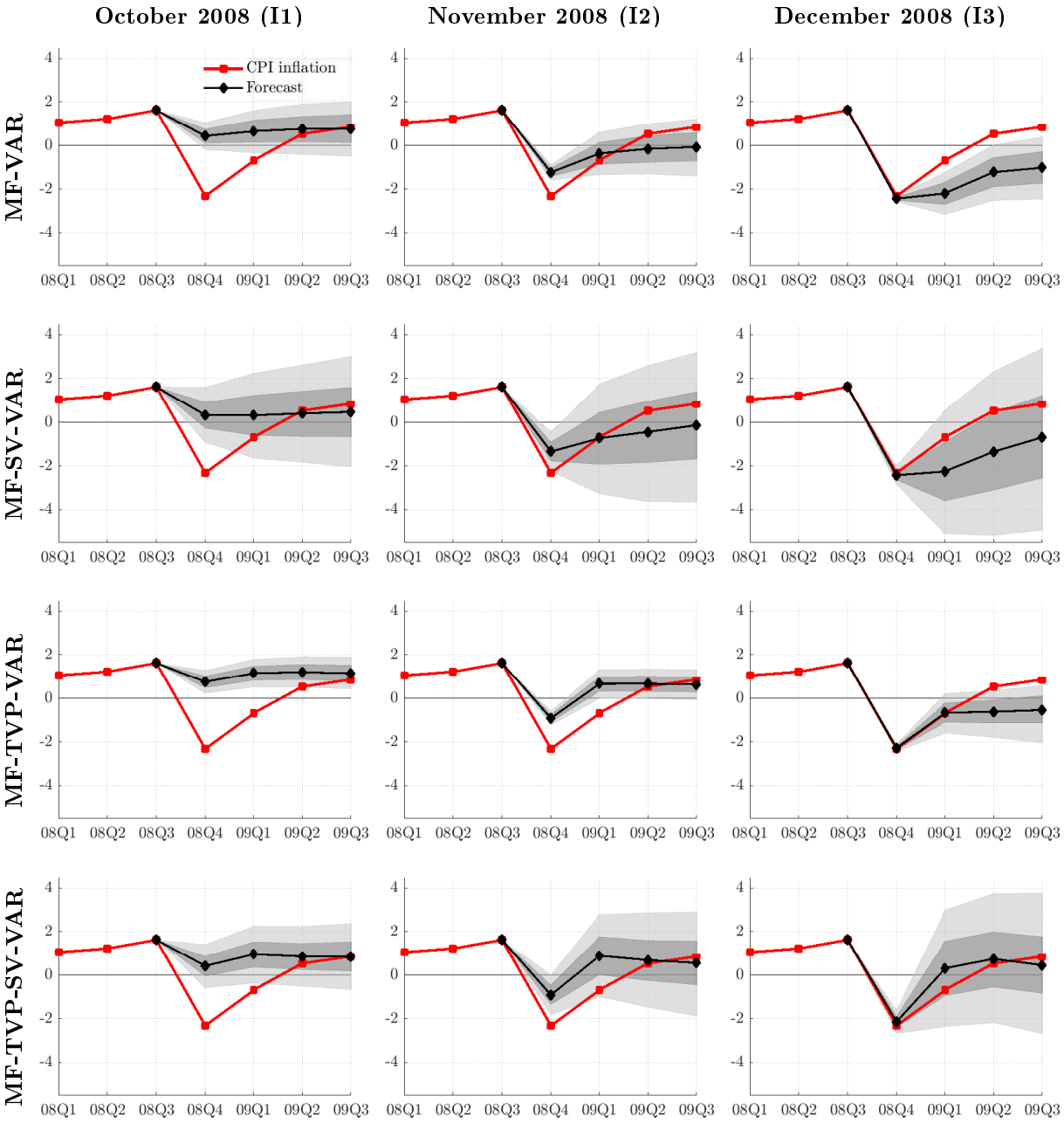

Notes: Rows refer to mixed-frequency models; columns refer to the forecast origins, i.e., the information sets. Red line indicates quarter-on-quarter real-time CPI inflation; black line is the mean of the predictive distribution. Shaded areas are 60% and 90% error bands from the predictive distributions.

of new data points affects the forecasts.

First, we consider the inflation forecasts computed with the vintage of October 2008 (first column). Note that in this month the models do not have any information on the current quarter except for the T-Bill rate of October. In October 2008, the models' posterior means are close to each other for each horizon—for the nowcast, all of them lie at roughly 0.5%, which is about three percentage points too high compared to the realization. The MF-VAR and the MF-TVP-VAR deliver narrow intervals, which assign only a small fraction of probability mass

Figure 2.5: Unemployment rate forecasts during the Great Recession

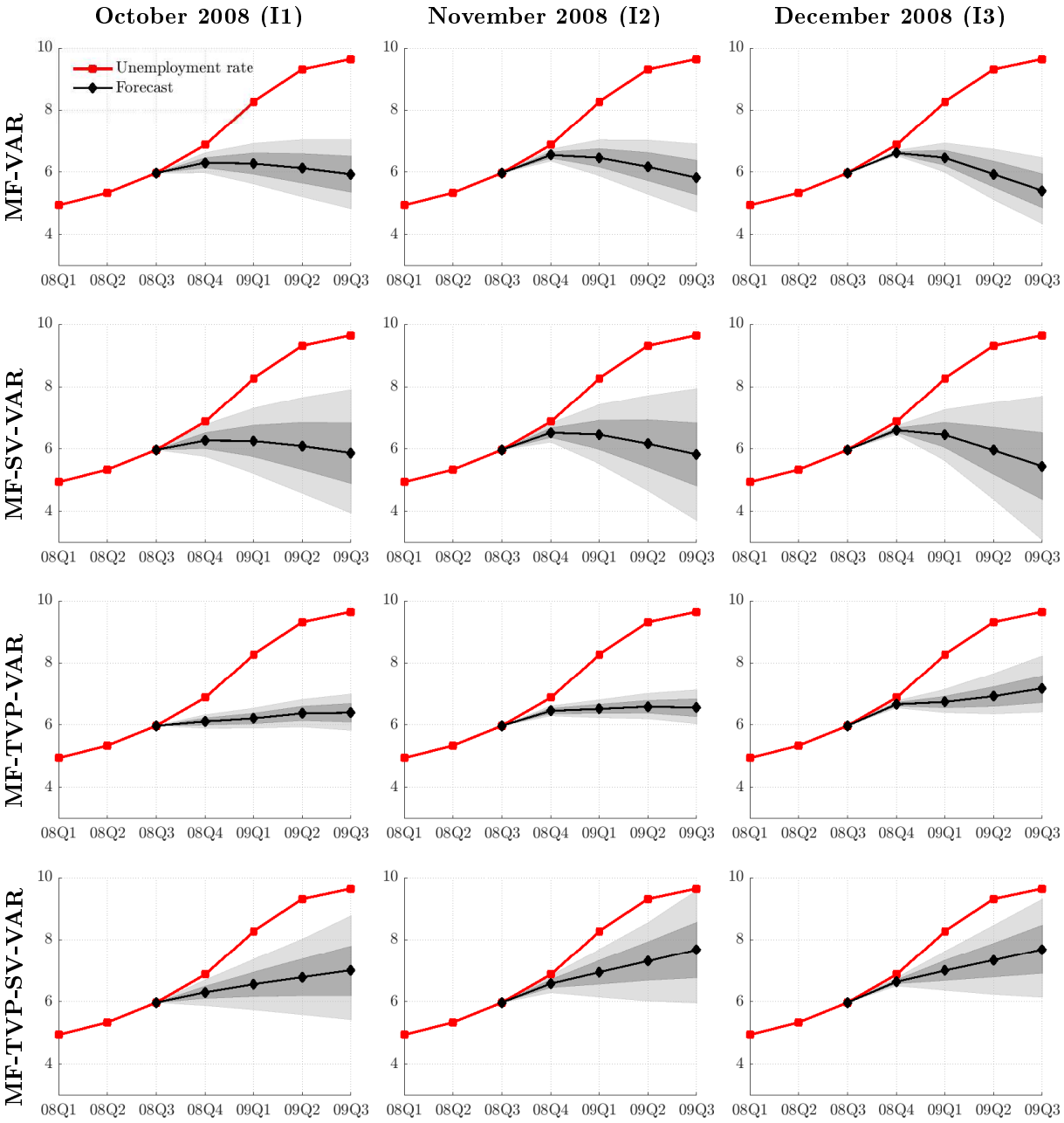

Notes: Rows refer to mixed-frequency models. columns refer to the forecast origins, i.e., the information sets. Blue line indicates quarter-on-quarter real-time unemployment rate; black line is the mean of the predictive distribution. Shaded areas are 60% and 90% probability bands from the predictive distributions.

to negative inflation rates. The MF-SV-VAR and the MF-TVP-SV-VAR in turn generate much wider intervals, clearly including negative inflation rates. However, the realization is not included in any interval. In November 2008, the posterior means are still similar, but become much more pessimistic. The models correctly anticipate a negative inflation rate for 2008Q4 (approx. -1%). Thus, as indicated in Section 2.5.1, the forecast errors become remarkably smaller due to the additional monthly observations. Moreover, while the constant coefficient VARs predict a slow recovery with negative inflation rates until 2009Q3, the TVP-VARs correctly anticipates

the recovery from 2009Q2 onward. In December 2008, the models produce a forecast error of almost zero for 2008Q4 with a narrow forecast interval. The subsequent recovery, however, is best predicted by the MF-TVP-SV-VAR. Driven by the pessimistic nowcasts, the remaining models forecast negative inflation rates for the entire forecast horizon. For the unemployment rate (Figure 2.5), the MF-TVP-SV-VAR also provides the best performance. While the 90% intervals do not contain the realizations for 2009Q1 until 2009Q3, only the VARs with time-varying coefficients predicts a prolonged increase in the unemployment rate. This increase in turn is more pronounced according to the MF-TVP-SV-VAR.

In summary, these results illustrate that the mixed-frequency models can translate intra-quarterly information into more precise point and density forecasts. Furthermore, this example supports the findings from Sections 2.5.1 and 2.5.2; it demonstrates the importance of combining stochastic volatility with time-varying parameters for accurate now- and forecasts.

2.5.6 Forecast combination

Instead of estimating a model that directly captures parameter instability, an obvious alternative is to estimate several models and generate forecasts using a combination of those. As shown by, for example, Clark and McCracken (2008), particularly forecasts from small-scale VARs can substantially benefit from this approach. Subsequently, we combine the forecasts from our models by applying both an equal-weighted combination scheme and the optimal prediction pool of Geweke and Amisano (2011). We derive the vector of optimal weights $\mathbf{w_t^{i,*}} = [w_{t,1}^i, \dots, w_{t,M}^i]'$ for variable i and M different models for each t by recursively minimizing the CRPS function:

$$\mathbf{w_t^{i,*}} = \underset{w_t^i}{\arg\min} \sum_{j=\tau+1}^{t} \left[\int_0^1 \text{QS}_\alpha \left(\sum_{m=1}^{M} w_{t,m}^i P_j(\alpha)^{-1}, y_j^i \right) \nu(\alpha) d\alpha \right], \tag{2.22}$$

$$\text{s.t.: } w_{t,m}^i \geq 0, \text{ for } \quad m = 1, \dots, M \quad \text{and} \quad \sum_{m=1}^{M} w_{t,m}^i = 1 \ \forall t, \tag{2.23}$$

where τ denotes a two-year warm-up sample. On the one hand, time-varying weights are highly informative regarding shifts in the relative forecast performance among a set of competing models (Pettenuzzo and Timmermann, 2017). On the other hand, changing weights can reflect important changes in the underlying economic structure (Del Negro et al., 2016).

Figure 2.6 displays the time-varying weights for $h=2$.[16] For GDP growth, a great deal of the total probability mass is assigned to the Q-SV-VAR and the Q-TVP-SV-VAR until the Great Recession hits the US economy. Thereafter, the MF-TVP-SV-VAR quickly gains importance by receiving a weight of roughly 50%, outweighing the Q-SV-VAR. For inflation, the MF-TVP-VAR obtains the largest weight until the Great Recession. Afterwards, the MF-TVP-SV-VAR receives the highest weight, confirming the results that parameter instability in each coefficient is important for inflation forecasts. Regarding the unemployment rate, Figure 2.6 confirms the findings from the previous sections; almost the entire probability mass is consistently assigned to MF-models with the MF-TVP-SV-VAR receiving the largest share the entire sample (about

[16] The figures for the remaining horizons look qualitatively similar and are available upon request.

Figure 2.6: Optimal prediction pools

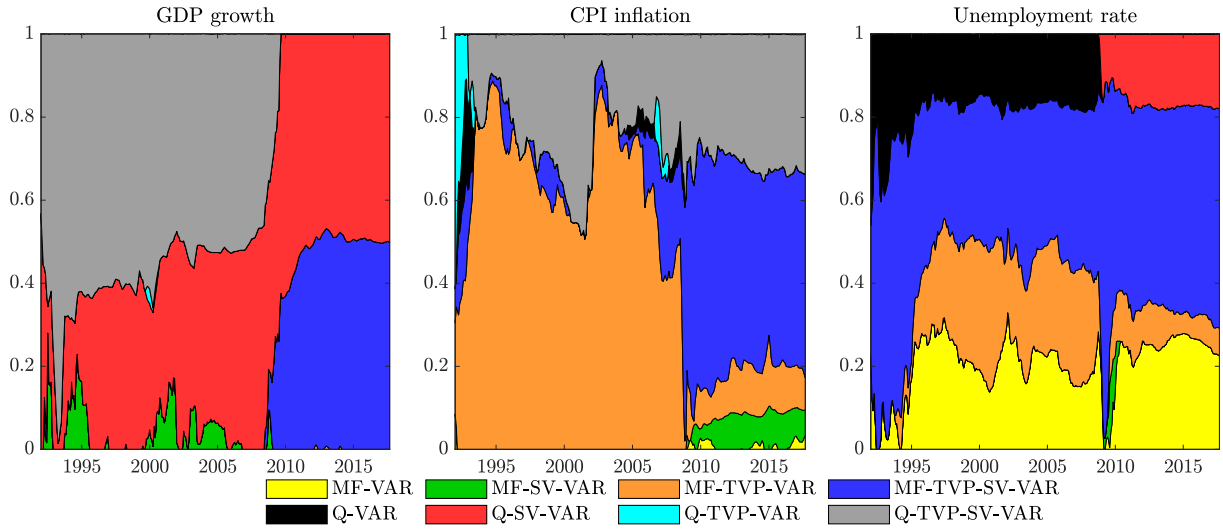

Notes: Probability weights for different models according to optimal prediction pool for $h = 2$. The weights are derived by recursively solving the minimization problem in (2.22).

40%). Thus, for each variable, the model that receives the largest weight at the end of the sample includes time-variation in both the VAR coefficients and the residual variances. Moreover, the MF-models' share at the end of the sample, is larger than those QF-models, supporting the importance of modeling intra-quarterly dynamics.

Table 2.4 depicts the point forecast performance of both combinations schemes relative to the benchmark model.[17] Both combination schemes provide strong gains in forecast accuracy across all variables and horizons. Notably, the optimal prediction pool outperforms the equal weighted average in almost each case, providing evidence that the increasing relevance of MF-models depicted by Figure 2.6 actually results in more precise forecasts. In the case of GDP growth, combining the forecast from MF and QF-VARs does not only (significantly) improve on the benchmark, but also on each individual model (see Table 2.2). At the one-year ahead horizon, the RMSE of the combined forecast is, on average 12% lower. For inflation, we find that combining the individual forecast does provide better results than those of the best performing models. In fact, the Q-TVP-SV-VAR provides a slightly better performance. Regarding the unemployment rate, combining forecasts from several VARs reduces the relative RMSEs with respect to the best performing individual model at each horizon with gains ranging from 4% to 8%.

2.6 Conclusion

Several studies show that modeling structural change improves forecast accuracy. We contribute to this discussion by investigating whether allowing for structural change in a mixed-frequency VAR setup further improves performance.

[17] The results regarding the density forecasts are qualitatively identical, which is why we do not report them. See Table 2.6 in the Appendix 2.A.3.

Table 2.4: Real-time forecast combination RMSEs

	1990-2017			2008-2017		
Combination scheme	**h = 2**	**h = 3**	**h = 4**	**h = 2**	**h = 3**	**h = 4**
	GDP growth					
Equal-weighting	0.95**	0.91***	**0.87*****	0.96	0.92**	**0.84*****
Optimal prediction pool	**0.93*****	0.88***	**0.88*****	**0.94**	**0.89***	0.85***
	Inflation					
Equal-weighting	0.86***	0.90***	0.88***	0.87***	0.91***	0.91***
Optimal prediction pool	**0.82*****	**0.84*****	**0.83*****	**0.84*****	**0.88*****	**0.90*****
	Unemployment rate					
Equal-weighting	0.81***	0.83***	0.84***	0.82	0.84*	0.85**
Optimal prediction pool	**0.75*****	**0.79*****	**0.81*****	**0.74**	**0.78***	**0.81****

Notes: RMSEs are reported as ratios to the benchmark. A ratio below unity indicates that the combination scheme outperforms the benchmark. Bold figures indicate the best performance for the variable and horizon. *, **, and *** denote significance at the 10%, 5%, and 1% level, respectively, according to the Diebold-Mariano test with Newey-West standard errors.

We conduct a rigorous real-time out-of-sample forecast experiment and generate predictions for GDP growth, CPI inflation, and the unemployment rate. Our findings show that modeling monthly dynamics substantially improves forecast accuracy. Nowcasts and short-term forecasts especially benefit from within-quarter information, while for longer horizons, the advantages vanish in most cases. The MF-TVP-SV-VAR provides, on average, the best point and density forecast performance. Both inflation and unemployment rate forecast benefit considerably from modeling both monthly dynamics and structural change. With regard to inflation, the MF-TVP-SV-VAR nowcasts are slightly more precise than those from the SPF. We obtain rather mixed results for the GDP growth; no model dominates over all horizons, though almost all nonlinear MF-models outperform their linear counterpart as well as the remaining quarterly models. Furthermore, we assess the forecast performance during the Great Recession and demonstrate how the inflow of monthly information alters inflation forecasts. We show that the combination of time-varying parameters and stochastic volatility yields overall the best performance for the downturn and subsequent recovery. Finally, using optimal prediction pools, we reveal the increased importance of the MF-VARs, notably the MF-TVP-SV-VAR, with the onset of the Great Recession, confirming the growing relevancy of modeling intra-quarterly dynamics and structural change.

Our models are small-scale VARs due to the large number of parameters that have to be estimated and our variables are rather standard in the literature. However, in the light of the recent developments regarding the usage of larger dataset for TVP-SV-VARs (Chan, 2019; Kapetanios et al., 2019; Petrova, 2019), our results suggest that introducing mixed-frequencies in these estimation procedures might lead to strong gains in nowcast accuracy.

2.A Appendix 2

2.A.1 Priors

For models with time-varying VAR coefficients, priors are based on a training sample, which consists of the first 8 years of the entire sample. In the following, variables denoted with OLS refer to OLS quantities based on the training sample. The length of the training sample is denoted by T_0.

AR-coefficients

For the benchmark VAR, we implement a diffuse Jeffrey's prior:

$$p(\beta, \Sigma) \propto |\Sigma|^{-(n+1)/2}. \tag{A.1}$$

For the nonlinear models, we use normal priors for the VAR-coefficients. To keep the models comparable with respect to the VAR coefficients, we choose an uninformative prior. In case of the Q-SV-VAR and the MF-SV-VAR, we employ the following prior:

$$p(\beta) \sim N\left(0, 1000 \times I_{k_\beta}\right). \tag{A.2}$$

For the TVP-models, we draw the VAR coefficients using the CK algorithm and initialize it with the following prior:

$$p(\beta_0) \sim N(0, 4 \times V(\hat{\beta}_{OLS})). \tag{A.3}$$

The prior for the covariance of the AR-coefficients ($Q = diag(q^2_{\beta_1}, \ldots, q^2_{\beta_{k_\beta}})$) follows an inverse-Wishart distribution:

$$p(Q) \sim IW(k_Q^2 \times T_0 \times V(\hat{\beta}_{OLS}), T_0). \tag{A.4}$$

Since we assume that Q is diagonal, this is equivalent to an inverse gamma prior for each element where k_Q is split into k_{Q_C} and $k_{Q_{AR}}$ for the intercepts and AR-coefficients, respectively.

Stochastic volatilities

The stochastic volatilities are drawn via the CK algorithm. Thus, additional priors for the diagonal elements of Σ_0 ($\log \sigma_0$), and the lower-triangular elements of A_0 ($a_{i,0}$) are required. We follow Primiceri (2005) in defining these prior distributions as:

$$p(\log \sigma_0) \sim N(\log \hat{\sigma}_{OLS}, I_n), \tag{A.5}$$

$$p(A_0) \sim N(\hat{A}_{OLS}, 4 \times V(\hat{A}_{OLS})). \tag{A.6}$$

The priors for the covariance of $\log \sigma_0$ and A_0 are inverse-Wishart distributed:

$$p(\Psi) \sim IW(k_\Psi^2 \times (1+n) \times I_n, 4), \tag{A.7}$$

$$p(\Phi_i) \sim IW(k_\Phi^2 \times (i+1) \times V(\hat{A}_{i,OLS}), i+1), \qquad i = 1, \ldots, k-1, \tag{A.8}$$

where i denotes the respective VAR-equation that has non-zero and non-one elements in the lower-triangular matrix A_t, i.e., for $n=4$ it is equation 2, 3, and 4.

Latent observations

The missing values of the quarterly series expressed at monthly frequency are replaced with an estimated latent state by applying a time-dependent CK algorithm. We initialize the unobserved state variable z_t with z_0 as actual observations from the monthly variables and constant values for the quarterly variables in levels from the last observations of our training sample:

$$p(z_0) \sim N(z_L, I_{np}). \tag{A.9}$$

Hence, $z_L = [\tilde{y}_0', \ldots, \tilde{y}_{0-p+1}']$ where $\tilde{y}_i$ contains actual values, if observed, and constant values in levels, thus zero growth rates, for missing observations.

Hyperparameters

The variability of β_t, a_t, and $\log \sigma_t$ depends on Q, Ψ, and Φ, respectively, and thus on the hyperparameters k_{Q_C}, $k_{Q_{AR}}$, k_Ψ, and k_Φ. Therefore, we follow Amir-Ahmadi et al. (2020) and use priors for those hyperparameters. Specifically, we employ an inverse gamma distribution with scale parameter and degrees of freedom equal to 0.1 and 2, respectively:

$$p(k_i) \sim IG(2, 0.1), \qquad i = Q_C, Q_{AR}, \Phi, \Psi. \tag{A.10}$$

This parameterization implies a loose prior with a mode of 0.05 and an infinite variance.

2.A.2 Specification of the Gibbs sampler

To estimate the models we employ a Gibbs sampler that consecutively draws from the conditional distribution. In the following, the general form of the MCMC algorithm according to Del Negro and Primiceri (2015) is outlined. To include the estimation of the hyperparameters, an additional Metropolis Hastings step is added to the Gibbs sampler. Denoting any vector of variables x over the sample T by $x^T = [x_1', \ldots, x_T']'$, the Gibbs sampler takes the following form:

1. Initialize β_t, Σ^T, A^T, s^T, Q, Ψ, Φ, k_Q, k_Φ, and k_Ψ.
2. Draw $\tilde{y}^T$ from $p(\tilde{y}^T | y^T, \beta^T, Q, \Sigma^T, A^T, \Psi, \Phi)$.
3. Draw β^T from $p(\beta^T | \tilde{y}^T, Q, \Sigma^T, A^T, \Psi, \Phi)$.
4. Draw Q from $p(Q | \tilde{y}^T, \beta^T, \Sigma^T, A^T, \Psi, \Phi)$.

5. Draw A^T from $p(A^T|\tilde{y}^T, \beta^T, Q, \Sigma^T, \Psi, \Phi)$.
6. Draw Φ from $p(\Phi|\tilde{y}^T, \beta^T, Q, \Sigma^T, A^T, \Psi)$.
7. Draw Ψ from $p(\Psi|\tilde{y}^T, \beta^T, Q, \Sigma^T, A^T, \Phi)$.
8. Draw s^T from $\tilde{p}(s^T|\tilde{y}^T, \beta^T, Q, \Sigma^T, A^T, \Psi, \Phi)$.
9. Draw Σ^T from $\tilde{p}(\Sigma^T|\tilde{y}^T, \beta^T, Q, A^T, s^T, \Psi, \Phi)$.
10. Draw k_{Q_C} from $p(k_{Q_C}|Q_C) = p(Q_C|k_{Q_C})p(k_{Q_C})$.
    Draw $k_{Q_{AR}}$ from $p(k_{Q_{AR}}|Q_{AR}) = p(Q_{AR}|k_{Q_{AR}})p(k_{Q_{AR}})$.
    Draw k_Ψ from $p(k_\Psi|\Psi) = p(\Psi|k_\Psi)p(k_\Psi)$.
    Draw k_ϕ from $\prod_{i=1}^{k-1} p(k_\Phi|\Phi_i) = p(\Phi_i|k_\Phi)p(k_\Phi)$.

The second step of this Gibbs sampler refers to drawing the latent observations. Since there are no latent observations in the quarterly models, the Gibbs sampler omits Step 2 for these models. Steps 3 to 8 belong to the block of drawing the joint posterior of $\tilde{p}(\theta, s^T|\tilde{y}^T, \Sigma^T)$ by drawing θ from $p(\theta|\tilde{y}^T, \Sigma^T)$ where $\theta = [\beta^T, A^T, Q, \Phi, \Psi]$. Subsequently, we draw s^T from $\tilde{p}(s^T|\tilde{Y^T}, \Sigma^T, \theta)$, and then Σ_t from $\tilde{p}(\Sigma_t|s^T, \theta)$. $\tilde{p}$ denotes the draws based on the approximate likelihood due to the KSC step, while p refers to draws based on the true likelihood (for further detail, see Del Negro and Primiceri, 2015). In Step 10, we include the Metropolis-Hastings within the Gibbs sampler to draw the hyperparameters.

For ease of exposition, in the following we use $\tilde{y}^T$ to indicate the data used in each step of the algorithm. If one considers quarterly models, however, $\tilde{y}^T$ has to be replaced by y^T. We employ 50000 burn-in iterations of the Gibbs sampler for each model and use every 4th draw of 20000 after burn-in draws for posterior inference.

Step 2: Drawing latent states z_t

Let $z_T = [z_1, \ldots, z_T]$ denote the sequence of state vectors consisting of the unobserved monthly states. Draws for z_t are obtained by using the CK algorithm, i.e., we run the Kalman filter until T to obtain $z_{T|T}$ as well as $P_{T|T}$ and draw z_T from $N(z_{T|T}, P_{T|T})$. Subsequently, for $t = T-1, \ldots, 1$ we draw z_t from $N(z_{t|t}, P_{t|t})$ by recursively updating $z_{t|t}$ and $P_{t|t}$.

Step 3: Drawing the AR-coefficient β^T

Conditional on the drawn states or the actual data, sampling the AR-coefficients proceeds as in Step 2 using the CK algorithm. In order to decrease computation time and efficiently simulate the draws, we apply the precision sampling approach by Chan and Jeliazkov (2009).

Step 4: Drawing the covariance of the VAR-coefficients Q

The posterior of the covariance of VAR-coefficients is inverse-Wishart distributed with scale matrix $\overline{Q} = Q_0 + e_t' e$, $e_t = \Delta\beta_t'$, and degrees of freedom $df_Q = T + T_0$, where Q_0 and T_0 denote the prior scale for Q and prior degrees of freedom, respectively.

Step 5: Drawing the elements of A^T

To draw the elements of A_T, we follow Primiceri (2005) and rewrite the VAR in (2.6) as follows:

$$A_t(\tilde{y}_t - Z_t'\beta_t) = \tilde{y}_t^* = \Sigma_t u_t, \tag{A.11}$$

where, taking into account that β_T and $\tilde{y}_t$ are known, y_t^* is observable. Due to the lower-triangular structure of A_t^{-1}, this system can be written as a system of k equations:

$$\hat{\tilde{y}}_{1,t} = \sigma_{1,t} u_{1,t}, \tag{A.12}$$

$$\hat{\tilde{y}}_{i,t} = -\hat{y}_{[1,i-1]} a_{i,t} + \sigma_{i,t} u_{i,t}, \qquad i = 2, \ldots, k, \tag{A.13}$$

where $\hat{\tilde{y}}_{[1,i-1]} = [\hat{\tilde{y}}_{1,t}, \ldots, \hat{\tilde{y}}_{i-1,t}]$. $\sigma_{i,t}$ and $u_{i,t}$ refer to the i-th elements of σ_t and u_t. Thus, under the block diagonal assumption of Φ, the RHS of equation i does not include $\hat{y}_{i,t}$, implying that one can recursively obtain draws for $a_{i,t}$ by applying an otherwise ordinary CK algorithm equation-wise.

Step 6: Drawing the covariance Φ_i of the elements of A^T

Φ_i has an inverse-Wishart posterior with scale matrix $\overline{\Phi}_i = \Phi_{0,i} + \epsilon_{i,t}'\epsilon_{i,t}$, $\epsilon_{i,t} = \Delta a_{i,t}'$, and degrees of freedom $df_{\Phi_i} = T + df_{\Phi_{i,0}}$ for $i = 1, \ldots, k$. $\Phi_{0,i}$, and $df_{\Phi_{i,0}}$ denote prior scale and prior degrees of freedom, respectively.

Step 7: Drawing the covariance Ψ of log-volatilities

As in Step 6, Ψ has an inverse-Wishart distributed posterior with scale matrix $\overline{\Psi} = \Psi_0 + \varepsilon_t'\varepsilon_t$, $\varepsilon_t = \Delta \log \sigma_t'^2$, and degrees of freedom $df_\Psi = T + df_{\Psi_0}$, where Ψ_0 and df_{Ψ_0} denote the prior scale and the prior degrees of freedom, respectively.

Step 8: Drawing the states of the mixture distribution s^T

Conditional on the volatilities, we independently draw a new value for the indicator matrix s^T from (see Kim et al., 1998):

$$PR(s_{i,t} = j|\tilde{y}^{**}, h_{i,t}) \propto q_j f_N(\tilde{y}^{**}|2h_{i,t} + m_j - 1.2704, \nu_j^2). \tag{A.14}$$

Step 9: Drawing the volatilities

The elements of Σ_t are drawn using the KSC algorithm. To this end, we employ the VAR rewritten as in (A.11). Taking squares and logarithms, we get

$$\tilde{y}_t^{**} = 2h_t + \nu_t, \tag{A.15}$$

and for the volatility process:

$$h_t = h_{t-1} + \varepsilon_t, \tag{A.16}$$

where $\tilde{y}_{i,t}^{**} = \log((\tilde{y}_{i,t}^*)^2 + c)$, $\nu_{i,t} = \log u_{i,t}^2$, $h_{i,t} = \log \sigma_{i,t}$, and c is set to a small but positive number to increase the robustness of the estimation process. To transform this

non-Gaussian system (ν_t is distributed according to a χ^2-distribution with one degree of freedom) into a Gaussian system, we resort to Kim et al. (1998) and consider a mixture of seven normal densities with component probabilities q_j, means $m_j - 1.2704$, and variances ν_j^2. The values for $\{q_j, m_j, \nu_j^2\}$ are chosen to match the moments of the log $\chi^2(1)$ distribution and given in Table 2.5.

Table 2.5: Gaussian mixtures for approximating the log-$\chi^2(1)$

ω	q_j	m_j	ν_j^2
1	0.0073	-10.1300	5.7960
2	0.1056	-3.9728	2.6137
3	0.0000	-8.5669	5.1795
4	0.0440	2.7779	0.1674
5	0.3400	0.6194	0.6401
6	0.2457	1.7952	0.3402
7	0.2575	-1.0882	1.2626

Kim et al. (1998).

Step 10: Drawing the hyperparameters $k_{Q_C}, k_{Q_{AR}}, k_\Psi$, and k_Φ

The prior hyperparameters of the scale matrix of the variance covariance matrix Q, Ψ, and Φ are drawn with a Metropolis within Gibbs step. Amir-Ahmadi et al. (2020) show that the acceptance probability for each draw i can be simplified to:

$$\alpha_{k_X}^i = min\left(\frac{p(X|k_X^*)p(k_X^*)q(k_X^*|k_X^{i-1})}{p(X|k_X^{i-1})p(k_X^{i-1})q(k_X^{i-1}|k_X^*)}, 1\right), \tag{A.17}$$

where $X = \{Q_C, Q_{AR}, \Psi, \Phi\}$. Q_C and Q_{AR} refer to the diagonal elements of Q with respect to the intercepts and AR-coefficients, respectively. $p(X|k_X^*)$ denotes the prior distribution of X, while $p(k_X^*)$ indicates the prior for the hyperparameter. $q(k_X^*|k_X^{i-1})$ labels the proposal distribution. We apply a random walk chain algorithm:

$$k_X^* = k_X^{i-1} + \xi_t, \qquad \xi_t \sim N(0, \sigma_{k_X}^2). \tag{A.18}$$

The standard deviation σ_{k_X} is adjusted according to the method proposed by Garthwaite et al. (2016):

$$\sigma_{k_X}^i = \sigma_{k_X}^{i-1} + c(\alpha^{i-1} - \alpha^*)/(i-1), \tag{A.19}$$

where $\alpha^* = 0.4$ is the target acceptance rate and $c = 1/[\alpha^*(1-\alpha^*)]$ is the optimal step size. We initialize k_X with the values used by Primiceri (2005), $k_Q = 0.01$, $k_\Psi = 0.1$, and $k_\Phi = 0.01$, and the standard deviation by $\sigma_{k_X} = 0.01$.

2.A.3 Additional results

Table 2.6: Real-time forecast combination CRPS

	1990-2017			2008-2017		
Combination scheme	**h = 2**	**h = 3**	**h = 4**	**h = 2**	**h = 3**	**h = 4**
	GDP growth					
Equal-weighting	1.01	0.93*	0.87***	0.95	0.90*	**0.81*****
Optimal prediction pool	**0.93***	**0.85*****	**0.86*****	**0.93*****	**0.86*****	0.83***
	Inflation					
Equal-weighting	0.89***	0.89***	0.83***	0.92**	0.87**	**0.77*****
Optimal prediction pool	**0.81*****	**0.79*****	**0.74*****	**0.83*****	**0.85*****	0.84***
	Unemployment rate					
Equal-weighting	0.82***	0.81***	0.80***	0.86***	0.84***	0.83**
Optimal prediction pool	**0.76*****	**0.77*****	**0.76*****	**0.77*****	**0.77*****	**0.77*****

Notes: The scores are reported as ratios to the benchmark. A ratio below unity indicates that the combination scheme outperforms the benchmark. Bold figures indicate the best performance for the variable and horizon. *, **, and *** denote significance at the 10%, 5%, and 1% level, respectively, according to a t-test on the average difference in scores relative to the benchmark model with Newey-West standard errors.

2.A.4 Additional figures

Figure 2.7: Time-varying parameters of the Q-TVP-SV-VAR

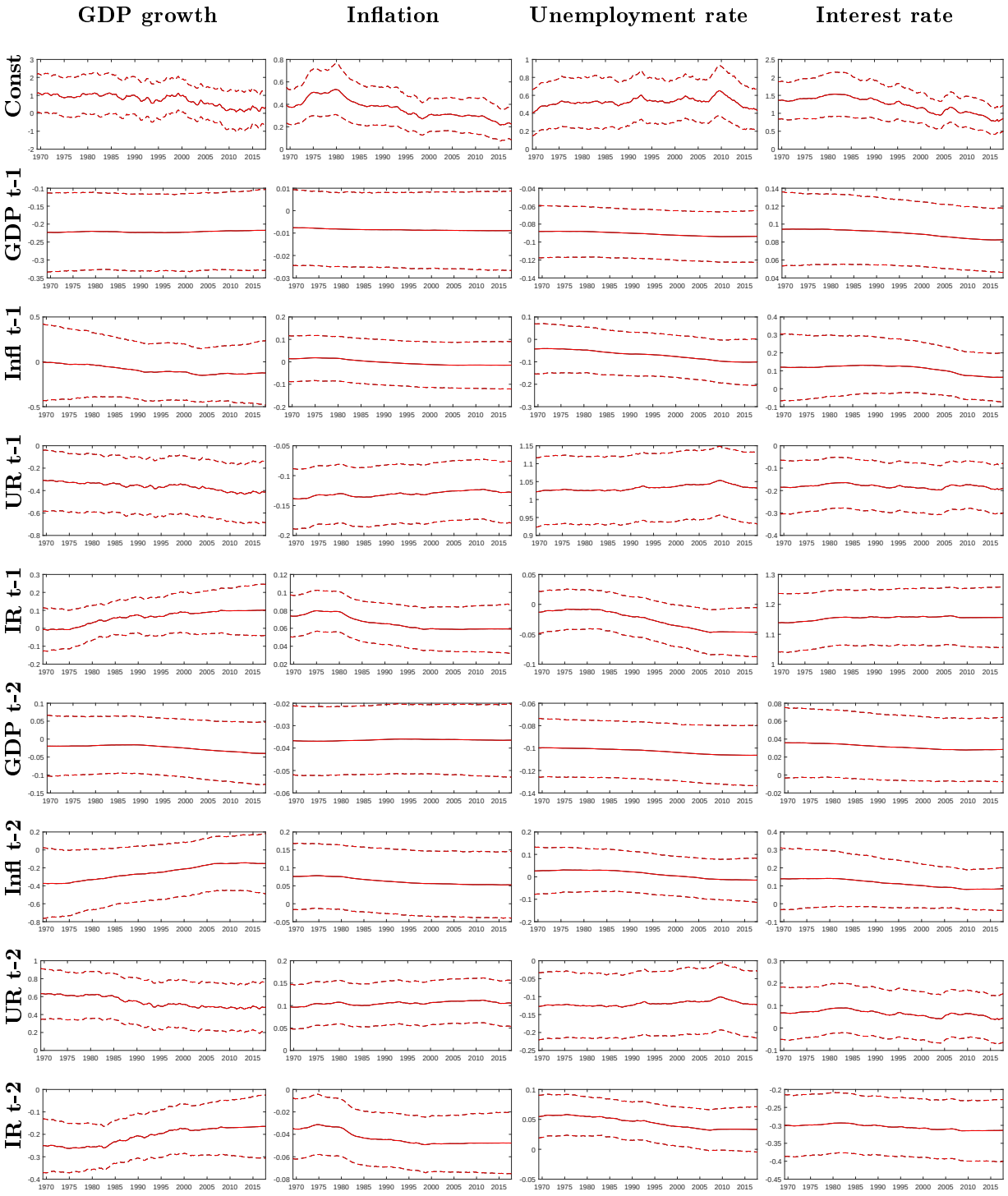

Notes: Figure depicts the time-varying parameters from the Q-TVP-SV-VAR. Columns refer to the variable and rows to the constant/lagged variable on which the variable is regressed. The dashed lines indicate 68% error bands. Results are based on the last data vintage

Figure 2.8: Time-varying parameters of the MF-TVP-SV-VAR

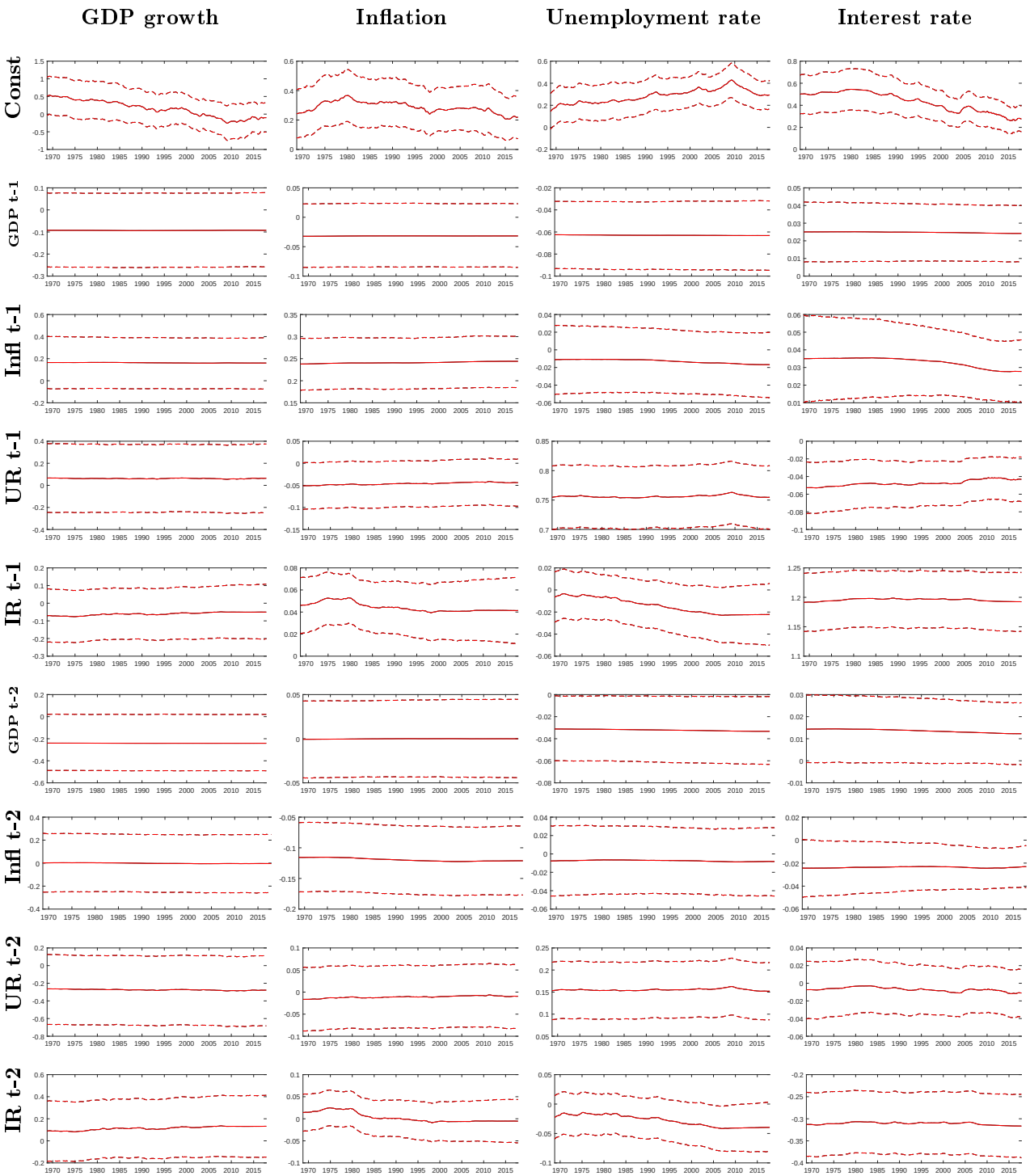

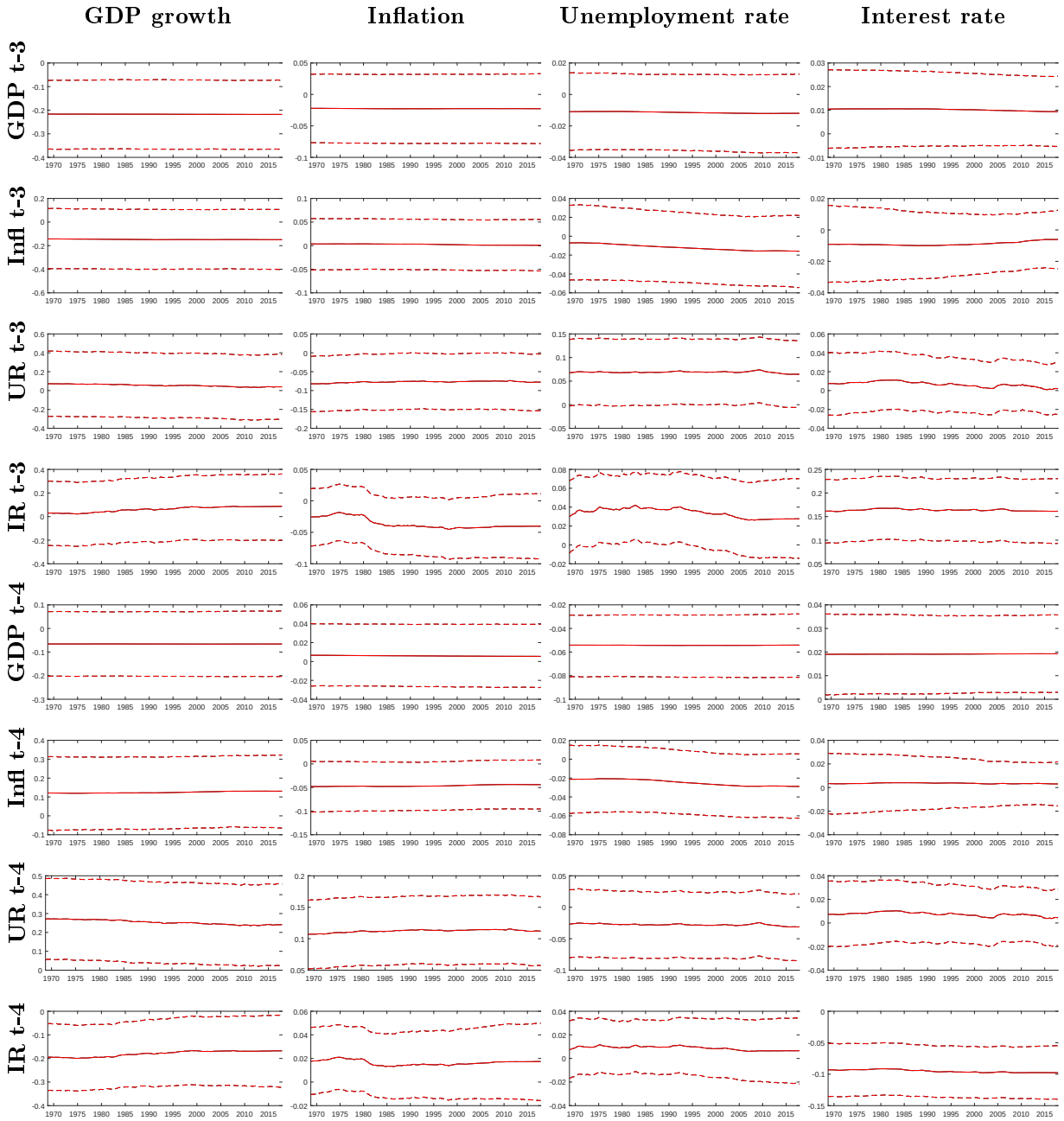

Notes: Figure depicts the time-varying parameters from the MF-TVP-SV-VAR. Columns refer to the variable and rows to the constant/lagged variable on which the variable is regressed. The dashed lines indicate 68% error bands. Results are based on the last data vintage.

Figure 2.9: Relative RMSEs

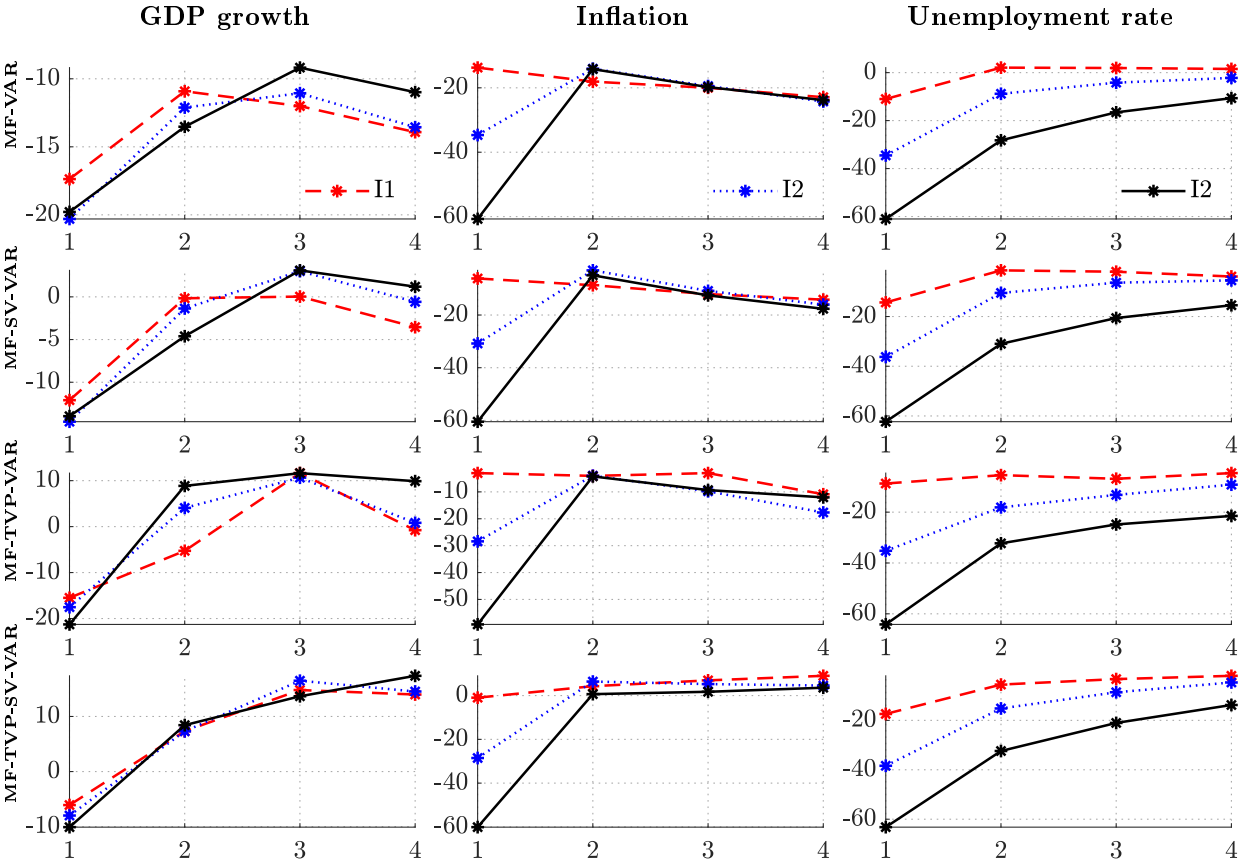

Notes: Figure depicts the relative RMSEs in terms of percentage gains compared to the benchmark model. Red, blue, and black lines refer to the information sets I1, I2, and I3 as outlined in Section 2.2, respectively. Sample: 1990–2017.

Figure 2.10: Comparison of model-based forecasts with Survey of Professional Forecasters

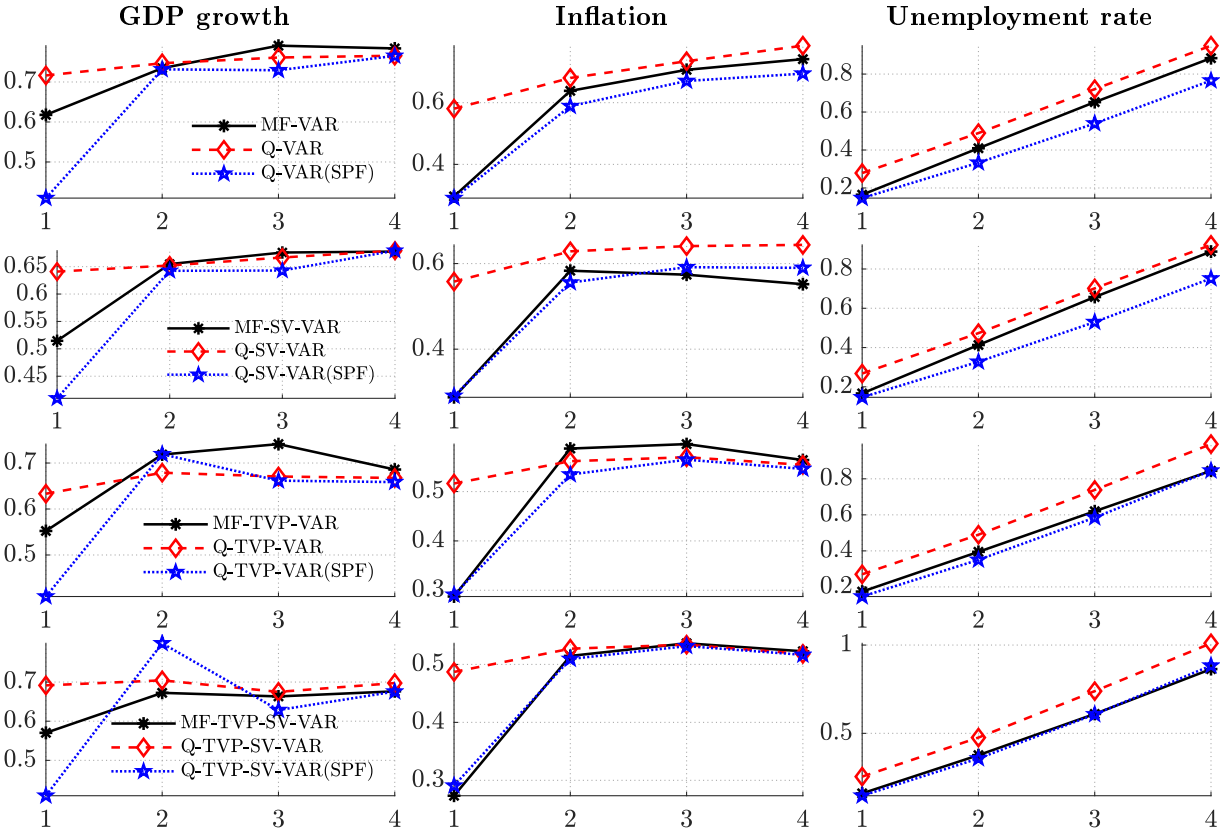

Notes: Figure depicts the RMSEs of the mixed-frequency VARs (solid lines), the quarterly VARs (dashed lines), and the quarterly VARs conditional on the SPF nowcasts (dotted lines) for the four horizons. To match the information set of SPF participants and models only forecasts from I2 are considered. Rows refer to models, columns refer to variables. Sample: 1990–2017.

Chapter 3

Does the Current State of the Business Cycle matter for Real-Time Forecasting? A Mixed-Frequency Threshold VAR approach.

Abstract

Macroeconomic forecasting in recessions is not easy due to the inherent asymmetry of business cycle phases and the increased uncertainty about the future path of the teetering economy. I propose a mixed-frequency threshold vector autoregressive model with common stochastic volatility in mean (MF-T-CSVM-VAR) that enables to condition on the current state of the business cycle and to account for time-varying macroeconomic uncertainty in form of common stochastic volatility in a mixed-frequency setting. A real-time forecasting experiment highlights the advantage of including the threshold feature for the asymmetry as well as the common stochastic volatility in mean in MF-VARs of different size for US GDP, inflation and unemployment. The novel mixed-frequency threshold model delivers better forecasts for short-term point and density forecasts with respect to GDP and unemployment– particularly evident for nowcasts during recessions. In fact, it delivers a better nowcast than the US Survey of Professional Forecasters for the sharp drop in GDP during the Great Recession in 2008Q4.

Keywords: Threshold VAR, Stochastic Volatility, Forecasting, Mixed-frequency models, Business Cycle, Bayesian Methods
JEL-Codes: C11, C32, C34, C53, E32

This study is a single-authored paper.
It is published as a Working & Discussion Papers Preprints, EconStor Direct.
`http://hdl.handle.net/10419/219312`

3.1 Introduction

Central banks, government agencies and the private sector turn to economic forecasts to gauge the current economic situation and future economic outlook. Having access to precise forecasts is crucial as a basis of decision-making. Making the right decision is particularly important in an uncertain and deteriorating economic environment, i.e. during the onset of a recession. Though, forecasts made at the beginning of recessions tend to err. Dovern and Jannsen (2017) uncover large systematic negative forecast errors made by professional forecasters for GDP growth during recessions. Chauvet and Potter (2013) reveal that forecasting GDP growth is generally more difficult in recessions than in expansions. In this paper I consider two potential reasons for these failures: First, insufficient good use of information about the current state of the business cycle in real time. Second, missing information about early business cycle indicators at a higher frequency than the variable to be predicted. The main contribution of this paper is to combine those two features into one novel model. Therefore, I set up a mixed-frequency threshold VAR with common stochastic volatility in mean (MF-T-CSVM-VAR) that simultaneously identifies the current state of the business cycle in real time and incorporates data with different frequencies.

Besides the significant benefits of mixed-frequency (MF) models that bear in mind frequency mismatches for forecasting, i.e. monthly indicators and quarterly GDP (see, i.e., Schorfheide and Song, 2015), a successful forecasting model needs to account for three well-documented business cycle characteristics. First, the business cycle can be characterized by the asymmetric dynamics in expansions and recessions. I model this asymmetry using the threshold feature by means of two distinct regimes within the VAR framework (T-VAR). This nonlinear VAR framework takes into account the nature of state dependent shock transmissions (see, i.e, Auerbach and Gorodnichenko, 2012; Caggiano et al., 2014; Mumtaz and Surico, 2015; Tenreyro and Thwaites, 2016). Second, business cycles can be characterized by co-movements among a broad range of different macroeconomic variables. Hence, I include a comprehensive business cycle index composed of a large data set as a predictor and threshold variable to identify the business cycle regimes in the T-VAR. And third, the business cycle often shares an increase (decrease) in macroeconomic uncertainty during recessions (expansions) as shown by, among others, Jurado et al. (2015). Clark (2011) and Clark and Ravazzolo (2015) point out the importance of time-varying volatilities for precise forecasts to account for changing uncertainty. On that account, I apply the concept of common stochastic volatility (CSV) as in Carriero et al. (2016) to account for the change in macroeconomic uncertainty over time. I add common stochastic volatility in the mean equation (CSVM) of the VAR as uncertainty can endogenously impact macroeconomic variables (see, i.e., Bloom, 2014; Carriero et al., 2018) and hence, can be beneficial for forecasting.

I stress the importance of considering these features of the business cycle for small and medium-scale MF-VARs in a real-time forecasting experiment on US GDP, inflation (CPI) and unemployment rate (UR). Overall, the nonlinear small-scale MF-T-VAR and MF-T-CSVM-VAR outperform their linear competitors on average across all variables and horizons. The best results are with regard to GDP and unemployment during recessions. The largest gains in relative forecast accuracy are during the steepest contraction in 2008Q4 during the Great Recession in which the MF-T-VAR even outperforms the GDP nowcast from the Survey of Professional

Forecasters (SPF). The medium-scale MF-CSVM-VAR performs best for forecast horizons two to four quarters ahead in which case it is quite competitive vis-á-vis the SPF for GDP. Accounting for macroeconomic uncertainty in form of CSVM generally contributes the most to density forecasts for all models and specifically to UR forecasts during recessions for small-scale models.

The novel fully-fledged MF-T-CSVM-VAR is based upon three extensions to the VAR which makes it flexible by switching on and off each feature as required. First is the MF-VAR in state-space form as in Schorfheide and Song (2015) to cope with unobserved low-frequency variables in mixed-frequency data.[1] Second is the T-VAR based on the Bayesian estimation algorithm proposed by Chen and Lee (1995). And third is the CSV based on Carriero et al. (2016) which additionally enters the mean equation as in Mumtaz and Theodoridis (2018). I utilize a Gibbs sampler to draw from each conditional posterior. Since VARs can suffer quite quickly from overparameterization and overfitting, I apply shrinkage in form of a Minnesota prior first proposed by Litterman (1986). I implement a flexible adaptive inverse-Gamma hyperprior on the overall and cross-variable shrinkage parameters. In case of regime dependent parameters, this prior setup allows for distinct shrinkage across regimes.

This paper adds to the literature on nonlinear forecast models in real time with a particular focus on mixed-frequency, the state of the business cycle, macroeconomic uncertainty and threshold VARs.[2] Alessandri and Mumtaz (2017) reveal a good forecasting performance of a T-VAR with financial condition regimes during the Financial Crisis 2008-2009. Reif (2020) shows improved forecasts with a T-VAR that includes a macroeconomic uncertainty index and conditions on periods of high and low uncertainty. Furthermore, Segnon et al. (2018) illustrate the importance of uncertainty on forecasting US GNP growth whereas Pierdzioch and Gupta (2019) highlight the predictive power of uncertainty on forecasting US recessions. In terms of informative content of the state of the business cycle, Chauvet and Potter (2013) and Carstensen et al. (2020) report an improved forecasting performance for AR models in recessions for horizons up to 2 quarters ahead that incorporate a business cycle factor and recession probabilities as predictors for US and German GDP, respectively. With regard to mixed-frequency and business cycle regimes, Bessec and Bouabdallah (2015) and Barsoum and Stankiewicz (2015) use univariate Markov-Switching models to account for the business cycle pattern in a mixed-frequency approach. They show that these models can accurately date the business cycle and forecast US GDP growth. Carriero et al. (2015b) reveal the benefits of stochastic volatility for forecasting in a mixed-frequency setup. Most closely related to my study in terms of nonlinear multivariate mixed-frequency models is the paper by Foroni et al. (2015).[3] They apply a Markov-Switching mixed-frequency bi-variate VAR for improved GDP forecasts. Yet, none of the contributions so far combine all of these beneficial features into one comprehensive model.

The remainder of the paper is structured as follows: Section 3.2 depicts the competing models and explains the estimation methodology. Section 3.3 provides a description of the data set and outlines the forecast setup. Section 3.4 presents the empirical results and Section 3.5 concludes.

[1] Foroni and Marcellino (2013) offer a detailed survey on different mixed-frequency methods.

[2] D'Agostino et al. (2013), Barnett et al. (2014), Ferrara et al. (2015) and Aastveit et al. (2017), among others, provide comprehensive comparisons of different nonlinear against linear models following the Great Recession.

[3] Götz and Hauzenberger (2018) and Heinrich and Reif (2020) combine mixed-frequency and time-varying parameter VARs, though this does not isolate the impact of the current state of the business cycle on forecasting.

3.2 Models

All models are estimated with Bayesian methods and can be written in state space form. The first subsection introduces the mixed-frequency (MF) block as the measurement equation which is necessary for all models. Subsequently, I present the different transition equations depending on the respective model. I start with the baseline MF-VAR followed by the common stochastic volatility in mean (CSVM). Finally, I extend the MF-VAR to the threshold VAR (MF-T-VAR) with and without CSVM. Thereafter, I describe the estimation algorithm and prior specifications.

3.2.1 Mixed-Frequency

The mixed-frequency block closely follows Schorfheide and Song (2015). Let y_t denote an $n \times 1$ vector of observable variables at monthly frequency t which is linked to the latent state vector z_t via the transformation matrix R_t:

$$y_t = R_t z_t \tag{3.1}$$

where the vector of variables is decomposed into $y_t = [y'_{q,t}, y'_{m,t}]'$ with n_q quarterly and n_m monthly variables. This vector contains missing values due to missing intra-quarterly values for $y_{q,t}$. Thus, a vector for one quarter is $[y_t\ y_{t-1}\ y_{t-2}]' = [[y'_{q,t}, y'_{m,t}]'\ [NaN', y'_{m,t-1}]'\ [NaN', y'_{m,t-2}]']'$ with missing values in month $t-1$ and $t-2$ of each quarter. The state vector includes p lags for the VAR. Hence, $z_t = [z'_{q,t}, z'_{m,t}]'$ is an $n(p+1) \times 1$ vector where $z_{q,t} = [\tilde{y}'_{q,t}, \ldots, \tilde{y}'_{q,t-p}]'$ is the unobserved quarterly variable at monthly frequency. $z_{m,t} = [y'_{m,t}, \ldots, y'_{m,t-p}]'$ is the vector of observed monthly variables.

The transformation from quarterly to monthly frequency is done according to a geometric mean of quarterly variables in levels $Y_{q,t}$ as in Mariano and Murasawa (2003):

$$Y_{q,t} = (\tilde{Y}_{q,t}\tilde{Y}_{q,t-1}\tilde{Y}_{q,t-2})^{1/3} \tag{3.2}$$

$$\Delta_3\, ln(Y_{q,t}) = y_{q,t} = (1/3\,\tilde{y}_{q,t} + 2/3\,\tilde{y}_{q,t-1} + \tilde{y}_{q,t-2} + 2/3\,\tilde{y}_{q,t-3} + 1/3\,\tilde{y}_{q,t-4}). \tag{3.3}$$

where the lower case denotes growth rates. R_t is a time-varying transformation matrix:

$$R_t = \begin{bmatrix} R_{1,t} & R_{2,t} \end{bmatrix}' \tag{3.4}$$

$$R_{1,t} = \begin{bmatrix} 1/3 * I_{nq} & 0_{nq\times n-1} & 2/3 * I_{nq} & 0_{nq\times n-1} & I_{nq} & 0_{nq\times n-1} & 2/3 * I_{nq} & 0_{nq\times n-1} & \ldots \\ 1/3 * I_{nq} & 0_{nq\times n-1} & 0_{nq\times (p-4)n} \end{bmatrix} \tag{3.5}$$

$$R_{2,t} = \begin{bmatrix} 0_{n-nq\times 1} & I_{n-nq} & 0_{n-nq\times pn} \end{bmatrix}. \tag{3.6}$$

The time variation in R_t follows Durbin and Koopman (2001) to deal with missing observations in y_t. If a variable is not observed at time t, the respective row in equation (3.1) is deleted and thus skipped in the respective estimation step of the Kalman filter.

3.2.2 Mixed-Frequency VAR

Conditional on the latent $\tilde{y}_{q,t}$, the $n \times 1$ vector $\tilde{y}_t = [\tilde{y}'_{q,t}, y'_{m,t}]'$ is modeled as a standard VAR with p lags, constant parameters and homoscedasticity:

$$\tilde{y}_t = A_0 + \sum_{l=1}^{p} A_l \tilde{y}_{t-l} + u_t \qquad u_t \sim \mathcal{N}(0, \Omega) \tag{3.7}$$

where A_0 is an $n \times 1$ vector of intercepts, A_l is $n \times n$ matrix of coefficients for $l = 1, \ldots, p$ and u_t denotes the $n \times 1$ error vector with a constant variance-covariance matrix Ω. The VAR(p) can be rewritten as a VAR(1) and completes the state space model with equation (3.1) for the MF-VAR:

$$z_t = C + A z_{t-1} + \upsilon_t \qquad \upsilon_t \sim \mathcal{N}(0, \Xi) \tag{3.8}$$

where $z_t = [\tilde{y}'_t, \ldots, \tilde{y}'_{t-p}]'$. C and A contain A_0 and $A_1, \ldots A_p$, respectively, in the first n rows for the VAR dynamics. Ξ contains Ω in the first n rows for the variance-covariance matrix.

3.2.3 Common stochastic volatility in mean

Common Stochastic Volatility (CSV) is based on Carriero et al. (2016). They exploit the finding that stochastic volatilities of different variables often share a comparable pattern. Thus, a single volatility factor is sufficient to capture the bulk of time variation in volatility. I extract a common factor f_t with loadings all restricted to one by decomposing the variance-covariance matrix of the error vector $u_t \sim \mathcal{N}(0, f_t \Sigma)$ from equation (3.7). The matrix Σ captures the difference in scaling among the variables and f_t accounts for the time-variation resulting in a time-varying variance-covariance matrix $\Omega_t = f_t \Sigma$.

This concept can be further enhanced by implementing CSV in the mean equation of the VAR (CSVM) :

$$\tilde{y}_t = A_0 + \sum_{l=1}^{p} A_l \tilde{y}_{t-l} + b h_{t-1} + \Sigma^{1/2} f_t^{1/2} \epsilon_t \qquad \epsilon_t \sim \mathcal{N}(0, I) \tag{3.9}$$

where $h_{t-1} = ln(f_{t-1})$ is the log volatility and $\Sigma^{1/2}$ is a lower triangular matrix such that $Var(u_t | f_t) = (\Sigma^{1/2} f_t^{1/2})(\Sigma^{1/2} f_t^{1/2})' = f_t \Sigma = \Omega_t$. h_t follows a random walk law of motion:

$$h_t = h_{t-1} + \varsigma_t \qquad \varsigma_t \sim \mathcal{N}(0, \phi) \tag{3.10}$$

which is, on the one hand, a parsimonious specification and on the other hand, as shown by Clark and Ravazzolo (2015), comparable in forecast accuracy to other specifications.

3.2.4 Mixed-frequency threshold VAR

The mixed-frequency Threshold VAR (MF-T-VAR) separates the linear VAR into different regimes, which in my case are expansions and recessions. The regimes are identified by a threshold variable y^*_{t-d} in form of a monthly business cycle index from the observed monthly vector

$y_{m,t}$, the delay parameter d and the respective threshold value r such that the VAR dynamics are modeled as follows:

$$\tilde{y}_t = A_{0,S_t} + \sum_{l=1}^{p} A_{l,S_t}\tilde{y}_{t-l} + \Sigma_{S_t}^{1/2}\epsilon_t \qquad \epsilon_t \sim \mathcal{N}(0, I) \tag{3.11}$$

$$\text{with } S_t = \begin{cases} 1 & \text{if } y^*_{t-d} \leq r \\ 2 & \text{otherwise.} \end{cases} \tag{3.12}$$

This model allows for different VAR coefficients $A_{0,S_t}, \ldots, A_{p,S_t}$ and variance-covariance matrix $Var(u_t) = \Sigma_{S_t}^{1/2}(\Sigma_{S_t}^{1/2})' = \Omega_{S_t}$ across regimes.

Furthermore, I extend the MF-T-VAR with common stochastic volatility in mean (MF-T-CSVM-VAR) such that equation (3.11) changes to:

$$\tilde{y}_t = A_{0,S_t} + \sum_{l=1}^{p} A_{l,S_t}\tilde{y}_{t-l} + b_{S_t}h_{t-1} + \Sigma_{S_t}^{1/2} f_t^{1/2}\epsilon_t \qquad \epsilon_t \sim \mathcal{N}(0, I) \tag{3.13}$$

and hence, $Var(u_t|f_t) = (\Sigma_{S_t}^{1/2} f_t^{1/2})(\Sigma_{S_t}^{1/2} f_t^{1/2})' = f_t\Sigma_{S_t} = \Omega_{t,S_t}$. On the one hand, the matrix Σ_{S_t} allows for different scalings across the regimes. On the other hand, the factor f_t grants time variation within the regime and permits feedback through the mean equation. Again, the law of motion for h_t follows a random walk as in equation (3.10).

Together with the measurement equation (3.1), the MF-T-CSVM-VAR(p) can be written down as a MF-T-CSVM-VAR(1) in state space form:

$$z_t = C_{S_t} + A_{S_t}z_{t-1} + B_{S_t}h_{t-1} + \upsilon_t \qquad \upsilon_t \sim \mathcal{N}(0, \Xi_{t,S_t}). \tag{3.14}$$

where $z_t = [\tilde{y}_t', \ldots, \tilde{y}_{t-p}']'$. C_{S_t} and A_{S_t} contain A_{0,S_t} and $A_{1,S_t}, \ldots A_{p,S_t}$, respectively, in the first n rows for the VAR dynamics. B_{S_t} contains b_{S_t} in the first n rows for the CSVM part. Ξ_{t,S_t} contains Ω_{t,S_t} in the first n rows for the time-varying variance-covariance matrix. A detailed description of the state space form of the MF-T-CSVM-VAR is in Appendix 3.A.1.

3.2.5 Prior specification and estimation

I estimate all VARs with an independent Normal-inverse-Wishart prior and impose Minnesota shrinkage on the VAR coefficients. This prior setup is more flexible compared to the dependent Normal-inverse-Wishart prior since the independence allows for cross-variable shrinkage in the variance component of the Normal prior amplifying forecast accuracy (see Carriero et al., 2015a). The prior mean on the first lag is 0 (0.9) if the respective variable is non-persistent (persistent) since all variables are transformed to be stationary (see Karlsson, 2013, for variations on the Minnesota prior). The prior variance for row j and column i of the coefficient matrix of lag l is set as follows:

$$Var(A_l^{j,i}) = \begin{cases} \frac{\lambda_1}{l^2} & \text{if } i = j \\ \frac{\lambda_1 \lambda_2 \sigma_{jj}^2}{l^2 \sigma_{ii}^2} & \text{if } i \neq j \\ \frac{\lambda_1 \lambda_3 \sigma_{jj}^2}{l^2 \sigma_{ii}^2} & \text{if } i \neq j \wedge j = y^* \\ 1000 & \text{if } l = 0 \end{cases} \tag{3.15}$$

where σ_{ii} is the residual standard error of an AR(p) for variable i. The amount of shrinkage is determined by the vector of hyperparameters $\Lambda = [\lambda_1, \lambda_2, \lambda_3]'$. λ_1 governs the overall and λ_2 the cross-variable shrinkage. Hence, it is assumed that lags on other variables contain less information compared to own lags if $\lambda_2 < 1$. Though, since the main concept of this paper is build around the importance of the business cycle, I apriori assume a stronger influence from the business cycle variables, namely the monthly BC index y^* and the log of the volatility factor h_t. Hence, I add λ_3 as an extra shrinkage parameter (denoted as BC shrinkage hereafter).[4] I facilitate regime-dependent shrinkage for the T-VARs to examine whether shrinkage is different in recessions and expansions. Thus, Λ is different across regimes Λ_{S_t} for $S_t = 1, 2$. The vector of shrinkage parameters is estimated using an inverse-Gamma hyperprior:[5]

$$p(\lambda_i) \sim \mathcal{IG}(\alpha, \beta_i) \qquad\qquad i = 1, 2, 3$$

with shape $\alpha = 0.1$ and scale $\beta_i = 0.044$ for $i = 1, 2$ and scale $\beta_i = \sqrt{0.044}$ for $i = 3$. I choose these values such that the prior is weakly informative and has a mode of 0.04 for $i = 1, 2$, which is in line with common values used for US data, and a mode of 0.2 which assigns apriori less shrinkage for the business cycle variables.[6]

The prior scale matrix for the inverse-Wishart is diagonal where the diagonal elements are the residual variances of ARs(p). The degrees of freedom are set to a minimum $n+2$ to resemble a rather loose prior. I follow Carriero et al. (2016) for the CSV by using an inverse-Gamma prior for the variance ϕ with mean 0.01 and scale 4. The stochastic volatility factor f_t has a Normal prior with mean 1 and variance 0.5. I fix $f_0 = 1$ for identification. I assume a uniform prior for the delay parameter $d \sim \mathcal{U}(1, p)$ as well as for the threshold parameter $r \sim \mathcal{U}(y_q^*, y_{1-q}^*)$, where $q = 0.10$ denotes the quantile of the threshold variable to avoid identification of outlier regimes instead of business cycle regimes. Further details on prior and initial values are given in Appendix 3.A.2.

I estimate the fully-fledged MF-T-CSVM-VAR with a Metropolis-within-Gibbs sampler. All the remainder models can be estimated by simply turning off the respective step within the

[4] A comparison between the standard cross-variable shrinkage $\lambda_3 == \lambda_2$ and the BC shrinkage $\lambda_3 \neq \lambda_2$ with respect to their point forecast accuracy is in Appendix 3.A.5, in which BC-shrinkage performs better.

[5] The concept of the Normal-inverse-Gamma mixture prior follows the idea of Geweke (1993) who shows that if $\alpha = \beta$, this is equivalent to a Student-t prior (see also Korobilis, 2013).

[6] See, e.g., Alessandri and Mumtaz (2017) for a T-VAR with overall shrinkage λ_1 and Carriero et al. (2015a) for the same value for cross-variable shrinkage λ_2. The mode of λ_3 is 5 times larger than the mode of λ_1 and λ_2 due to the importance of the monthly BC index for estimating the latent monthly GDP. The value approximately resembles the strong correlation between the BC index and GDP at quarterly frequency. This correlation is, depending on the data vintage, between 4 and 5.5 times larger than the second highest correlation for GDP.

sampler. The conditional MF part is estimated along the lines of Schorfheide and Song (2015) with a Kalman filter. The conditional T-VAR is based on Chen and Lee (1995). Hence, r is drawn with a random walk Metropolis-Hastings. The prior for λ_i is natural conjugate for the conditional posterior distribution and thus, follows an inverse-Gamma distribution. The draws for the stochastic volatility are carried out with the algorithm of Jacquier et al. (2002).[7] The MCMC sampler has 30000 draws. The first 25000 are burn-in draws while the last 5000 draws are for inference. The lag length is set to $p = 6$ as in the MF-VAR of Schorfheide and Song (2015). A detailed description of the sampler is in Appendix 3.A.3.

3.2.6 Predictive density

The predictive densities are simulated within the MCMC sampler. Let T denote the size of the respective real-time data vintage. Since real-time data contains ragged edges due to publication lags, the Kalman filter fills in missing values at the end of each vintage up to T. I apply iterated multistep forecasts $\tilde{y}_{T+h_m}$ for the remaining monthly forecast horizons $h_m = 1, \ldots, 12$, which are drawn at iteration s of the MCMC sampler for the MF-T-CSVM-VAR from:

$$p(\tilde{y}^{(s)}_{T+h_m} | \tilde{y}^{(s)}_{1:T+h_m-1}, \theta^{(s)}_{S_{T+h_m}}) \\ \sim \mathcal{N}(C^{(s)}_{S_{T+h_m}} + A^{(s)}_{S_{T+h_m}} \tilde{y}^{(s)}_{(T+h_m-p:T+h_m-1)} + b^{(s)}_{1,S_{T+h_m}} h^{(s)}_{T+h_m-1}, \Omega^{(s)}_{T+h_m,S_{T+h_m}}) \quad (3.16)$$

where $\tilde{y}_{1:T} = [\tilde{y}_1, \ldots, \tilde{y}_T]'$ and θ contains all remaining parameters of the model. For both T-VARs, the first forecast is conditional on the state S_t at time T and evolves according to equation (3.12) with respect to the threshold value $r^{(s)}$. I draw a sequence of $f^{(s)}_{T+h_m}$ common volatility factors for $h_m = 1, \ldots, 12$ according to the random walk law of motion as in equation (3.10) to forecast the time varying volatilities $\Omega^{(s)}_{T+h_m,S_{T+h_m}} = f^{(s)}_{T+h_m} \Sigma^{(s)}_{S_{T+h_m}}$.

3.3 Data and forecast setup

3.3.1 Data setup

The data set includes US real-time data covering March 1967 until December 2017 from the Archival FRED database and the FRED-MD monthly database provided by McCracken and Ng (2016). The historical vintages start in February 2001 up to December 2017. This provides a total of 203 vintages including the 2001 and 2008/09 recession for the real-time forecasting experiment. The target variables to be forecasted are Real Gross Domestic Product (GDP), the Unemployment Rate (UR) and the Consumer Price Index (CPI).

I distinguish between two variable sets with respect to size–a small-scale and a medium-scale set. Since GDP is in quarterly frequency, the small-scale set requires a monthly business cycle index to accurately estimate the intra-quarterly values of GDP. Here I distinguish between two indices. As a benchmark index, I choose Industrial Production (IP) as it is generally considered

[7] This algorithm draws f_t date by date for $t = 1, \ldots, T$ instead of in one block as in Kim et al. (1998). Hence, it can accommodate the stochastic volatility in mean.

to be good predictor for GDP (see, i.e., Foroni et al., 2015; Brave and Butters, 2010). Since the business cycle is characterized by co-movements among a broad range of different macroeconomic variables, I utilize the Chicago Fed National Activity Index (CFNAI) as a more comprehensive business cycle index. The index is based on the first principle component from a data set containing 85 monthly macroeconomic variables. I choose this index for three reasons. First, the index allows for accurately classifying the economy into recessions and expansions (see, i.e., Berge and Jorda, 2011; Brave, 2009) and hence, can be used as a threshold variable in equation (3.12). Second, it is good for nowcasting GDP (see Brave and Butters, 2014). And third, it starts quite early in March 1967, is in monthly frequency and the real-time data vintages are publicly available since February 2001. As the index neither cover interest rates nor stock market data, I additionally include in both small-scale sets the yield spread (YS), measured as the difference between the 10-year and the 3-month treasury bill rate, and the S&P 500 index. Both variables are good predictors for the business cycle (see, i.e., Chauvet and Potter, 2005; Liu and Moench, 2016) as well as for the target variables (see, i.e., Estrella and Mishkin, 1997; Estrella, 2005; Evgenidis et al., 2020). Hence, the two small-scale sets include GDP, CPI, UR, YS, S&P 500 and IP or CFNAI as a business cycle index.

The medium scale set is based on the evidence in the literature that medium-scale VARs in many cases outperform small-scale VARs (see, i.e., Bańbura et al., 2010; Koop, 2013). Carriero et al. (2019) shown that large-scale VARs in many cases do not outperform medium-scale VARs with 13-14 hand-picked variables. Hence, I append the small-scale set with two important variables from each of the four categories of the CFNAI–namely, 1) production and income, 2) labour market, 3) personal consumption and housing and 4) sales, orders and inventories–in exchange for the CFNAI.[8] This provides me with 13 variables for the medium-scale set and allows to analyse whether the CFNAI index alone or the individual variables are crucial for precise forecasts. These variables are Industrial Production, Capacity Utilization, Average Weekly Hours, All Employees-Total Nonfarm, Housing Starts, Real Personal Consumption Expenditures, Real Manufacturing and Trade Sales and New Orders Durable Goods. This variable set is quite standard for medium-scale VARs for US data and is similar to data sets of other US studies (see, i.e., Schorfheide and Song, 2015; Carriero et al., 2016, 2019).

All variables are transformed to be stationary. The CFNAI is taken as a real-time three month moving average to filter out some of the volatility since it is shown to better reflect the business cycle. Table 3.1 provides a quick overview about the included variables in each set. A full list of all variables with the respective transformation and source is in Appendix 3.A.6.

[8] The importance is measured in terms of factor loadings in the principle component analysis. Furthermore, the choice is also based on availability in real time over the time span February 2001 - December 2017. A full list of all monthly indicators and their loadings can be found here: `https://www.chicagofed.org/~/media/publications/cfnai/background/cfnai-background-pdf.pdf`.

Table 3.1: Sets of Variables

	Small Benchmark^b	Small	Medium^{med}
GDP	x	x	x
CPI	x	x	x
Unemployment Rate	x	x	x
Yield Spread	x	x	x
S&P 500	x	x	x
CFNAI		x	
Industrial Production	x		x
Capacity Utilization			x
Average Weekly Hours			x
Employment			x
Housing Starts			x
Consumption			x
Manufacturing & Trade Sales			x
New Orders Durable Goods			x

Notes: For the remainder, a model M with a medium variable set is denoted by M^{med} and the benchmark model with M^b. A list of the data with source and transformation can be found in Appendix 3.A.6.

Combining the data sets with the different models described in Section 3.2, I analyse a total of seven models for the forecasting experiment:[9]

1. MF-VAR^b: Mixed-frequency VAR (small benchmark)
2. MF-VAR: Mixed-frequency VAR (small)
3. MF-CSVM-VAR: Mixed-frequency VAR with common stochastic volatility in mean (small)
4. MF-T-VAR: Mixed-frequency threshold VAR (small)
5. MF-T-CSVM-VAR: Mixed-frequency threshold VAR with common stochastic volatility in mean (small)
6. MF-VAR^{med}: Mixed-frequency VAR (medium)
7. MF-CSVM-VAR^{med}: Mixed-frequency VAR with common stochastic volatility in mean (medium)

3.3.2 Forecast setup

I apply an expanding window to the 203 real-time data vintages from February 2001 until December 2017. Since GDP is in quarterly frequency, all forecasts are evaluated at $h = 1, \ldots, 4$ quarters

[9] Due to the nonlinearity, T-VARs become quite tedious and time-consuming to estimate with increasing scale. Hence, I do not include medium-scale T-VARs.

ahead which relates to the quarterly averages of monthly forecast $h_m = 1, \ldots, 12$. Monthly GDP is taken in quarterly growth rates via the transformation matrix R_t in equation (3.4). Hence, in the end I obtain quarterly averages of monthly GDP in quarterly growth rates, quarterly averages of monthly CPI inflation and quarterly averages of monthly unemployment rates as final forecast values.

The timing and availability of the data is vital since forecasts are made in real time. I assume that forecasts are made at the end of each month as the CFNAI is published in the last week of the month and is crucial for the estimation of the threshold VAR. The forecaster has only the information at its disposal as in real time. Thus, the data set includes so called "ragged edges" due to publication lags and data revisions. Only the yield spread and the S&P 500 are available without a lag. All other variables have a publication lag according to the ALFRED and Fred MD real-time data base.

The timing is crucial for $h = 1$ which constitutes a nowcast as it refers to the quarter in which the forecast is made. Lets take for example the real-time data vintage 2008M2 for nowcasting 2008Q1. The publication lags at the end of the vintage for January to February 2008 are filled with forecasts by the Kalman Filter, while the forecast for March 2008 is simulated by equation (3.16) for $h_m = 1$. Thus, the quarterly nowcast $h = 1$ is an average of January, February and March, where January and February are from the Kalman Filter and March from forecast $h_m = 1$. The decomposition of the nowcast in data vintage 2008M1 and 2008M3 in Kalman filter predictions and predictions simulated by equation (3.16) is analog.

3.4 Results

This section starts with a brief presentation of the in-sample and out-of-sample results concerning the regime identification of the MF-T-CSVM-VAR.[10] Next, I show in-sample results with respect to shrinkage and common stochastic volatility. After that, I present the results from the out-of-sample forecasting experiment. The forecast accuracy is evaluated with respect to point and density forecasts. Additional to the full sample, I analyse the forecast accuracy conditional on recession and expansion subsamples. Furthermore, I compare the nowcast accuracy against the Survey of Professional Forecasters with a special focus on the Great Recession.

3.4.1 Regimes

The important feature of T-VARs is the ability to separate samples into different regimes in a data driven manner defined by the threshold variable. Figure 3.1a depicts the Chicago Fed National Activity Index along with the estimated threshold r and the regime $S_t = 1$ for the final data vintage 1967M4-2017M12. The state $S_t = 1$ clearly identifies a recession regime as it closely matches the NBER recessions. Furthermore, the threshold value of -0.59 is similar to the one found in Berge and Jorda (2011) with -0.72 and thus confirms the good ability of the CFNAI for classifying economic activity into recessions and expansions.

[10] Results for the MF-T-VAR are quantitatively similar and available upon request.

Figure 3.1: Chicago Fed National Activity Index and threshold regimes

(a) In-sample

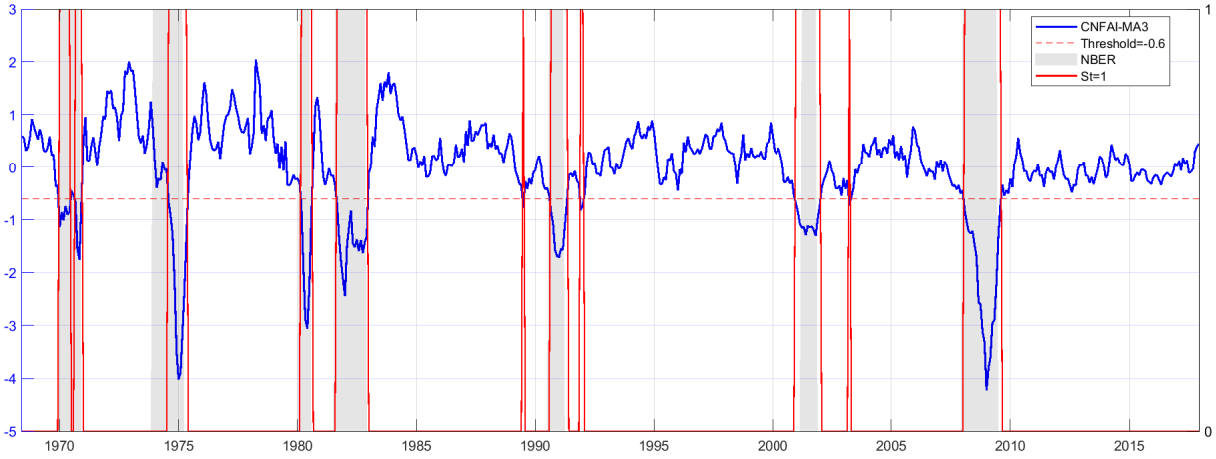

(b) Out-of-sample

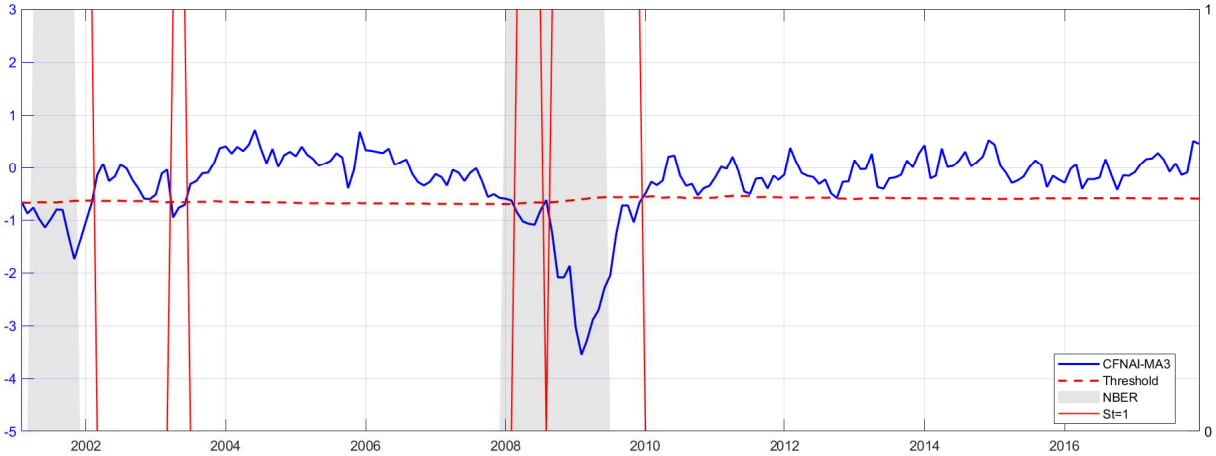

Notes: Panel (a) corresponds to the in-sample estimation of the final data vintage 1967M4-2017M12. Panel(b) corresponds to the real-time recursive out-of-sample nowcasts 2001M2-2017M12. Hence, each point t on the x-axis corresponds to the information set as of period t. The solid and the dashed red line denote the mode and mean of the posterior densities of the recession regime $S_t = 1$ and the threshold value r, respectively. The blue solid line displays the three-month-moving average of the Chicago Fed National Activity Index. Shaded areas correspond to the recessions dated by the NBER.

Since the CFNAI includes monthly economic indicators, which are prone to revisions, Figure 3.1b displays the real-time out-of-sample nowcast results for the regimes together with the time varying threshold value r over the expanding recursive out-of-sample 2001M2-2017M12. The threshold value is quite stable over time. It starts at roughly -0.7 and remains around that value in the first part of the out-of-sample period. After that, it increased slightly to approximately -0.6 right after the Great Recession in 2009. Overall, the real-time estimates significantly differ to the final estimates only in three occasions–the beginning and the end of the Great Recession and the 2008M8 vintage. These differences are due to revisions. The onset of the Great Recession as well as the short recovery in 2008M8 have been revised downwards quite heavily at a later vintage. Furthermore, the Great Recession regime prevails 6 month longer out-of-sample compared to

only 2 month longer in-sample. Again, this is evident in data revisions as the index has been revised upwards at a later stage. In summary, the CFNAI is able to accurately and timely date the business cycle in-sample and out-of-sample.

3.4.2 In-sample results

Table 3.2 displays the posterior mean of the shrinkage parameters. According to equation (3.15), a lower value for λ_i is associated with stronger shrinkage. Four points deserve to be stressed here. First, the amount of shrinkage increases with model size as in Bańbura et al. (2010). Second, there is strong cross-variable shrinkage which is in line with Carriero et al. (2015a). Third, the shrinkage for the business cycle variables, CFNAI and CSVM, is less than for the remaining variables. This is a first indication of the importance of those variables for accurate forecasts. And fourth, there is a stronger overall shrinkage and less cross-variable shrinkage in the recession regime implying that information emerging from other variables can be crucial for forecasts during recessions where information coming from their own past is more important in expansions.

Table 3.2: Shrinkage

		MF	MF-CSVM	MF-T	MF-T-CSVM	MF^{med}	MF-$CSVM^{med}$	MF^{b}
		Overall, Cross-Variable and BC Shrinkage						
λ_1	$S_t = 1$	0.275	0.181	0.131	0.069	0.112	0.120	0.096
	$S_t = 2$			0.208	0.162			
$\lambda_1\lambda_2$	$S_t = 1$	0.005	0.002	0.007	0.003	0.003	0.002	0.010
	$S_t = 2$			0.003	0.002			
$\lambda_1\lambda_3$	$S_t = 1$	0.028	0.016	0.038	0.016	-	0.042	-
	$S_t = 2$			0.035	0.015			

Notes: λ_i refers to posterior mean and $\lambda_i\lambda_j$ to posterior mean of the product. A larger value implies less shrinkage. Since the medium-scale MF^{med} and benchmark MF^{b} do neither contain the CFNAI index nor the CSVM, they do not include any BC shrinkage via λ_3. $S_t = 1$ identifies the recession regime.

Figure 3.2 shows the common stochastic volatility for the final vintage for the MF-CSVM-VAR and the MF-T-CSVM-VAR. Both models show qualitatively similar results. Though, the values for the MF-T-CSVM-VAR are somewhat smaller during recessions since the model accounts for the difference in scaling across business cycle regimes due to $\Sigma_1 \neq \Sigma_2$ in equation (3.13). Up to 1987 one can observe a period of high volatility with its peak around the recession 1980-1981. The prolonged period of low volatility from 1987 until 2007 is referred to as the Great Moderation. The Great Recession induce another strong increase in volatility around 2008/2009 followed by a subsequent slow-down to levels similar to the Great Moderation. This supports the finding of Clark (2009) that the Great Recession only interrupts the Great Moderation, but does not end it. Overall, the pattern closely follows the macroeconomic uncertainty index by Jurado et al. (2015). Hence, the volatility factor corresponds closely to the macroeconomic uncertainty

which spikes upwards in most recessions. This pattern is also well reflected in the volatility of the monthly GDP estimates (see Figure 3.6 in Appendix 3.A.4).

Figure 3.2: Common stochastic volatility

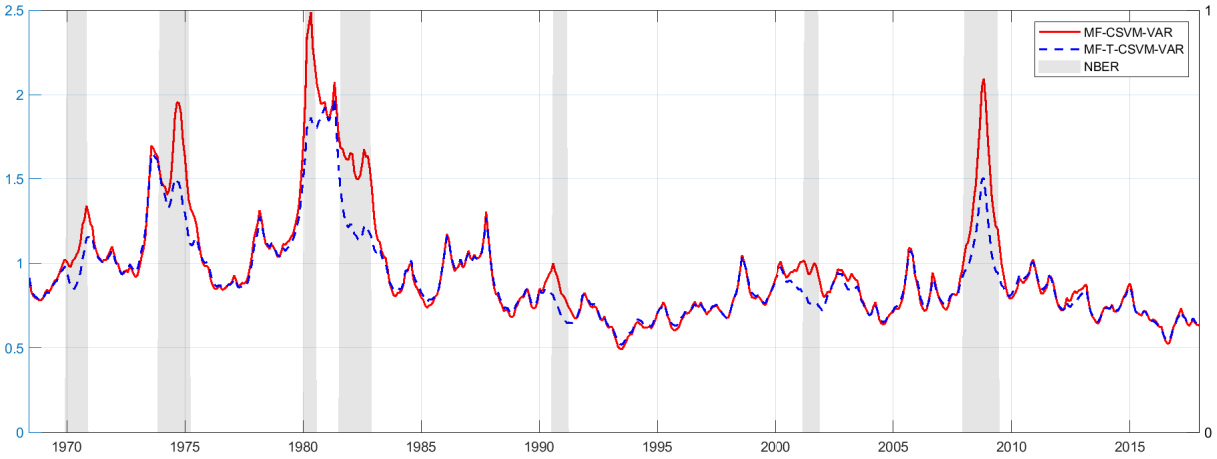

Notes: The lines indicate the posterior mean from the common stochastic volatility factor f_t as standard deviations. The red solid line and blue dashed line refer to MF-CSVM-VAR and MF-T-CSVM-VAR, respectively, from the final data vintage. Shaded areas correspond to the recessions dated by the NBER. Sample: 1967M4-2017M12.

3.4.3 Point forecast evaluation

The point forecast accuracy is measured as the root-mean-squared error (RMSE):

$$\text{RMSE}_h^M = \sqrt{\frac{1}{T_f}\sum_t \left(y_{t+h} - \hat{y}_{t+h}^M\right)^2} \tag{3.17}$$

relative to the benchmark model:

$$\text{relative RMSE}_h^M = \frac{\text{RMSE}_h^M}{\text{RMSE}_h^b}, \tag{3.18}$$

where M denotes the model, b the benchmark model, $\hat{y}_{t+h}$ the posterior mean as the point forecast, y_{t+h} the actual value and T_f the recursive sample size. I apply a Diebold-Mariano test with Newey-West standard errors to roughly gauge the statistical significance of the results. GDP is measured in annualized percentage changes for comparison with the SPF in Section 3.4.5.

Table 3.3 displays the relative RMSE for the full out-of-sample period. The best performance on average across all horizons and variables is obtained for the MF-T-CSVM-VAR with a reduction of 11% in relative RMSEs. The MF-T-VAR shows the highest relative forecasting accuracy in terms of nowcasting. In contrast, both medium-scale VARs reveal their strength with increasing forecasting horizon. The CSVM contributes the most for forecast horizons exceeding the nowcast $h > 1$ and for the UR.

For GDP, we can observe a significant gain in nowcast accuracy with regard to the MF-VAR and MF-T-VAR by 12%. The MF-CSVM-VAR^{med} reveals the best accuracy with gains up to 15%

for horizons $h > 1$. In terms of CPI, only models that include CSVM can significantly improve the benchmark, whereas the relative improvements are rather moderate with maximum 9%. In contrast, the relative improvements for UR are the largest, though they are rarely significant. Of notable mention here is the MF-T-CSVM-VAR with relative gains up to 22%. Again, the MF-T-VAR shows a strong performance for the nowcast.

Table 3.3: Relative RMSEs

Model	h=1	h=2	h=3	h=4
	GDP			
MF-VAR	**0.88*****	0.91***	0.93***	0.98**
MF-CSVM-VAR	0.93	0.90**	0.90***	0.95**
MF-T-VAR	0.88***	0.92**	0.91***	0.93***
MF-T-CSVM-VAR	0.90***	0.90**	0.88***	0.92***
MF-VAR^{med}	0.90*	0.88**	0.86*	0.87**
MF-CSVM-VAR^{med}	0.93	**0.87*****	**0.85*****	**0.86*****
MF-VAR^{b}	*0.50*	*0.63*	*0.68*	*0.67*
	Inflation			
MF-VAR	1.00	1.03	0.99	0.99
MF-CSVM-VAR	0.99	0.97***	0.95***	0.96***
MF-T-VAR	**0.97**	1.01	1.00	0.99
MF-T-CSVM-VAR	0.98	**0.96***	0.97	0.96**
MF-VAR^{med}	0.99	0.98	0.96	0.94
MF-CSVM-VAR^{med}	0.98**	0.97*	**0.94****	**0.91*****
MF-VAR^{b}	*0.21*	*0.29*	*0.28*	*0.28*
	Unemployment Rate			
MF-VAR	0.92	0.88	0.89	0.90*
MF-CSVM-VAR	0.89	0.80*	**0.79***	**0.80****
MF-T-VAR	**0.84***	0.84*	0.88*	0.90*
MF-T-CSVM-VAR	0.85	**0.78***	0.80*	0.81*
MF-VAR^{med}	1.00	1.03	1.07	1.09
MF-CSVM-VAR^{med}	1.00	0.97	0.96	0.96
MF-VAR^{b}	*0.16*	*0.39*	*0.63*	*0.87*

Notes: The relative RMSEs are expressed as ratios relative to the benchmark model. A figure below unity indicates that the model outperforms the benchmark. The benchmark is reported in absolute terms in italic figures (the last column of each panel). Bold figures indicate the best performance for the variable and horizon. *, **and ***denote significance at the 10%, 5% and 1% level, respectively, according to the Diebold-Mariano test with Newey-West standard errors. GDP is measured in annualized growth rates. Out-of-sample: 2001M2-2017M12.

Since the paper emphasizes the relationship between the state of the business cycle and forecasting, it is of particular interest to examine the two regimes, recession and expansion, separately. Therefore, I divide the sample into two subsamples consistent with the recession and expansion dates according to the NBER business cycle dating committee. The left and right panel of Table 3.4 present the relative RMSE for the recession and expansion subsample, respectively. For the recessions, the highest precision across all horizons and variables on average is shown by the MF-T-CSVM-VAR with a reduction of 15% in relative RMSEs which improved by 4% compared to the full sample. Moreover, two additional results stand out. First, the

relative nowcast precision of the T-VARs increased even more for GDP and UR compared to the full sample. The MF-T-VAR is best for GDP with a reduction of 15%. The MF-T-CSVM-VAR reduces the relative RMSE of UR by 38%. Second, gains in forecast accuracy for the CPI are again rather moderate and often insignificant. However, it is a different story for the expansion subsample. The MF-CSVM-VAR works well with a drop of 4% in relative RMSE on average over all variables and horizons. It is also noticeable that every model with CSVM beats its counterpart without CSVM during expansions with largest gains again for the UR.

Table 3.4: Relative RMSEs for recessions and expansions

	NBER Recessions				NBER Expansions			
Model	h=1	h=2	h=3	h=4	h=1	h=2	h=3	h=4
	GDP							
MF-VAR	0.93**	0.92	0.93**	0.97**	**0.86*****	0.90***	0.93***	0.99
MF-CSVM-VAR	1.05	0.92	0.90**	0.93***	0.88***	0.89**	0.91**	0.97
MF-T-VAR	**0.85*****	0.94**	0.93	0.91**	0.90**	0.90*	0.89***	0.94
MF-T-CSVM-VAR	0.91**	**0.91**	**0.88****	0.90**	0.90**	0.89*	0.88***	0.93*
MF-VAR^{med}	0.93	0.92	0.90	0.87	0.89	0.84**	0.83*	0.86
MF-CSVM-VAR^{med}	0.98	0.94	0.89	**0.87****	0.92	**0.82*****	**0.82****	**0.85****
MF-VAR^{b}	*0.75*	*1.13*	*1.29*	*1.27*	*0.45*	*0.51*	*0.53*	*0.53*
	Inflation							
MF-VAR	1.03	1.06	1.03	1.01	0.98***	0.99	0.96***	0.97***
MF-CSVM-VAR	1.02	0.99	**0.97*****	0.98*	0.96***	0.93***	0.94***	0.94***
MF-T-VAR	**0.96**	1.04	1.04	1.01	0.99	0.97	0.96**	0.96**
MF-T-CSVM-VAR	0.98	**0.99**	0.98	0.98	0.98	0.93**	0.95**	0.95**
MF-VAR^{med}	1.01	1.03	1.02	0.98	0.96***	**0.92*****	0.90***	0.90**
MF-CSVM-VAR^{med}	1.01	1.00	0.98	**0.95**	**0.96*****	0.92***	**0.90*****	**0.88*****
MF-VAR^{b}	*0.41*	*0.60*	*0.54*	*0.52*	*0.16*	*0.20*	*0.22*	*0.22*
	Unemployment Rate							
MF-VAR	0.72**	0.75**	0.80***	0.83***	1.04	1.05	1.08	1.05
MF-CSVM-VAR	0.66**	0.64**	0.69***	0.73***	1.02	0.99	**0.99**	**0.95**
MF-T-VAR	0.64*	0.73**	0.80***	0.83***	**0.96**	**0.97**	1.05	1.06
MF-T-CSVM-VAR	**0.61***	**0.61****	**0.68*****	**0.72*****	0.98	0.99	1.04	1.02
MF-VAR^{med}	0.82*	0.80*	0.78**	0.77**	1.11*	1.30***	1.57***	1.67***
MF-CSVM-VAR^{med}	0.94	0.87	0.84*	0.83**	1.04	1.09	1.22**	1.26***
MF-VAR^{b}	*0.29*	*0.84*	*1.48*	*2.07*	*0.13*	*0.26*	*0.36*	*0.48*

Notes: The relative RMSEs are expressed as ratios relative to the benchmark model. A figure below unity indicates that the model outperforms the benchmark. The benchmark is reported in absolute terms in italic figures (the last column of each panel). Bold figures indicate the best performance for the variable and horizon. *, **and ***denote significance at the 10%, 5% and 1% level, respectively, according to the Diebold-Mariano test with Newey-West standard errors. GDP is measured in annualized growth rates. The left and right panel refers to periods that the NBER identifies as recessions and expansions, respectively. Out-of-sample: 2001M2-2017M12.

Since the results with respect to the business cycle regimes indicate a significant difference in forecast performance for GDP and UR, it is of peculiar interest to examine the development of the relative RMSE over time for both variables. Thereby, I focus on the nowcast of GDP and UR as they reveal the largest gains in recessions. Figure 3.3 depicts the cumulative sum of RMSE

for the nowcast of GDP and UR. I subtract the cumulative sum of the benchmark model such that positive values indicate a better performance and the benchmark is indicated by a zero line.

Figure 3.3: Relative cumulative sum of squared nowcast errors

(a) GDP

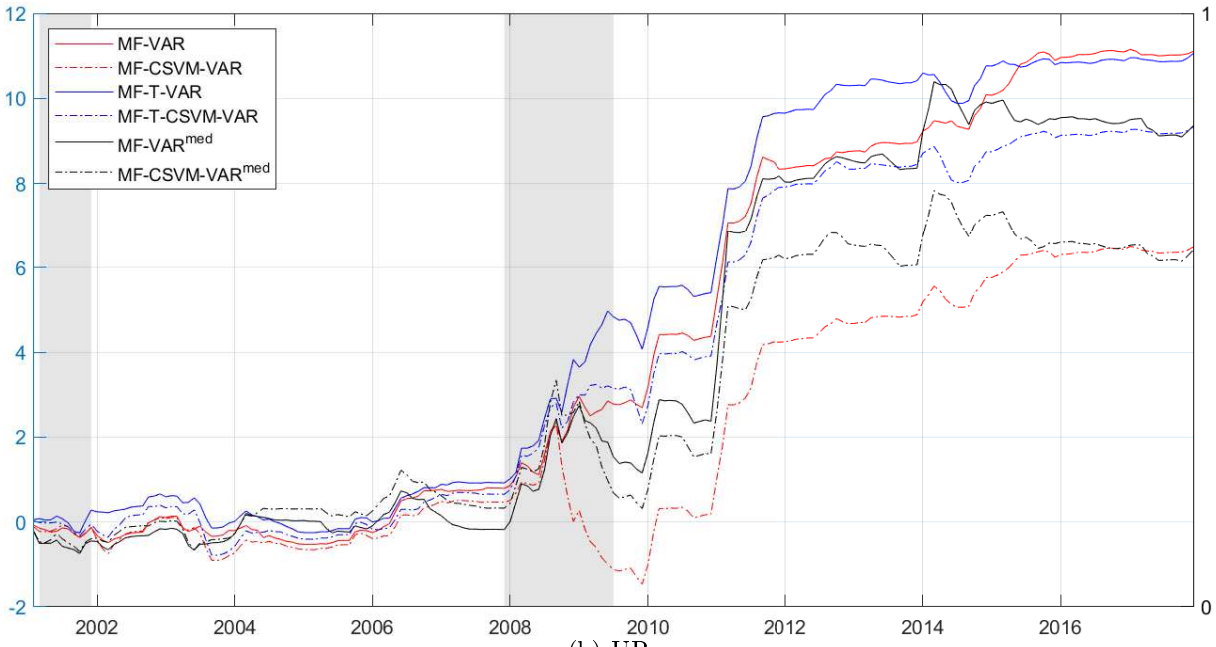

(b) UR

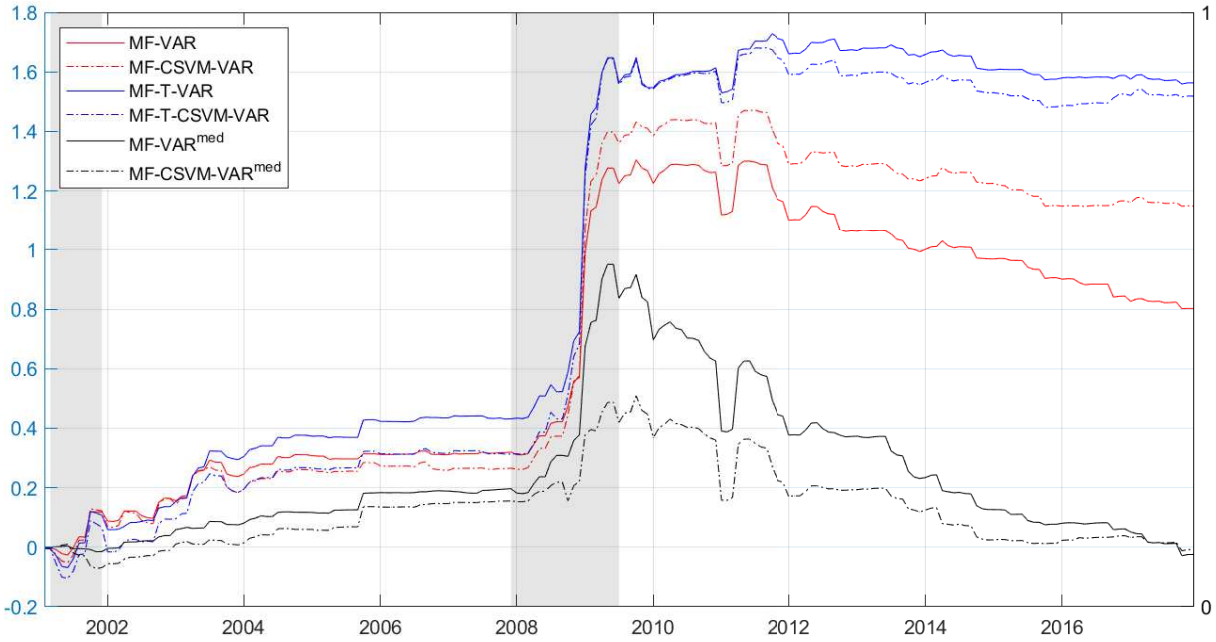

Notes: Lines refer to the relative cumulative sum of squared forecast errors at horizon $h = 1$ in difference to the benchmark. A value above zero indicates a better forecast accuracy. GDP is measured in annualized growth rates. Shaded areas correspond to the recessions dated by the NBER. Out-of-sample: 2001M2-2017M12

Regarding GDP, the MF-T-VAR improves upon all models during and following the first recession in 2001. Thereafter, the accuracy converges among all models up to the point that

they fail to beat the benchmark. All models start to improve after 2006 but diverge considerably with the start of the Great Recession, more specifically, during the largest decline of GDP in 2008Q4 in which the MF-T-VAR outperforms all other models by quite a margin. One can see another large kink in the first quarter of 2011 during which GDP drops by roughly 1%. Though, in this occasion all models equally enhance relative the benchmark.

In contrast, UR depicts a more stable pattern. Right from the first sharp increase in the UR in the middle of 2001, the MF-T-VAR starts to steadily improve upon all other models with a sharp increase again during the Great Recession. Following the Great Recession, all linear models decline relative to the benchmark, whereas both T-VARs maintain their relative levels. This decline in forecast accuracy is particularly striking for both medium-scale VARs during the long recovery in the labour market following the Great Recession.

In summary, the MF-T-VAR and MF-T-CSVM-VAR provide by far the most accurate nowcasts during recessions, with the nowcast for GDP and UR clearly standing out. This gains are mainly driven by deteriorating times during the recession periods, in particular the severe conditions during the Great Recession. This shows that it is important to timely incorporate information on the current state of the business cycle into forecasting models for point forecasts of GDP and UR–however CPI does not benefit from it. Accounting for time-varying macroeconomic uncertainty in form of CSVM increases point forecast accuracy for forecast horizons beyond the nowcast on average over all variables–notably for UR during recessions. The medium-scale MF-CSVM-VAR^{med} reveals precise forecasts for GDP and CPI for horizons exceeding the nowcast $h > 1$.

3.4.4 Density forecast evaluation

Recently more and more interest and importance in the literature on forecasting is shifted towards density forecasts to account for the uncertainty surrounding point forecasts (see Wright, 2019). I employ the continuous ranked probability score (CRPS) introduced by Matheson and Winkler (1976) to evaluate the entire forecast density. I follow Gneiting and Ranjan (2011) and apply the score function:

$$S(p_t^M, y_{t+h}, \nu(u)) = \int_{-0}^{1} \mathrm{QS}_u(P_t^M(u)^{-1}, y_{t+h})\nu(u)du, \tag{3.19}$$

where $\mathrm{QS}_u(P_t^M(u)^{-1}, y_{t+h}) = 2(I\{y_{t+h} < P_t^M(u)^{-1}\} - u)(P_t^M(u)^{-1} - y_{t+h}^M)$ is the quantile score for forecast quantile $P_t^M(u)^{-1}$ of model M at level $0 < u < 1$. $I\{y_{t+h} < P_t^M(u)^{-1}\}$ denotes an indicator function which is one in case of $y_{t+h} < P_t^M(u)^{-1}$ and zero otherwise. p_t^M denotes the predictive density and $(P_t^M)^{-1}$ the inverse of the cumulative predictive density for model M. $\nu(u)$ is a weighting function. I use a simple uniform weighting scheme $\nu(u) = 1$. Thus, the average CRPS is:

$$\mathrm{CRPS}_h^M = \frac{1}{T_f} \sum_t S(p_t^M, y_{t+h}, 1). \tag{3.20}$$

A lower value signifies a better fit of the predictive density with respect to the true data density. I evaluated the CRPS as a ratio relative to the benchmark:

$$\text{relative CRPS}_h^M = \frac{CRPS_h^M}{CRPS_H^b} \tag{3.21}$$

To gauge equal predictive forecast accuracy, I regress the differences between the CRPS and the benchmark on a constant. Inference is based on a t-test with Newey-West standard errors.

Table 3.5 shows the relative CRPS for the entire sample and Table 3.6 displays the results conditional on the business cycle state according the NBER chronology. The overall result of the density forecasts support the results of the point forecasts in Section 3.4.3. On average over all variables and horizons, the MF-T-CSVM-VAR still beats all other models with a decline of 11% in CRPS. The result enhances to an overall reduction of 18% during recessions. While the MF-T-CSVM-VAR still performs best during expansions, the reduction in relative CRPS is lower with 8%.

Similar to the point forecasts, the best performance for the nonlinear MF-T-VAR and MF-T-CSVM-VAR is during the recession periods for the nowcast of GDP and UR. However, the difference for the MF-T-VAR to the benchmark for GDP is even larger with a decline in the relative CRPS by 19% compared to 15%. The same holds for the MF-T-CSVM-VAR for UR, though the incline from 39% to 41% is only minor. Furthermore, the improvement due to CSVM in recessions for forecast horizons $h > 1$ is even more pronounced for each model. Thus, the contribution of adding CSVM is best when analysing the whole predictive density as it takes into account the change in volatility over time.

All in all, the results from the density forecast evaluation confirmed the point forecast results. For GDP and UR, one can achieve even better results in terms of the nowcasts during recessions. Therefore, the MF-T-VAR and MF-T-CSVM-VAR can also very well reflect the uncertainty surrounding the point forecast that is associated with periods of high volatility during recessions. The CSVM feature again works particularly well for forecast horizons exceeding the nowcast $h > 1$ but is even more pronounced.

3.4.5 Nowcast comparison with the Survey of Professional Forecasters

In general, any forecasting model has a hard time to beat survey or institutional forecasts (see discussion in Wright, 2019). Nevertheless, these forecasts also perform rather poorly for GDP during recessions (see, i.e., Dovern and Jannsen, 2017; Sinclair, 2019). With promising results for the GDP nowcast from the MF-T-VAR during recessions, it is worth comparing this model's nowcast against the Survey of Professional Forecasters (SPF) from the Federal Reserve Bank of Philadelphia.

The SPF has two limitations for an exact evaluation against the MF-T-VAR. First, the SPF reports only once a quarter and hence, I can compare it only on a quarterly basis which cuts the out-of-sample period to 64 observations. Second, it is difficult to exactly match the information set with the corresponding SPF deadlines in real time. The questionnaires are send to the participants at the end of the first month of each quarter at the time of the publication

Table 3.5: Relative CRPS

Model	h=1	h=2	h=3	h=4
	GDP			
MF-VAR	0.89***	0.90***	0.94***	0.98***
MF-CSVM-VAR	0.91***	0.88***	0.89***	0.94***
MF-T-VAR	**0.88****	0.89***	0.92***	0.94***
MF-T-CSVM-VAR	0.89***	0.87***	0.87***	0.91***
MF-VAR^{med}	0.93**	0.88**	0.88*	0.89**
MF-CSVM-VAR^{med}	0.94*	**0.86****	**0.85****	**0.86****
MF-VAR^{b}	*0.27*	*0.33*	*0.36*	*0.35*
	Inflation			
MF-VAR	1.00	1.03	0.99	0.99
MF-CSVM-VAR	0.98*	**0.94****	0.92***	0.92***
MF-T-VAR	0.98	1.00	0.98	0.98
MF-T-CSVM-VAR	0.98	0.95*	0.93***	0.93***
MF-VAR^{med}	0.98**	0.97	0.95	0.93
MF-CSVM-VAR^{med}	**0.97****	0.95***	**0.91****	**0.88****
MF-VAR^{b}	*0.11*	*0.14*	*0.14*	*0.14*
	Unemployment Rate			
MF-VAR	0.97	0.93	0.92*	0.92
MF-CSVM-VAR	0.92*	0.84***	0.80***	**0.79****
MF-T-VAR	**0.88****	0.85***	0.87***	0.87***
MF-T-CSVM-VAR	0.88***	**0.82****	**0.80****	0.80***
MF-VAR^{med}	1.02	1.11*	1.22**	1.29***
MF-CSVM-VAR^{med}	0.99	0.99	1.03	1.05
MF-VAR^{b}	*0.09*	*0.20*	*0.31*	*0.43*

Notes: The relative CRPS are expressed as ratios relative to the benchmark model. A figure below unity indicates that the model outperforms the benchmark. The benchmark is reported in absolute terms in italic figures (the last column of each panel). Bold figures indicate the best performance for the variable and horizon. *, **and ***denote significance at the 10%, 5% and 1% level, respectively, according to the difference in mean test with Newey-West standard errors. GDP is measured in annualized growth rates. The out-of-sample goes from 2001M2-2017M12.

of the Bureau of Economic Analysis' advance report. The deadline to submit the forecasts is at late in the second to third week of the second month of each quarter. Hence, the information set for the SPF is in between the end of the first and end of the second month, though the exact timing depends on the date of submission of each participant. As the CFNAI is crucial for the MF-T-VAR and is only published at the end of each month, I compare it against the SPF across the three information sets–I1, I2 and I3–defined as the end of the first, second and third month of each quarter, respectively. Hence, the MF-T-VAR starts each quarter with I1 with an information disadvantage of roughly two to three weeks against the SPF. This information set does not contain a value for the CFNAI concerning the current quarter as it has a publication lag of one month. The information set continues with I2 with an advantage of an additional week of data releases which includes the first monthly figure of the CFNAI of the current quarter. The final set I3 takes the whole current quarter into account which includes the first and second monthly figure of the CFNAI of the current quarter.

Table 3.6: Relative CRPS for recessions and expansions

	NBER Recessions				NBER Expansions			
Model	h=1	h=2	h=3	h=4	h=1	h=2	h=3	h=4
	GDP							
MF-VAR	0.95	0.93	0.92***	0.96**	**0.87*****	0.89***	0.94***	0.99**
MF-CSVM-VAR	1.00	0.90	0.91	0.94	0.88***	0.87***	0.88***	0.94**
MF-T-VAR	**0.81*****	0.94**	0.94	0.91**	0.90***	0.88***	0.91***	0.95**
MF-T-CSVM-VAR	0.87***	**0.89**	**0.89****	0.91**	0.90***	0.86***	0.87***	0.91***
MF-VAR^{med}	0.92	0.95	0.92	**0.86**	0.93*	0.86***	0.87*	0.89
MF-CSVM-VAR^{med}	0.93	0.95	0.92	0.86*	0.95	**0.83*****	**0.83*****	**0.86*****
MF-VAR^{b}	*0.46*	*0.64*	*0.75*	*0.72*	*0.25*	*0.29*	*0.30*	*0.30*
	Inflation							
MF-VAR	1.05	1.11*	1.08	1.06	0.98***	0.99	0.96***	0.97***
MF-CSVM-VAR	0.97	**0.96**	**0.96**	1.01	0.98	0.94***	0.90***	0.89***
MF-T-VAR	**0.94**	1.05	1.08*	1.07**	0.99	0.97	0.95***	0.96***
MF-T-CSVM-VAR	0.94	0.98	0.98	1.02	0.99	0.94***	0.91***	0.90***
MF-VAR^{med}	1.02	1.09**	1.10	1.06	**0.96*****	0.92***	0.91***	0.90**
MF-CSVM-VAR^{med}	0.98	1.01	1.00	**0.99**	0.97**	**0.92*****	**0.88*****	**0.85*****
MF-VAR^{b}	*0.21*	*0.32*	*0.27*	*0.23*	*0.09*	*0.11*	*0.12*	*0.13*
	Unemployment Rate							
MF-VAR	0.75***	0.72***	0.74***	0.77***	1.04	1.03	1.04	1.03
MF-CSVM-VAR	0.63***	0.58***	0.61***	0.65***	1.02	0.97	**0.94**	**0.89****
MF-T-VAR	0.63***	0.67***	0.73***	0.76***	**0.96**	**0.95**	0.96	0.96
MF-T-CSVM-VAR	**0.59*****	**0.55*****	**0.59*****	**0.64*****	0.98	0.96	0.94	0.92
MF-VAR^{med}	0.82***	0.80**	0.77**	0.76**	1.09*	1.26***	1.53***	1.68***
MF-CSVM-VAR^{med}	0.88**	0.85*	0.82*	0.80*	1.03	1.06	1.17**	1.24***
MF-VAR^{b}	*0.17*	*0.53*	*1.00*	*1.45*	*0.07*	*0.15*	*0.21*	*0.29*

Notes: The relative CRPS are expressed as ratios relative to the benchmark model. A figure below unity indicates that the model outperforms the benchmark. The benchmark is reported in absolute terms in italic figures (the last column of each panel). Bold figures indicate the best performance for the variable and horizon. *, **and ***denote significance at the 10%, 5% and 1% level, respectively, according to the difference in mean test with Newey-West standard errors. GDP is measured in annualized growth rates. The left and right panel refers to periods that the NBER identifies as recessions and expansions, respectively. Out-of-sample: 2001M2-2017M12.

Table 3.7 shows the nowcast errors relative to the SPF. For the full sample, there is an increase in accuracy with incoming information. For I1, with an information disadvantage, the MF-T-VAR performs worse than the SPF but breaks even with new information in I2 and I3. For recessions, the MF-T-VAR beats the SPF already in I1 with gains increasing from 9% up to 29% with incoming new information at the end of the each month. On the contrary, the SPF dominates the expansion subsample independent of the information set.

Figure 3.4 displays the GDP nowcast errors (bars) for the SPF and the MF-T-VAR for I1, I2 and I3 together with the annualized GDP growth rates (solid line). The sequence of bars at each point in time is ordered as SPF, I1, I2 and I3. Errors are defined as actual minus forecast $y_{(t+h)} - \hat{y}_{(t+h)}$. Hence, negative errors indicate a too optimistic forecast for negative growth rates and too pessimistic forecast for positive growth rates. Thus, if the MF-T-VAR beats the SPF and

Table 3.7: Relative RMSEs for GDP nowcast - Comparison of MF-T-VAR with Survey of Professional Forecasters

	I1	I2	I3	I1	I2	I3	I1	I2	I3
	Full sample			Recessions			Expansions		
MF-T-VAR	1.06	1.00	0.98	0.91	0.85	0.71	1.15	1.10	1.12

Notes: The relative RMSEs are expressed as ratios relative to the SPF. A figure below unity indicates that the model outperforms the benchmark. Out-of-sample: 2001M2-2017M12.

new information reduces nowcast errors, the bars should ascend (descend) for negative (positive) errors from left to right at a specific point in time. Overall, the SPF and MF-T-VAR tend to make similar nowcast errors over time with a correlation of 0.85, 0.87 and 0.85 for I1, I2 and I3, respectively. 2001Q3, 2008Q1 and 2008Q4 render the steepest downturns in GDP with negative forecast errors in the full sample coinciding with recessions. Thus, both the MF-T-VAR as well as the SPF are too optimistic in downturns during recessions. However, in both occasions the negative forecast error is lower for the MF-T-VAR. This is already present for I1 and decreased even further with more information in I2 and I3–particularly evident for the largest forecast error in 2008Q4. On the contrary, large negative forecast errors present in expansion, i.e. first quarter of 2011 with annualized GDP growth of -1.5%, can not be diminished by the M-T-VAR.

Figure 3.4: GDP nowcast errors - Comparison of MF-T-VAR with Survey of Professional Forecasters

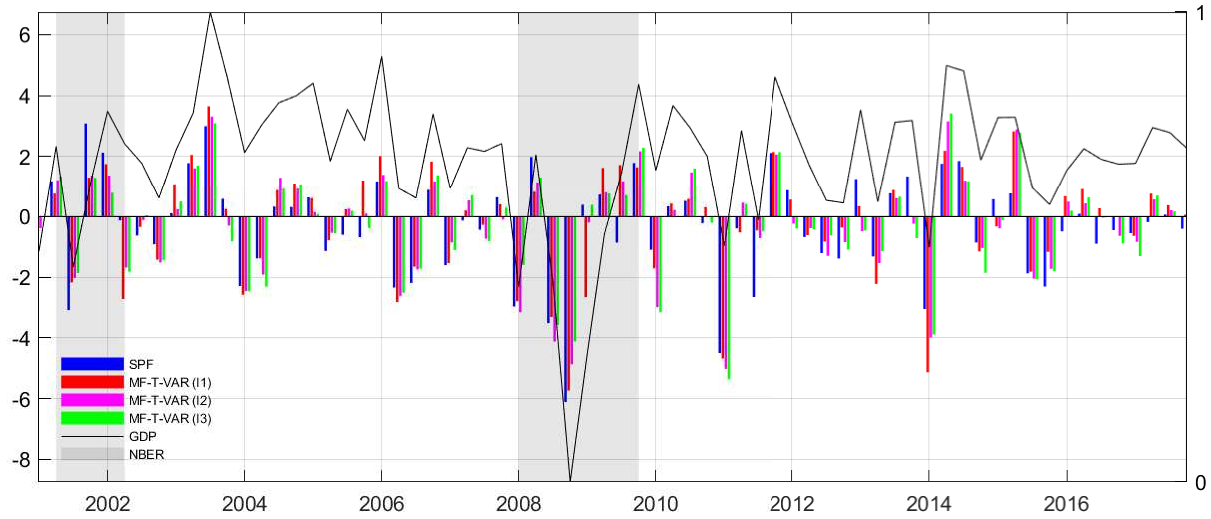

Notes: The black solid line refers to actual GPD in annualized growth rates. The forecast errors are defined as $(y_{t+h} - \hat{y}_{t+h})$ for $h = 1$. Hence, a negative value indicates that the forecast is too optimistic for negative GDP growth rates. The blue, red, magenta and green bars refer to the nowcast error of the SPF and MF-T-VAR for information set I1, I2 and I3, respectively. Shaded areas correspond to the recessions dated by the NBER. Out of sample: 2001Q1 - 2017Q4

Overall, the MF-T-VAR can help to lower systematic negative nowcast errors made by SPF in recessions as described by Dovern and Jannsen (2017), though in expansions the SPF is still a benchmark hard to beat. For information on other models and forecast horizons I refer to

Figure 3.7 in Appendix 3.A.4. In short, the medium-scale MF-VARs can keep up with the SPF concerning GDP for forecast horizons $h > 1$ and even perform better by small margin for $h = 4$.

3.4.6 Nowcasting during the Great Recession

Unsurprisingly, the largest forecast errors according to Figure 3.4 occur in 2008Q4 during the Great Recession with the largest drop in GDP. Thus, it is of great interest how the different models and the SPF perform during that time in detail. Figure 3.5 presents the entire nowcast densities together with point nowcasts and the actual GDP value. Each panel includes the different monthly information sets. Hence, I1, I2 and I3 refer to 2008M10, 2008M11 and 2008M12.

Figure 3.5: GDP nowcast densities - 2008Q4 during the Great Recession

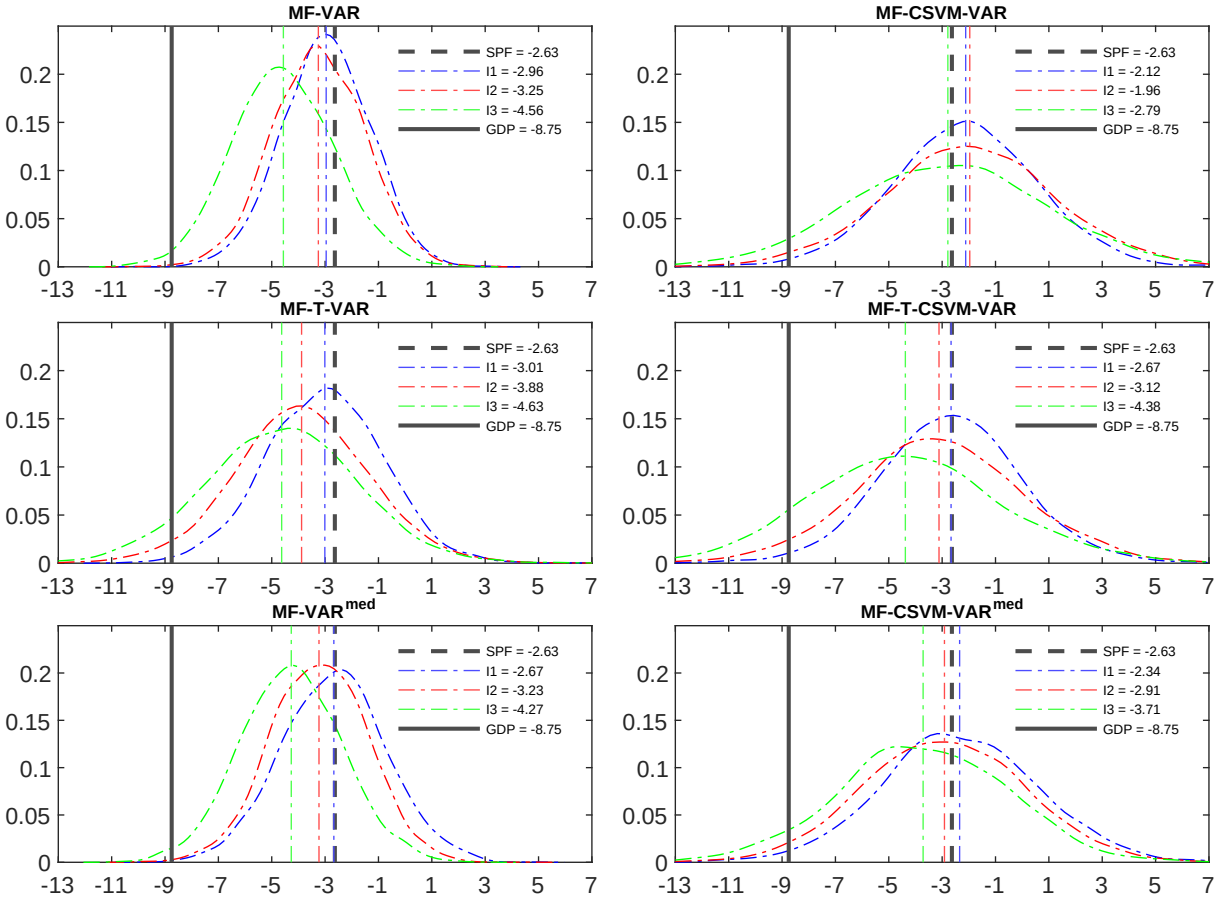

Notes: Figures refer to each model with its nowcast densities (based on a normal kernel density estimate) and the respective mean (dashed-dotted line). Within each figure, the blue, the red and the green dashed-dotted line refer to 2008M10, 2008M11 and 2008M12 vintage, respectively. The SPF nowcast is shown by a black dashed line while the final value for GDP by a black solid line.

There are two main results to consider. First, all models with CSVM show significant wider tails in the predictive density. Thus, the time-varying volatility clearly takes the heightened uncertainty during that time into account and thus, enhances density nowcasts. Second, for MF-T-VAR, MF-T-CSVM-VAR and MF-VAR, all dashed-dotted lines are left of the dashed line and right of the solid line, denoting means of the forecast densities, SPF nowcast and final GDP value, respectively. Hence, these models nowcast better than the SPF from information set I1 onward.

Overall, if a forecaster is interested in both point and density forecasts, it is best to include information about the business cycle in form of an index, regime dependent parameters and additionally account for macroeconomic uncertainty in form of common time-varying volatility.

3.5 Conclusion

Macroeconomists have a hard time to forecast and even nowcast during recessions. Especially following the Great Recession in 2008/09, this problem has aroused interest in recent research on forecasting. To approach this problem, this paper proposes a novel VAR that can handle mixed-frequency data and recurring business cycle regimes and common stochastic volatility in mean as important business cycle features in real time. To this end, I combined a mixed-frequency VAR (MF-VAR) with a threshold VAR (T-VAR) which additionally accounts for time-varying macroeconomic uncertainty in form of common stochastic volatility in mean (CSVM). I utilize the Chicago Fed National Activity Index as business cycle index for the threshold variable to date the business cycle in real time. A Minnesota prior is used for all VARs where the shrinkage parameter is estimated with an adaptive Normal-inverse-Gamma prior. This allows to determine the amount of shrinkage and furthermore permits for different shrinkage across business cycle regimes and variables.

In a real-time forecasting experiment for US GDP, CPI and UR, the MF-T-CSVM-VAR outperforms on average across all variables and horizons linear MF-VARs without the business cycle features of different size with respect to point and density forecasts. The difference in performance is especially pronounced for nowcasts for GDP and UR during recessions. The MF-T-VAR even reduces GDP nowcast errors made by the Survey of Professional Forecasters (SPF) during the sharp drop in economic activity of 2008Q4 during the Great Recession. Thus, the results suggest that it is valuable for the short-term forecast during recessions to identify the current state of the economy and incorporate this information into the model. By contrast, the medium-scale MF-CSVM-VAR reveals accurate GDP forecasts for horizons of two to four quarters ahead in which case it is quite competitive to the SPF. The time-varying volatility CSVM provides the largest gains for UR forecasts–notably density forecasts for two to four quarters ahead.

3.A Appendix 3

3.A.1 State-Space representation

I follow Schorfheide and Song (2015) and split the state vector z_t from equation (3.1) such that it contains only the latent variable $z_t = z_{q,t} = [\tilde{y}'_{q,t}, \ldots, \tilde{y}'_{q,t-p}]'$ to decrease computation time. Let the remaining monthly variables be $z_{m,t-1} = [y'_{m,t-1}, \ldots, y'_{m,t-p}]'$. Hence, the measurement equation for the MF-T-CSVM-VAR can be written as:

$$y_t = C_{m,S_t} + R_{q,S_t} z_{q,t} + R_{m,S_t} z_{m,t-1} + B_{m,S_t} h_{t-1} + \Upsilon_{S_t}$$

where

$$\begin{aligned}
C_{m,S_t} &= \begin{bmatrix} 0_{nq,1} & A_{0m,S_t} \end{bmatrix}' \\
B_{m,S_t} &= \begin{bmatrix} 0_{nq,1} & b_{m,S_t} \end{bmatrix}' \\
R_{q,S_t} &= \begin{bmatrix} R_{q1,S_t} & R_{q2,S_t} \end{bmatrix}' \\
R_{q1,S_t} &= \begin{bmatrix} 1/3 * I_{nq} & 2/3 * I_{nq} & I_{nq} & 2/3 * I_{nq} & 1/3 * I_{nq} & 0_{nq \times nq*p} \end{bmatrix} \\
R_{q2,S_t} &= \begin{bmatrix} 0_{n-nq \times 1} & A_{mq,S_t} \end{bmatrix} \\
R_{m,S_t} &= \begin{bmatrix} R_{m1,S_t} & R_{m2,S_t} \end{bmatrix}' \\
R_{m1,S_t} &= \begin{bmatrix} 0_{nq \times nm*(p)} \end{bmatrix} \\
R_{m2,S_t} &= \begin{bmatrix} 0_{nq,nm*p} & A_{mm,S_t} \end{bmatrix}'.
\end{aligned}$$

with A_{0m,S_t} containing the intercepts for $y_{m,t}$, b_{m,S_t} being the parameters that relate $y_{m,t}$ to h_{t-1}, A_{mm,S_t} being a $(nm \times nm*p)$ matrix containing all VAR parameters that relates $y_{m,t}$ to $[y'_{m,t-1}, \ldots, y'_{m,t-p}]'$ and A_{mq,S_t} being a $(nm \times nq*p)$ matrix containing all VAR parameters that relates $y_{m,t}$ to $[\tilde{y}'_{q,t-1}, \ldots, \tilde{y}'_{q,t-p}]'$. The error term is divided into $\Upsilon_{S_t} = [0_{nq,1} u_{nm,t}]$. The transition equation is adjusted as follows:

$$z_{q,t} = C_{q,S_t} + A_{q,S_t} z_{q,t-1} + A_{m,S_t} z_{m,t-1} + B_{q,S_t} h_{t-1} + \upsilon_t \qquad \upsilon_t \sim \mathcal{N}(0, \Xi_{S_t}).$$

where

$$\begin{aligned}
C_{q,S_t} &= \begin{bmatrix} A_{0q,S_t} & 0_{nq*p,1} \end{bmatrix}' \\
B_{q,S_t} &= \begin{bmatrix} b_{q,S_t} & 0_{nq*p,1} \end{bmatrix}' \\
A_{q,S_t} &= \begin{bmatrix} A_{qq,S_t} & I_{nq*p,nq*(p+1)} \end{bmatrix}' \\
A_{m,S_t} &= \begin{bmatrix} A_{qm,S_t} & 0_{nq*p,nm*(p+1)} \end{bmatrix}'.
\end{aligned}$$

with A_{0q,S_t} containing the intercepts for $\tilde{y}_{q,t}$, b_{q,S_t} being the parameters that relate $\tilde{y}_{q,t}$ to h_{t-1}, A_{qq} being a $(nq \times nq * p)$ matrix containing all VAR parameters that relates $z_{q,t}$ to $z_{q,t-1}$ and A_{qm} being a $(nq \times nm * p)$ matrix containing all VAR parameters that relates $z_{q,t}$ to $z_{m,t-1}$.

3.A.2 Priors

VAR-coefficients

I use an independent Normal-inverse-Wishart Minnesota prior for the VAR parameters. The prior mean on the first lag is 0 (0.9) if the respective variable is non-persistent (persistent) since all variables are transformed to be stationary. Thus, the prior mean for row j and column i of the coefficient matrix of lag l is set as follows:

$$E(A_l^{j,i}) = \begin{cases} 0.9 & \text{if } i = j \text{ and } l = 1 \text{ and j is persistent} \\ 0 & \text{if } i = j \text{ and } l = 1 \text{ and j is non-persistent} \\ 0 & \text{otherwise.} \end{cases}$$

The prior variance for row j and column i of the coefficient matrix of lag l is set as follows:

$$Var(A_l^{j,i}) = \begin{cases} \frac{\lambda_1}{l^2} & \text{if } i = j \\ \frac{\lambda_1 \lambda_2 \sigma_{jj}^2}{l^2 \sigma_{ii}^2} & \text{if } i \neq j \\ \frac{\lambda_1 \lambda_3 \sigma_{jj}^2}{l^2 \sigma_{ii}^2} & \text{if } i \neq j \wedge j = y^* \\ 1000 & \text{if } l = 0 \end{cases}$$

where σ_{ii} is the residual standard error of an AR(p) for variable i. The amount of shrinkage is determined by the vector of hyperparameters $\Lambda = [\lambda_1, \lambda_2, \lambda_3]'$. λ_1 governs the overall shrinkage. λ_2 applies cross-variable shrinkage and λ_3 as an extra shrinkage parameter for the business cycle variables, namely the business cycle index y^* (CFNAI) and the uncertainty factor h_t (CSVM). The prior variance for row j of the coefficient on h_{t-1} is $Var(b^{j,1}) = \frac{\lambda_1 \lambda_3 \sigma_{jj}^2}{\overline{\sigma^2}}$ where $\overline{\sigma^2}$ is the mean of the residual standard errors of AR(p) for each variable rescaled to have a variance of one. Starting values are $\Lambda = [0.04, 1, 1]'$ such that there is no cross-variable shrinkage and the overall shrinkage is in line with standard values picked for US data.

The prior scale matrix for the inverse-Wishart is diagonal:

$$p(\Omega) \sim \mathcal{IW}(S, \nu)$$

with $S = diag(\sigma_{11}^2, \ldots, \sigma_{NN}^2)$ where σ_{ii}^2 is again the residual variance of an AR(p) for variable i. The degrees of freedom ν are set to a minimum to account for a loose prior. The same prior is used across regimes $S_t = 1, 2$.

Shrinkage

I utilize a hyperprior to determine the degree of shrinkage in form of an inverse-Gamma prior:

$$p(\lambda_i) \sim \mathcal{IG}(\alpha, \beta_i) \qquad i = 1, 2, 3$$

with shape $\alpha = 0.1$ and scale $\beta_i = 0.044$ for $i = 1, 2$ and scale $\beta_i = \sqrt{0.044}$ for $i = 3$ such that it is weakly informative and has a mode of 0.04 for $i = 1, 2$ which is in line with common values used for US data and with 0.2 for $i = 3$ giving a priori a less shrinkage for the business cycle variables assuming that those variables are more important.

Threshold variable

I assume a uniform prior for the delay d and threshold parameter r:

$$\begin{aligned} d &\sim \mathcal{U}(1, p) \\ r &\sim \mathcal{U}(y_q^*, y_{1-q}^*). \end{aligned}$$

where p is the maximum number of lags in the VAR and y_q^* denotes the qth quantile of the threshold variable. The quantile is set to 10% to avoid outlier regimes. Given the real-time information content regarding the NBER business cycle dating, recessions account for about 15% to 20% of observations such that 10% is a general reasonable lower bound.

The initial value for the threshold value r is crucial since it is the first rough guess for the classification of the different regimes. Hence, I set it according to the lowest quadratic score for the first real-time data vintage of size $t = 1, \ldots, T$ defined as:

$$r^{\text{init}} = \arg\min_r \sum^r \sum^t (\text{NBER}_t - I(y_t^* < r))^2$$

where the range of r is over the discrete $\mathcal{U}(y_q^*, y_{1-q}^*)$ with step size of 0.1, NBER_t is a dummy for the real-time business cycle dates according to the NBER and $I(y_t^* < r)$ is an indicator function. After the first real-time data vintage, I use iteratively the final estimate of r as the next starting value.

Common stochastic volatility

The CSV prior setting mainly follows Carriero et al. (2016). I initialize the factor f_t with a Normal prior:

$$f_t \sim \mathcal{N}(1, 0.5)$$

and the variance of the innovations of the random walk law of motion by an inverse-Gamma distribution:

$$\phi \sim \mathcal{IG}(4, 0.04)$$

Furthermore, $f_t \Sigma$ is identified up to scale. Hence, I fix $f_0 = 1$ for identification.

Latent state

I follow Schorfheide and Song (2015) for the prior on the latent state variable $z_{q,t}$ and initialize the Kalman filter with a Normal prior:

$$p(z_{q,0}) \sim N(z_{q,-1}, I).$$

where I use a training sample of one year to estimate $z_{q,-1}$ with a linear MF-VAR based on actual observations for the monthly variables, interpolated values for the quarterly latent values and VAR parameters resting on their prior means.

3.A.3 Metropolis-within-Gibbs sampler

In the following I explain in detail each step of the MCMC algorithm for the MF-T-CSVM-VAR since all other models can be estimated by skipping the respective step in the sampler and in the conditioning set. I employ a total of 30000 iterations where the first 25000 are used as burn-in draws. A vector of variables over time T is denoted by $x^T = [x_1', \dots, x_T']'$. For the remainder A_{S_t} indicates the coefficient matrix of all VAR(p) dynamics including A_{0,S_t} and b_{1,S_t} for $S_t = 1, 2$ as it is estimated in the same step. The sequence for the MCMC is as follows:

1. Initialize A_1, Λ_1, Σ_1, A_2, Λ_2, Σ_2 , r, d, ϕ, f^T
2. $p(\tilde{y}^T | A_1, \Lambda_1, \Sigma_1, A_2, \Lambda_2, \Sigma_2, r, d, \phi, f^T, y^T)$
3. $p(A_1 | \tilde{y}^T, \Lambda_1, \Sigma_1, A_2, \Lambda_2, \Sigma_2, r, d, \phi, f^T)$
4. $p(\Sigma_1 | \tilde{y}^T, A_1, \Lambda_1, A_2, \Lambda_2, \Sigma_2, r, d, \phi, f^T)$
5. $p(A_2 | \tilde{y}^T, A_1, \Lambda_1, \Sigma_1, \Lambda_2, \Sigma_2, r, d, \phi, f^T)$
6. $p(\Sigma_2 | \tilde{y}^T, A_1, \Lambda_1, \Sigma_1, A_2, \Lambda_2, r, d, \phi, f^T)$
7. $p(\Lambda_1 | \tilde{y}^T, A_1, \Sigma_1, A_2, \Lambda_2, \Sigma_2, r, d, \phi, f^T)$
8. $p(\Lambda_2 | \tilde{y}^T, A_1, \Lambda_1, A_2, \Sigma_1, \Sigma_2, r, d, \phi, f^T)$
9. $p(r | \tilde{y}^T, A_1, \Lambda_1, \Sigma_1, A_2, \Lambda_2, \Sigma_2, d, \phi, f^T)$
10. $p(d | \tilde{y}^T, A_1, \Lambda_1, \Sigma_1, A_2, \Lambda_2, \Sigma_2, r, \phi, f^T)$
11. $p(\phi | \tilde{y}^T, A_1, \Lambda_1, \Sigma_1, A_2, \Lambda_2, \Sigma_2, r, d, f^T)$
12. $p(f^T | \tilde{y}^T, A_1, \Lambda_1, \Sigma_1, A_2, \Lambda_2, \Sigma_2, r, d, \phi)$

After step 2., one can drop the conditioning on the data y^T since the data does not provide any further information after condition on the latent state $\tilde{y}^T$. Conditional on r, d and $\tilde{y}^T$, the sample is split into two regimes $S_t = 1, 2$. Furthermore, conditional on f^T, one can transform $\check{y}^T = \frac{1}{\sqrt{f^T}} \tilde{y}^T$. Hence, step 3.-6. are standard draws from the multivariate Normal distribution for $p(A_{S_t} | \cdot)$ and from the inverse-Wishart for $p(\Sigma_{S_t} | \cdot)$ based on the subsamples and transformed

variables $\check{y}^T$. Drawing the variance ϕ of log-volatilities is, conditional on f_t, from an inverse-Gamma distribution.

The Gibbs sampler includes two Metropolis-Hastings step. Step 9. uses a random walk for the threshold r and step 12. an independence chain Metropolis-Hastings for the stochastic volatility f_t. Apart from the standard draws, the remaining steps draw from the following conditional posterior distributions:

2. Step: Latent states $z_{q,t}$ to obtain $\tilde{y}_{q,t}$:
   Draws for $z_{q,t}$ are based on the algorithm by Carter and Kohn (1994). To this end, I apply the Kalman filter until T to estimate the mean $z_{q,T|T}$ as well as the covariance matrix $P_{T|T}$. Hence, I draw $z_{q,T}$ from $N(z_{q,T|T}, P_{T|T})$. After backward smoothing the state vector recursively for $t = T-1, \ldots, 1$, I draw $z_{q,t}$ from $N(z_{q,t|t}, P_{t|t})$

7. and 8. Step: Shrinkage parameters Λ_{S_t}:
   To simplify notation, I drop the index S_t. Conditional on all other parameters, $\Lambda = [\lambda_1, \lambda_2, \lambda_3]'$ only affects the VAR coefficients through its prior dependence. Since the prior variance $Var(A) = \underline{V}$ is diagonal, one can operate row-wise by selecting the respective elements containing λ_i from the prior variance. Hence, the conditional posterior simplifies to:

$$p(\lambda_i|\lambda_{-i}, \tilde{y}^T, A, \Sigma, r, d, \phi, f^T) \propto p(A_i|\lambda_i)p(\lambda_i) \qquad \forall\, i = 1, 2, 3$$

   where $p(A_i|\lambda_i)$ denotes prior distribution of all elements of A associated with λ_i and $p(\lambda_i)$ indicates the prior distribution for the hyperparameter. λ_{-i} are the remainder shrinkage parameters excluding i. The conditional posterior $p(\lambda_i|\ldots) \sim \mathcal{IG}(\overline{a}, \overline{b})$ is inverse-Gamma with posterior shape and scale:

$$\begin{aligned}
\overline{a} &= \underline{a} + 1/2 * k_i \\
\overline{b} &= 1/2 * \left((vec(A_i) - vec(\underline{A}_i))'\underline{V}^{-1}(vec(A_i) - vec(\underline{A}_i)) + \underline{b}\right)
\end{aligned}$$

   where k_i refers to the number of parameters attached to λ_i, $\underline{a}$ and $\underline{b}$ indicate prior shape and scale and $vec()$ is the vectorization operator. $\underline{A}_i$ denotes the prior mean of A_i.

9. Step: Threshold value r:
   The conditional posterior distribution of r is analytical infeasible given by:

$$p(r|\cdot) = |\Sigma|_1^{T_1}|\Sigma|_2^{T_2} exp\left(-\sum_{S_t=1}^{2}(\check{Y}_{S_t} - \check{X}_{S_t}A_{S_t})'\Sigma_{S_t}^{-1}(\check{Y}_{S_t} - \check{X}_{S_t}A_{S_t})\right)$$

where T_1 and T_2 are the sample size of regime 1 and 2, respectively. Since the prior for r is uniform, the acceptance probability for the Metropolis-Hastings step at iteration s is

$$\alpha_r^s = min\left(\frac{p(r^*|\cdot)}{p(r^{s-1}|\cdot)}, 1\right) \quad \text{for } S_t = 1, 2$$

where the proposal r^* is generated by a random walk:

$$r^* = r^{s-1} + \vartheta \qquad \vartheta \sim N(0, \sigma_r^2).$$

The standard deviation σ_r is adjusted in iteration s according to the method proposed by Garthwaite et al. (2016):

$$\sigma_r^s = \sigma_r^{s-1} + c(\alpha^{s-1} - \alpha^*)/(s-1),$$

where $\alpha^* = 0.4$ is the target acceptance rate and $c = 1/[\alpha^*(1-\alpha^*)]$ is the optimal step size.

10. Step: Delay parameter d:

    The conditional posterior distribution $p(d|\cdot)$ is a multinomial distribution:

$$p(d|\cdot) = \frac{L(A_1, A_2, \Sigma_1, \Sigma_2, r, d|\check{y}^T)}{\sum_{d=1}^{p} L(A_1, A_2, \Sigma_1, \Sigma_2, r, d|\check{y}^T)}$$

    where $L(\cdot|\check{y}^T)$ denotes the likelihood function conditional on the transformed latent state $\check{y}^T$ and $\sum_{d=1}^{p}$ adds up all likelihoods based on the support of the uniform prior $d \sim \mathcal{U}(1, p)$ with p being the lag order of the VAR.

12. Step: Stochastic volatility f_t:

    The draw is based on the algorithm by Jacquier et al. (2002). For each draw of f_t, given the random walk law of motion, only the knowledge of f_{t+1} and f_{t-1} is relevant:

$$p(f_t|f_{-t}, \ldots) = p(f_t|f_{t-1}, f_{t+1}, \ldots)$$

    such that the conditional posterior is the product of a Normal density arising from the likelihood and a log-Normal density arising from the random walk law of motion of $h_t = ln(f_t)$. A log-Normal density is taken as a proposal and then progresses for $t = 1, \ldots, T$ cycling through T Metropolis-Hastings steps. I refer to Jacquier et al. (2002) for more details. One simply needs to adjust for the exact likelihood of the VAR model and the exact law of motion for the for stochastic volatility in case-by-case.

3.A.4 Additional figures

Figure 3.6: Monthly GDP from the MF-T-CSVM-VAR

(a) in monthly growth rates

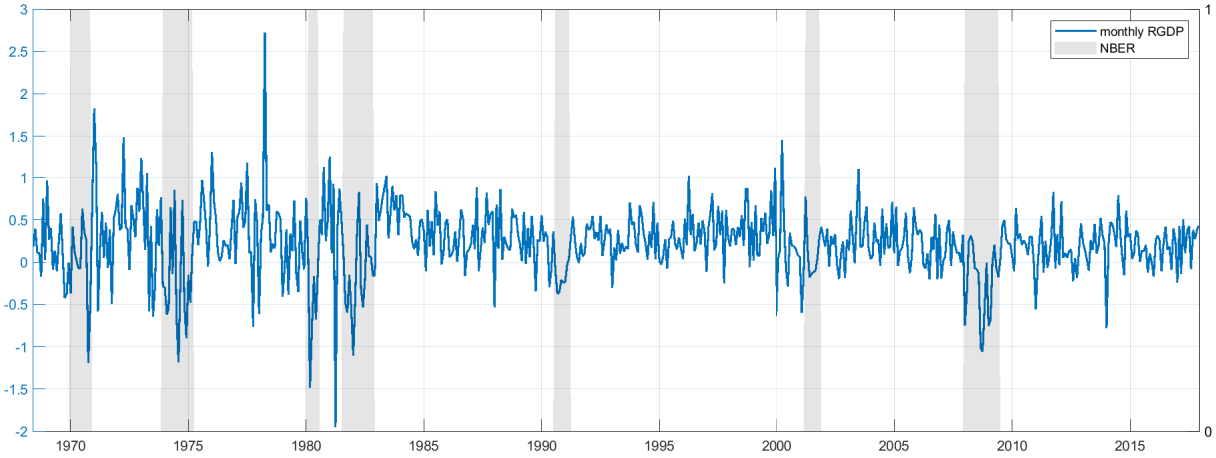

(b) in quarterly growth rates

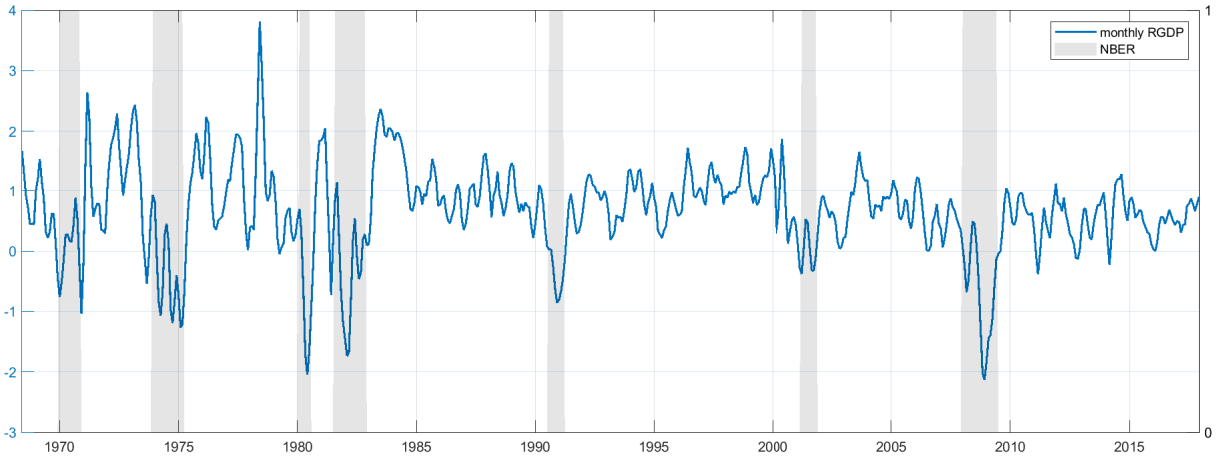

Notes: Panel (a) corresponds to $\tilde{y}_{q,t}$ from equation (3.3). Panel (b) corresponds to $y_{q,t}$ from equation (3.3). Shaded areas correspond to the recessions dated by the NBER. Sample: 1967M4-2017M12

Figure 3.7: Relative RMSEs for GDP - Comparison with Survey of Professional Forecasters

(a) Full sample

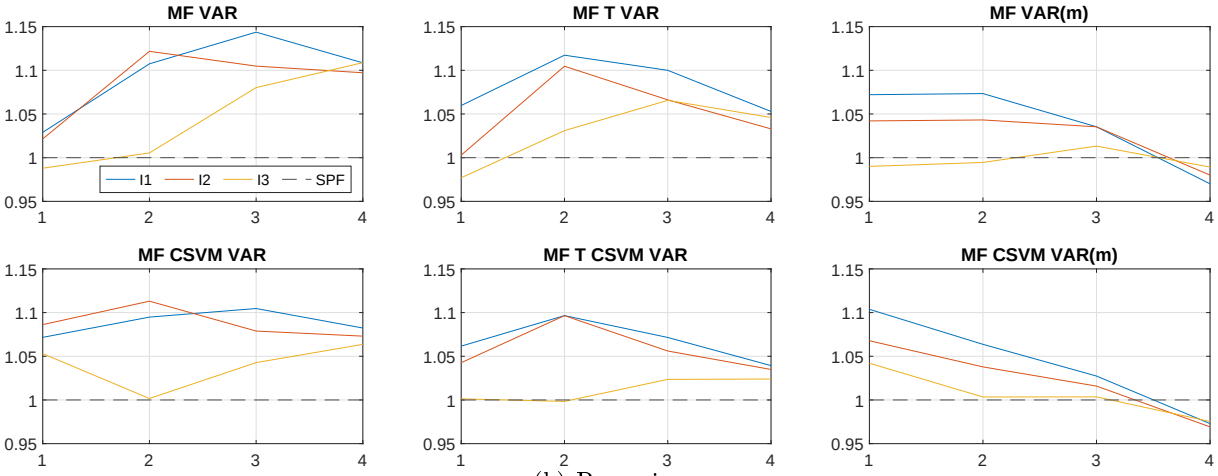

(b) Recession

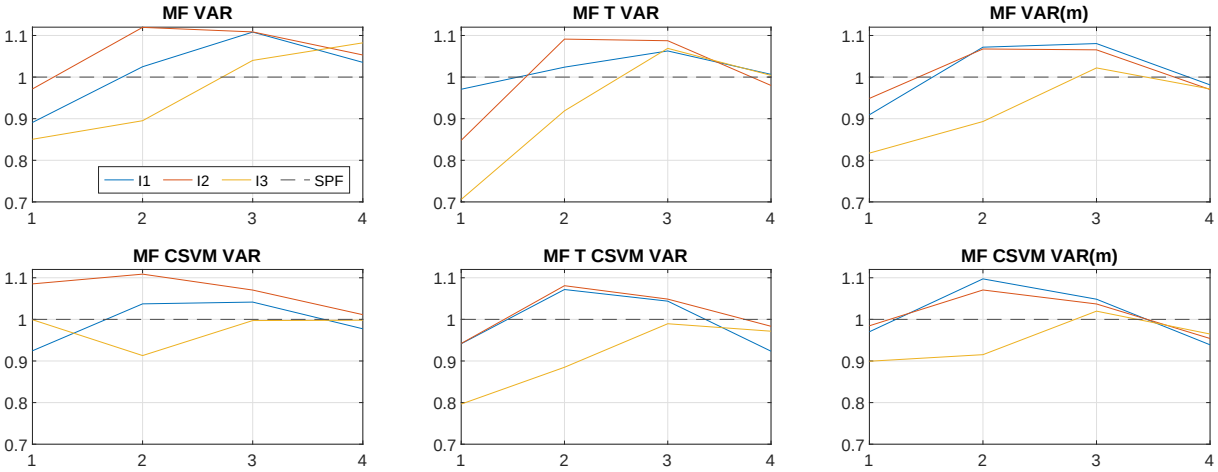

(c) Expansion

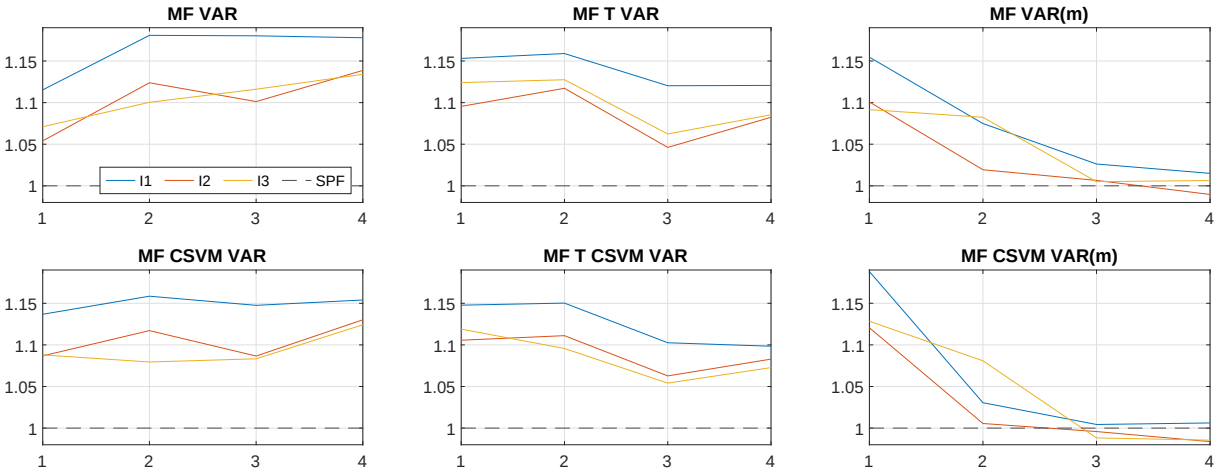

Notes: The relative RMSEs are expressed as ratios relative to the SPF for horizons $h = 1, \ldots, 4$. A figure below unity indicates that the model outperforms the SPF. The blue, red and yellow line belong to information set I1, I2 and I3, respectively, as explained in Section 3.4.5. Figure (a) refers to the full sample. Figure (b) and (c) refer to the NBER recession and expansion subsample, respectively. Out-of-sample: 2001M2-2017M12

Figure 3.8: Relative RMSEs for UR - Comparison with Survey of Professional Forecasters

(a) Full sample

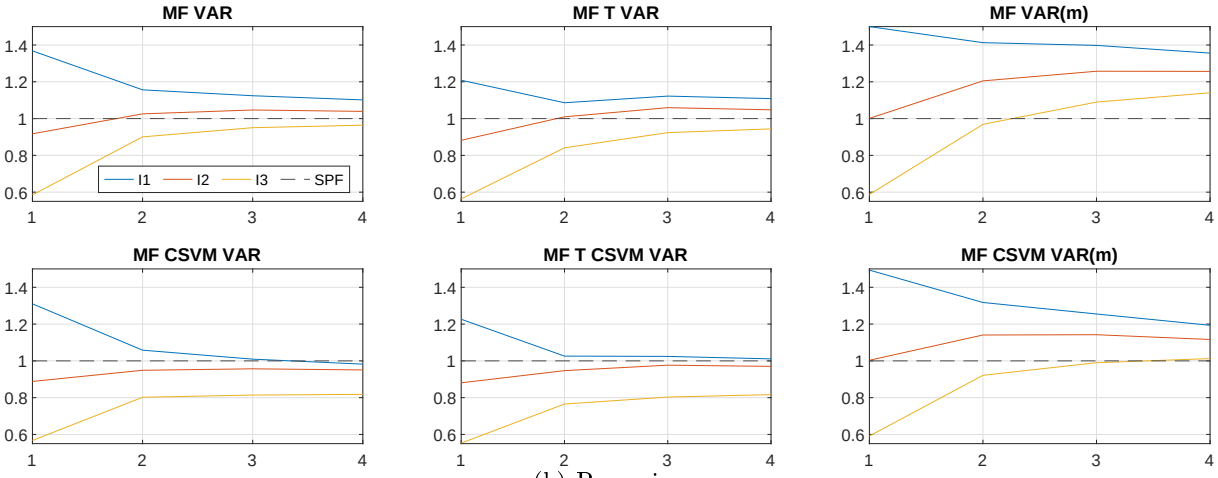

(b) Recession

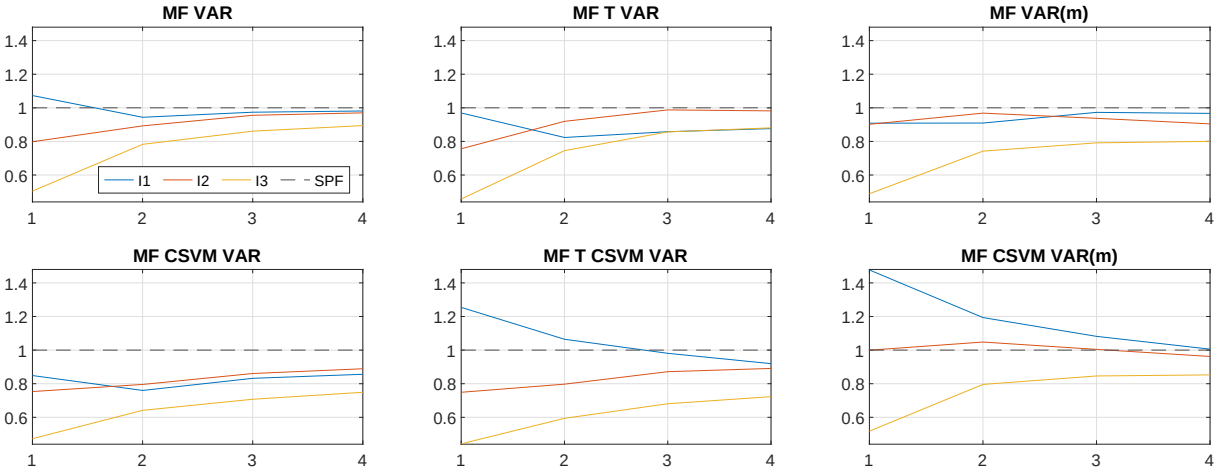

(c) Expansion

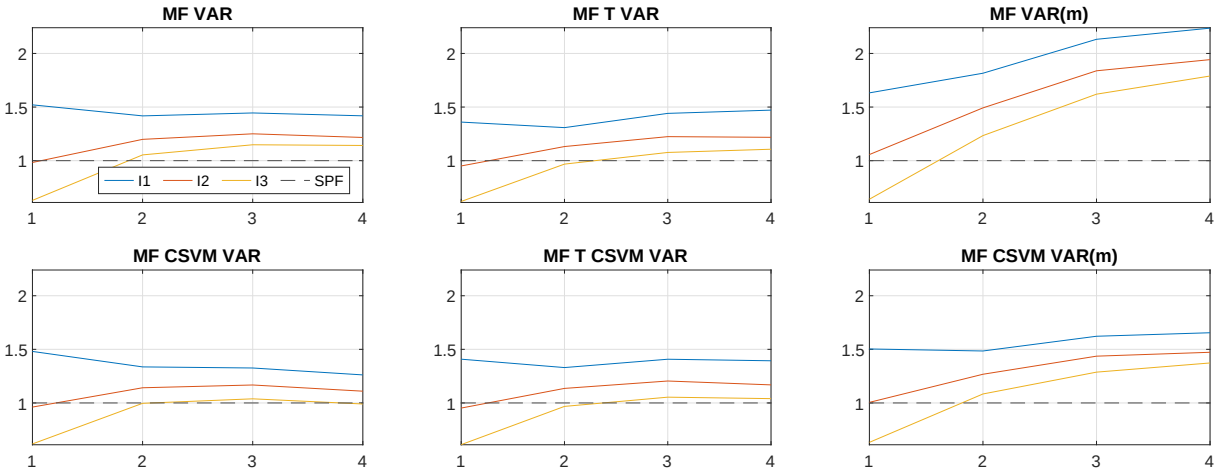

Notes: The relative RMSEs are expressed as ratios relative to the SPF for horizons $h = 1, \ldots, 4$. A figure below unity indicates that the model outperforms the SPF. The blue, red and yellow line belong to information set I1, I2 and I3, respectively, as explained in Section 3.4.5. Figure (a) refers to the full sample. Figure (b) and (c) refer to the NBER recession and expansion subsample, respectively. Out-of-sample: 2001M2-2017M12.

3.A.5 Shrinkage and forecasting

Each model that contains either the CFNAI business cycle index and/or the CSVM uncertainty factor have an separate cross variable shrinkage parameter λ_3 such that those variables might get less shrinkage due to their importance for forecasting. However, the standard Minnesota prior usually comes with a single cross variable shrinkage parameter ($\lambda_3 = \lambda_2$). Hence, I compare those two shrinkage setups with respect to their point forecast accuracy. Figure 3.9 displays a heatmap based on the relative RMSEs. The relative RMSEs are expressed as ratios relative to the same model with cross variable shrinkage. A figure below unity indicates that the model with BC shrinkage ($\lambda_3 \neq \lambda_2$) performs better.

The first detail one notice is that RMSEs are significantly reduced for GDP and UR during recessions for both T-VARs. While this is noticeable for GDP only for h=1, it is significantly better for UR across all forecast horizons. However, also for UR the improvements are strongest with up to 11% in relative RMSEs for the MF-T-CSVM-VAR for h=1. This advantage is no longer present in expansion in any way. Neither the small-scale nor the medium-scale VARs can improve their RMSEs by BC shrinkage during expansions.

In summary, the influence of the BC shrinkage on forecasting accuracy is stronger in times of recessions than expansions. Whereby the advantages in recession outweigh the slight disadvantages in expansion for the full sample. That means less shrinkage for CFNAI and CSVM is beneficial during recessions emphasizing the important information for short term forecasting contained in both BC variables during deteriorating times.

Figure 3.9: Relative RMSEs - BC Shrinkage against Cross Variable Shrinkage

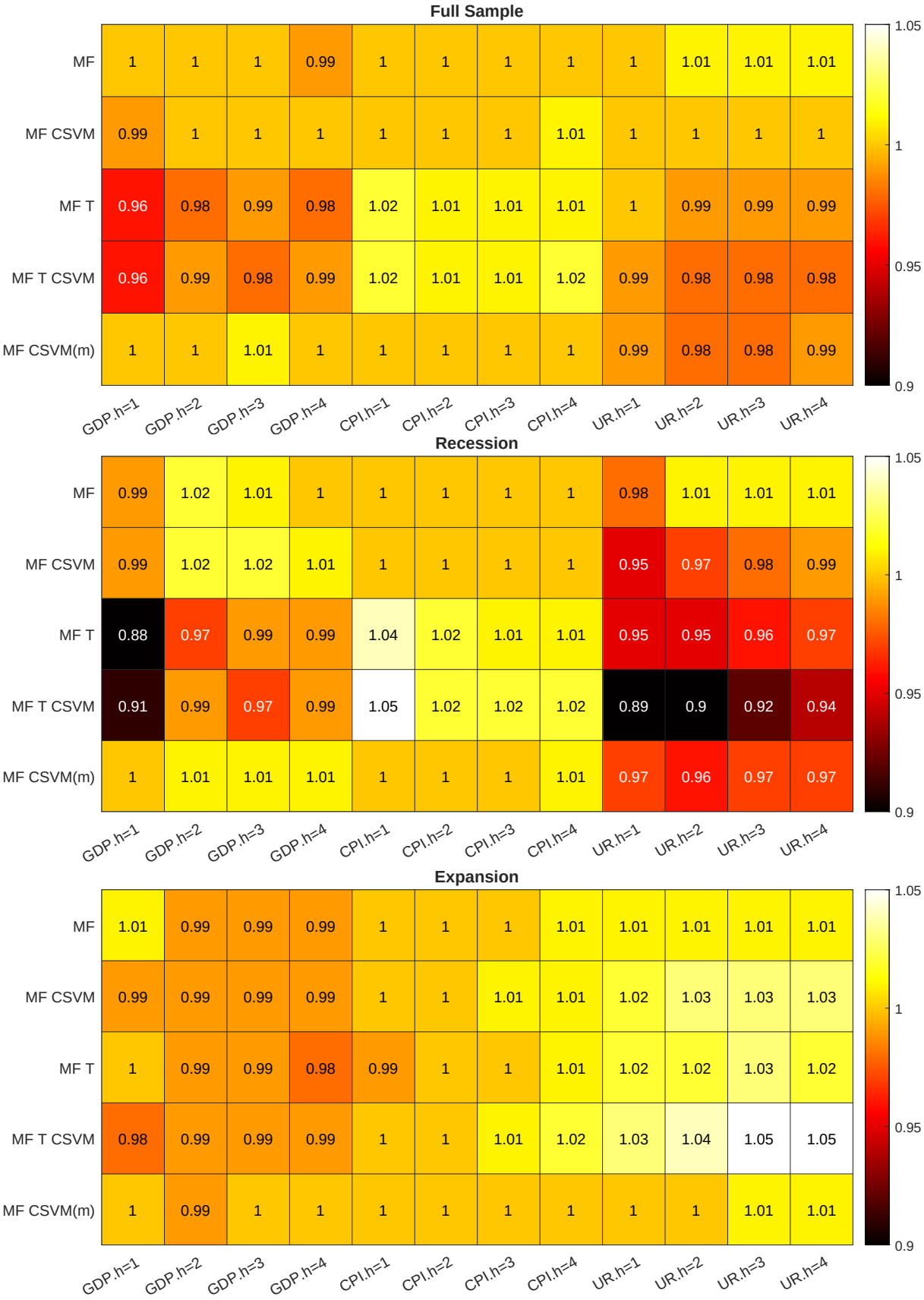

Notes: The relative RMSEs are expressed as ratios relative to the same model with cross variable shrinkage ($\lambda_3 = \lambda_2$). A figure below unity indicates that the model with BC shrinkage ($\lambda_3 \neq \lambda_2$) performs better. Hence, a panel with a darker shade corresponds to an increase in forecast accuracy. MF-VAR^{med} and MF-VAR^{b} are left out since the do not include λ_3. The upper, middle and lower panel belong to the full sample, the recession subsample and expansion subsample, respectively. Out-of-sample: 2001M2-2017M12.

3.A.6 Data set

Name	Transformation	ALFRED Code
Real Gross Domestic Product (GDP)	1	GDPC1
Consumer Price Index for All Urban Consumers: All Items (CPI)	1	CPIAUCSL
Civilian Unemployment Rate	4	UNRATE
All Employees: Total Nonfarm Payrolls	1	PAYEMS
Yield Spread (YS), 10-year - 3-month treasury bill rate	4	GS10-TB3MS
S&P 500 Index	1	(FRED-MD)
Chicago Fed National Activity Index	4	(Chicago Fed)
Industrial Production Index	1	INDPRO
Capacity Utilization: Total Industry	2	TCU
Housing Starts: Total	3	HOUST
Real Personal Consumption Expenditures	1	PCEC96
Index of Aggregate Weekly Hours	2	AWHI
Real Manufacturing and Trade Sales	1	(FRED-MD)
New Orders Durable Goods	1	(FRED-MD)

Transformation: 1. $\Delta ln(y_t)$ 2. Δy_t 3. $ln(y_t)$ 4. y_t. Additional Sources: Chicago Fed `https://www.chicagofed.org/publications/cfnai/index`. FRED-MD `https://research.stlouisfed.org/econ/mccracken/fred-databases/`.

Bibliography

Aastveit, K. A., A. Carriero, T. E. Clark, and M. Marcellino (2017). Have standard VARs remained stable since the crisis? Journal of Applied Econometrics 32(5), 931–951.

Alessandri, P. and H. Mumtaz (2017). Financial conditions and density forecasts for US output and inflation. Review of Economic Dynamics 24, 66–78.

Amir-Ahmadi, P., C. Matthes, and M.-C. Wang (2020). Choosing prior hyperparameters: With applications to time-varying parameter models. Journal of Business & Economic Statistics 38(1), 124–136.

Auerbach, A. J. and Y. Gorodnichenko (2012). Measuring the Output Responses to Fiscal Policy. American Economic Journal: Economic Policy 4(2), 1–27.

Bańbura, M., D. Giannone, and L. Reichlin (2010). Large Bayesian vector auto regressions. Journal of Applied Econometrics 25(1), 71–92.

Banbura, M. and A. van Vlodrop (2018). Forecasting with Bayesian vector autoregressions with time variation in the mean. Tinbergen Institute Discussion Paper 2018-025/IV, Tinbergen Institute.

Barnett, A., H. Mumtaz, and K. Theodoridis (2014). Forecasting UK GDP growth and inflation under structural change. A comparison of models with time-varying parameters. International Journal of Forecasting 30(1), 129–143.

Barsoum, F. and S. Stankiewicz (2015). Forecasting GDP growth using mixed-frequency models with switching regimes. International Journal of Forecasting 31(1), 33–50.

Berge, T. J. and O. Jorda (2011). Evaluating the Classification of Economic Activity into Recessions and Expansions. American Economic Journal: Macroeconomics 3(2), 246–77.

Bessec, M. and O. Bouabdallah (2015). Forecasting GDP over the business cycle in a multi-frequency and data-rich environment. Oxford Bulletin of Economics and Statistics 77(3), 360–384.

Blanchard, O. J. and M. W. Watson (1986). Are business cycles all alike? In The American business cycle: Continuity and change, pp. 123–180. University of Chicago Press.

Bloom, N. (2014). Fluctuations in uncertainty. The Journal of Economic Perspectives 28(2), 153–175.

Brave, S. (2009). The Chicago Fed National Activity Index and business cycles. Chicago Fed Letter (268), 1.

Brave, S. and R. A. Butters (2010). Chicago Fed National Activity Index turns ten-analyzing its first decade of performance. Chicago Fed Letter (273), 1.

Brave, S. A. and R. Butters (2014). Nowcasting using the Chicago Fed National Activity Index. Economic Perspectives 38(1).

Brave, S. A., R. A. Butters, and A. Justiniano (2019). Forecasting economic activity with mixed frequency BVARs. International Journal of Forecasting 35(4), 1692–1707.

Caggiano, G., E. Castelnuovo, and N. Groshenny (2014). Uncertainty shocks and unemployment dynamics in US recessions. Journal of Monetary Economics 67, 78–92.

Carriero, A., T. E. Clark, and M. Marcellino (2015a). Bayesian VARs: specification choices and forecast accuracy. Journal of Applied Econometrics 30(1), 46–73.

Carriero, A., T. E. Clark, and M. Marcellino (2015b). Realtime nowcasting with a Bayesian mixed frequency model with stochastic volatility. Journal of the Royal Statistical Society: Series A 178(4), 837–862.

Carriero, A., T. E. Clark, and M. Marcellino (2016). Common Drifting Volatility in Large Bayesian VARs. Journal of Business & Economic Statistics 34(3), 375–390.

Carriero, A., T. E. Clark, and M. Marcellino (2018). Measuring uncertainty and its impact on the economy. Review of Economics and Statistics 100(5), 799–815.

Carriero, A., A. B. Galvao, and G. Kapetanios (2019). A comprehensive evaluation of macroeconomic forecasting methods. International Journal of Forecasting 35(4), 1226–1239.

Carstensen, K., M. Heinrich, M. Reif, and M. H. Wolters (2020). Predicting ordinary and severe recessions with a three-state markov switching dynamic factor model. An application to the German business cycle. International Journal of Forecasting 36(3), 829–850.

Carter, C. K. and R. Kohn (1994). On Gibbs sampling for state space models. Biometrika 81(3), 541–553.

Chan, J. C. C. (2019). Large hybrid time-varying parameter VARs. CAMA Working Papers 2019–77, Centre for Applied Macroeconomic Analysis, Crawford School of Public Policy, The Australian National University.

Chan, J. C. C. and E. Eisenstat (2017). Bayesian model comparison for time-varying parameter VARs with stochastic volatility. Journal of Applied Econometrics 33(4), 509–532.

Chan, J. C. C. and I. Jeliazkov (2009). Efficient simulation and integrated likelihood estimation in state space models. International Journal of Mathematical Modelling and Numerical Optimisation 1(1-2), 101–120.

Chauvet, M. and S. Potter (2005). Forecasting recessions using the yield curve. Journal of Forecasting 24(2), 77–103.

Chauvet, M. and S. Potter (2013). Forecasting output. Handbook of Economic Forecasting 2(Part A), 141–194.

Chen, C. W. and J. C. Lee (1995). Bayesian inference of threshold autoregressive models. Journal of Time Series Analysis 16(5), 483–492.

Chiu, C.-W. J., H. Mumtaz, and G. Pintér (2017). Forecasting with VAR models: Fat tails and stochastic volatility. International Journal of Forecasting 33(4), 1124–1143.

Clark, T. E. (2009). Is the Great Moderation over? An empirical analysis. Economic Review 94(Q IV), 5–42.

Clark, T. E. (2011). Real-time density forecasts from Bayesian vector autoregressions with stochastic volatility. Journal of Business & Economic Statistics 29(3), 327–341.

Clark, T. E. and M. W. McCracken (2008). Forecasting with small macroeconomic VARs in the presence of instabilities. In D. E. Rapach and M. E. Wohar (Eds.), Forecasting in the Presence of Structural Breaks and Model Uncertainty, pp. 93–147. Emerald Publishing.

Clark, T. E. and F. Ravazzolo (2015). Macroeconomic forecasting performance under alternative specifications of time-varying volatility. Journal of Applied Econometrics 30(4), 551–575.

D'Agostino, A., L. Gambetti, and D. Giannone (2013). Macroeconomic forecasting and structural change. Journal of Applied Econometrics 28(1), 82–101.

Del Negro, M., R. B. Hasegawa, and F. Schorfheide (2016). Dynamic prediction pools: An investigation of financial frictions and forecasting performance. Journal of Econometrics 192(2), 391–405.

Del Negro, M. and G. E. Primiceri (2015). Time varying structural vector autoregressions and monetary policy: A corrigendum. Review of Economic Studies 82(4), 1342–1345.

Diebold, F. X. and R. S. Mariano (1995). Comparing predictive accuracy. Journal of Business & Economic Statistics 13(3), 253–263.

Dovern, J. and N. Jannsen (2017). Systematic errors in growth expectations over the business cycle. International Journal of Forecasting 33(4), 760–769.

Durbin, J. and S. J. Koopman (2001). Time Series Analysis by State Space Methods. Number 9780198523543 in OUP Catalogue. Oxford University Press.

Estrella, A. (2005). Why does the yield curve predict output and inflation? The Economic Journal 115(505), 722–744.

Estrella, A. and F. S. Mishkin (1997). The predictive power of the term structure of interest rates in Europe and the United States: Implications for the European Central Bank. European Economic Review 41(7), 1375–1401.

Evgenidis, A., S. Papadamou, and C. Siriopoulos (2020). The yield spread's ability to forecast economic activity: What have we learned after 30 years of studies? Journal of Business Research 106, 221–232.

Faust, J. and J. H. Wright (2009). Comparing Greenbook and reduced form forecasts using a large realtime dataset. Journal of Business & Economic Statistics 27(4), 468–479.

Faust, J. and J. H. Wright (2013). Forecasting inflation. Handbook of Economic Forecasting 2(Part A), 2–56.

Ferrara, L., M. Marcellino, and M. Mogliani (2015). Macroeconomic forecasting during the Great Recession: The return of non-linearity? International Journal of Forecasting 31(3), 664 – 679.

Foroni, C., P. Guérin, and M. Marcellino (2015). Markov-switching mixed-frequency VAR models. International Journal of Forecasting 31(3), 692–711.

Foroni, C. and M. Marcellino (2013). A survey of econometric methods for mixed-frequency data. Working Paper 2013/06, Norges Bank.

Foroni, C. and M. Marcellino (2014). A comparison of mixed frequency approaches for nowcasting euro area macroeconomic aggregates. International Journal of Forecasting 30(3), 554–568.

Garthwaite, P. H., Y. Fan, and S. A. Sisson (2016). Adaptive optimal scaling of Metropolis–Hastings algorithms using the Robbins–Monro process. Communications in Statistics-Theory and Methods 45(17), 5098–5111.

Geweke, J. (1993). Bayesian treatment of the independent Student-t linear model. Journal of Applied Econometrics 8, S19–S40.

Geweke, J. and G. Amisano (2011). Optimal prediction pools. Journal of Econometrics 164(1), 130–141.

Ghysels, E. (2016). Macroeconomics and the reality of mixed frequency data. Journal of Econometrics 193(2), 294–314.

Ghysels, E., P. Santa-Clara, and R. Valkanov (2004). The MIDAS touch: Mixed data sampling regression models. CIRANO Working Papers 2004s-20, CIRANO.

Gneiting, T. and R. Ranjan (2011). Comparing density forecasts using threshold and quantile weighted scoring rules. Journal of Business & Economic Statistics 29(3), 411–422.

Götz, T. B. and K. Hauzenberger (2018). Large mixed-frequency VARs with a parsimonious time-varying parameter structure. Discussion Papers 40/2018, Deutsche Bundesbank.

Heinrich, M. (2020). Does the current state of the business cycle matter for real-time forecasting? A mixed-frequency threshold VAR approach. EconStor Preprints 219312, ZBW - Leibniz Information Centre for Economics.

Heinrich, M. and M. Reif (2020). Real-time forecasting using mixed-frequency VARs with time-varying parameters. CESifo Working Paper Series 8054, CESifo Group Munich.

Jacquier, E., N. G. Polson, and P. E. Rossi (2002). Bayesian analysis of stochastic volatility models. Journal of Business & Economic Statistics 20(1), 69–87.

Jurado, K., S. C. Ludvigson, and S. Ng (2015). Measuring uncertainty. The American Economic Review 105(3), 1177–1216.

Kapetanios, G., M. Marcellino, and F. Venditti (2019). Large time-varying parameter VARs: A nonparametric approach. Journal of Applied Econometrics 34(7), 1027–1049.

Karlsson, S. (2013). Forecasting with Bayesian vector autoregression. Handbook of Economic Forecasting 2, 791–897.

Kim, S., N. Shephard, and S. Chib (1998). Stochastic volatility: likelihood inference and comparison with ARCH models. The Review of Economic Studies 65(3), 361–393.

Koop, G. M. (2013). Forecasting with medium and large Bayesian VARs. Journal of Applied Econometrics 28(2), 177–203.

Korobilis, D. (2013). Hierarchical shrinkage priors for dynamic regressions with many predictors. International Journal of Forecasting 29(1), 43–59.

Krüger, F., T. E. Clark, and F. Ravazzolo (2017). Using entropic tilting to combine BVAR forecasts with external nowcasts. Journal of Business & Economic Statistics 35(3), 470–485.

Kuzin, V., M. Marcellino, and C. Schumacher (2011). MIDAS vs. mixed-frequency VAR: Nowcasting GDP in the euro area. International Journal of Forecasting 27(2), 529–542.

Litterman, R. B. (1986). Forecasting with Bayesian vector autoregressions – five years of experience. Journal of Business & Economic Statistics 4(1), 25–38.

Liu, W. and E. Moench (2016). What predicts US recessions? International Journal of Forecasting 32(4), 1138–1150.

Mariano, R. S. and Y. Murasawa (2003). A new coincident index of business cycles based on monthly and quarterly series. Journal of Applied Econometrics 18(4), 427–443.

Mariano, R. S. and Y. Murasawa (2010). A coincident index, common factors, and monthly real GDP. Oxford Bulletin of Economics and Statistics 72(1), 27–46.

Matheson, J. E. and R. L. Winkler (1976). Scoring rules for continuous probability distributions. Management Science 22(10), 1087–1096.

McCracken, M. W. and S. Ng (2016). FRED-MD: A monthly database for macroeconomic research. Journal of Business & Economic Statistics 34(4), 574–589.

McCracken, M. W., M. T. Owyang, and T. Sekhposyan (2015). Real-time forecasting with a large, mixed frequency, Bayesian VAR. Working Paper 2015-30, Federal Reserve Bank of St. Louis.

Mumtaz, H. and P. Surico (2015). The transmission mechanism in good and bad times. International Economic Review 56(4), 1237–1260.

Mumtaz, H. and K. Theodoridis (2018). The changing transmission of uncertainty shocks in the US. Journal of Business & Economic Statistics 36(2), 239–252.

Ng, S. and J. H. Wright (2013). Facts and challenges from the Great Recession for forecasting and macroeconomic modeling. Journal of Economic Literature 51(4), 1120–1154.

Perez-Quiros, G., E. Rots, and D. Leiva-Leon (2020). Real-time weakness of the global economy: a first assessment of the coronavirus crisis. Working Paper Series 2381, European Central Bank.

Petrova, K. (2019). A quasi-Bayesian local likelihood approach to time varying parameter VAR models. Journal of Econometrics 212(1), 286–306.

Pettenuzzo, D. and A. Timmermann (2017). Forecasting macroeconomic variables under model instability. Journal of Business & Economic Statistics 35(2), 183–201.

Pierdzioch, C. and R. Gupta (2019). Uncertainty and forecasts of US recessions. Studies in Nonlinear Dynamics & Econometrics Forthcoming.

Primiceri, G. E. (2005). Time varying structural vector autoregressions and monetary policy. Review of Economic Studies 72(3), 821–852.

Reif, M. (2020). Macroeconomic Uncertainty and Forecasting Macroeconomic Aggregates. Studies in Nonlinear Dynamics & Econometrics Forthcoming.

Schorfheide, F. and D. Song (2015). Real-Time forecasting with a mixed-frequency VAR. Journal of Business & Economic Statistics 33(3), 366–380.

Segnon, M., R. Gupta, S. Bekiros, and M. E. Wohar (2018). Forecasting US GNP growth: The role of uncertainty. Journal of Forecasting 37(5), 541–559.

Sims, C. A. (2002). The role of models and probabilities in the monetary policy process. Brookings Papers on Economic Activity 2002(2), 1–40.

Sims, C. A. and T. Zha (2006). Were there regime switches in U.S. monetary policy? American Economic Review 96(1), 54–81.

Sinclair, T. M. (2019). Continuities and discontinuities in economic forecasting. RPF Working Paper 2019-003, The George Washington University.

Tenreyro, S. and G. Thwaites (2016). Pushing on a string: US monetary policy is less powerful in recessions. American Economic Journal: Macroeconomics 8(4), 43–74.

Wolters, M. H. (2015). Evaluating point and density forecasts of DSGE models. Journal of Applied Econometrics 30(1), 74–96.

Wright, J. H. (2019). Some observations on forecasting and policy. International Journal of Forecasting 35(3), 1186 – 1192.

Zadrozny, P. A. (1988). Gaussian-likelihood of continuous-time ARMAX models when data are stocks and flows at different frequencies. Econometric Theory 4(1), 108–124.

Erklärung zum selbständigen Verfassen der Arbeit:

Ich erkläre hiermit, dass ich meine Doktorarbeit "Macroeconomic Forecasting and Business Cycle Analysis with Nonlinear Models" selbstständig und ohne fremde Hilfe angefertigt habe und dass ich als Koautor maßgeblich zu den weiteren Fachartikeln beigetragen habe. Alle von anderen Autoren wörtlich übernommenen Stellen, wie auch die sich an die Gedanken anderer Autoren eng anlehnenden Ausführungen der aufgeführten Beiträge wurden besonders gekennzeichnet und die Quellen nach den mir angegebenen Richtlinien zitiert.

[Markus Heinrich]